

# NATIONAL ADVISORY COMMITTEE FOR AERONAUTICS

TECHNICAL NOTE 2640

INTERACTION OF COLUMN AND LOCAL BUCKLING  
IN COMPRESSION MEMBERS

By P. P. Bijlaard and G. P. Fisher

Cornell University



Washington

March 1952

## NATIONAL ADVISORY COMMITTEE FOR AERONAUTICS

## TECHNICAL NOTE 2640

## INTERACTION OF COLUMN AND LOCAL BUCKLING

## IN COMPRESSION MEMBERS

By P. P. Bijlaard and G. P. Fisher

## S U M M A R Y

The actual buckling stress  $\sigma_{cr}$  can be calculated from the first author's exact theory as well as by his method of split rigidities. Both methods yield practically identical results. By the latter method simple formulas are obtained which express the actual buckling stress  $\sigma_{cr}$  directly in terms of the column and local or plate buckling stresses. Columns with box, I-, H-, and T-sections and angles are considered separately. Interaction of practically significant magnitude occurs only in cases of flexural and torsional buckling. In these cases the additional effect of distortion of the cross section is also taken into account. The theory includes buckling in the plastic range. No post-buckling phenomena are considered in the theoretical part of the paper.

Tests were carried out for a considerable range of ratios of corrected free length to radius of gyration on two sections, for one of which the local buckling stress was in the plastic domain, and for the other, in the elastic domain. The experimental buckling stresses are in excellent agreement with those predicted by the theory.

## I N T R O D U C T I O N

It is customary to consider that a column may buckle in either one of two ways: (a) By deflection of the entire column in a half wave of length equal to the effective column length (column buckling) or (b) by plate buckling of its component webs and flanges in shorter or longer half waves (local or plate buckling). In the first case it is tacitly assumed that no distortion of cross section occurs, while in the second the lines of intersection of the midplanes of the various plates are assumed to remain straight. For a given column, buckling is supposed to occur at the lower of the two critical stresses, column or local. In reality, however, there is an interaction of these two modes of buckling, so that the real buckling stress  $\sigma_{cr}$  will be smaller than either of the buckling stresses for column or local buckling.

With column buckling the buckling stress  $\sigma_1$  is determined by the Euler or Engesser load. In figure 1  $\sigma_1$  is plotted against the ratio  $\beta = a/b$  of the half wave length  $a$  to the web width  $b$ , for example, for a column section like that in figure 2(a). On the other hand, with local buckling, which assumes the lines of intersection of the middle planes of the plates to remain straight, the buckling stress is given by  $\sigma_2$  in figure 1. The latter becomes minimum for a ratio  $\beta_1 = a/b$  of order of magnitude 1. If no interaction is taken into account for  $\beta < \beta_2$  in figure 1 the minimum plate buckling stress  $(\sigma_2)_{\min}$  is smaller than  $\sigma_1$ . Hence for an I-section with an effective buckling length  $a$ , where  $a/b < \beta_2$ , the plate buckling stress  $\sigma_2$  is governing and web and flanges will buckle in relatively short waves. If  $a/b > \beta_2$  the column buckling stress  $\sigma_1$  governs and the column buckles as a whole in a single half wave.

Actually the buckling deflection consists of a deflection  $w_1$  of the member as a whole, as it occurs with column buckling, and a deflection  $w_2$  of the web, as it occurs with plate buckling (fig. 2(b)). Assuming first an infinite rigidity against column buckling,  $w_1$  will be zero and a buckling of the web will occur at a stress  $\sigma_2$  with a maximum deflection  $w_2$  and in waves with a half wave length  $a$  of the order of magnitude of the web width  $b$  ( $a/b = \beta_1$  in fig. 1). This web deflection  $w_2$  will cause an external moment in the column as a whole. It will result in an entirely negligible internal moment in the column, however, since the latter is practically exclusively caused by the deflection of the flanges alone. Hence, assuming the column again to have a finite rigidity, this deflection  $w_2$  has the same effect as an initial deflection  $w_i < w_2$  of the entire column, causing an external but not an internal moment. It is well-known that an initial deflection  $w_i$  of a column causes an extra deflection of about  $[\sigma_C / (\sigma_E - \sigma_C)] w_i$ , where  $\sigma_C$  is the actual compressive force and  $\sigma_E$  is the elastic buckling stress of the column (see reference 1). Since, for the very small half wave length  $a$  of the deflection  $w_2$ , the column buckling stress  $\sigma_1$  for multiple-wave buckling is in most cases very high as compared with the plate buckling stress  $\sigma_2$  (compare  $\sigma_1$  and  $\sigma_2$  for  $a/b = \beta_1$  in fig. 1), this means that the deflection  $w_2$  causes a column deflection  $w_1$  which is smaller than  $[\sigma_2 / (\sigma_1 - \sigma_2)] w_2$  and hence very small as compared with  $w_2$ . This extra deflection  $w_1$  increases the deflecting forces  $-\tau_x dx dy (\partial^2 w / \partial x^2)$  that act on an element  $t dx dy$  of the web, while it increases only slightly the restraining forces acting on that element. Since  $w_1 \ll w_2$  the increase of the deflecting forces will be relatively

small, so that the actual buckling stress  $\sigma_{cr}$  will be only slightly less than  $\sigma_2$  (compare  $\sigma_{cr}$  and  $\sigma_2$  for  $a/b = \beta_1$  in fig. 1).

If, on the other hand, the I-section has an effective buckling length  $a$  which is larger than the limiting value  $a_2 = \beta_2 b$ , so that  $\beta = a/b$  is larger than  $\beta_2$  in figure 1, buckling will occur in a single half wave. In this case, besides the deflection  $w_1$  of the member as a whole, a small deflection  $w_2$  of the web (fig. 2(b)) will also occur because of the deflecting forces  $-\tau_x dx dy (\partial^2 w / \partial x^2)$  that act on each element  $t dx dy$ .

In this case, in a similar way as above, the extra deflection  $w_2$  will be of the order of magnitude  $[\sigma_1 / (\sigma_2 - \sigma_1)] w_1$  which is small as compared with  $w_1$  because for  $a/b \geq \beta_2$ , in most cases,  $\sigma_2$  is very much larger than  $\sigma_1$  (fig. 1). The deflection  $w_2$  increases the external moment in the column while it practically does not increase its internal moment. Since, however,  $w_2$  is small with respect to  $w_1$ , the actual buckling stress  $\sigma_{cr}$  will be only slightly smaller than  $\sigma_1$ . The qualitative conclusions above are fully worked out quantitatively in the theoretical part of the paper and are confirmed, in particular, by study of the interaction equations (74) and (75).

Considerable interaction occurs and governs the actual buckling stress only if the individual buckling stresses  $\sigma_1$  and  $\sigma_2$  have their smallest value for a half wave length about equal to the effective column length. This happens, for example, with angles and T-sections, where for flexural buckling as well as for torsional buckling (which is a simplified form of plate buckling) both individual buckling stresses  $\sigma_1$  and  $\sigma_2$  are the smaller the larger the length of the column. In the latter case interaction actually occurs between three individual modes of buckling (fig. 3).

In the theoretical part of the paper the exact theory for determining the actual buckling stress  $\sigma_{cr}$  of arbitrary plate assemblies is given. It leads to transcendental buckling conditions for  $\sigma_{cr}$  which have to be solved by trial and error. Furthermore, by the first author's method of split rigidities design formulas are derived which express  $\sigma_{cr}$  directly in the individual buckling stresses  $\sigma_1$  and  $\sigma_2$  and for a column with T-section in  $\sigma_1$ ,  $\sigma_2$ , and  $\sigma_3$ . As is customary, in all derivations column deflections by shear were neglected.

In the experimental part of the investigation stress-strain tests were carried out on square tube columns. Column tests were then carried out using the stress-strain data to study the interaction of local and column buckling.

This investigation was carried out at Cornell University under the sponsorship and with the financial assistance of the National Advisory Committee for Aeronautics. The theoretical part was carried out by Professor P. P. Bijlaard and the experimental part was carried out by Professor G. P. Fisher. The project was directed by Professor George Winter, who is also at Cornell University.

### S Y M B O L S

a	half wave length of buckling
L	column and plate length
b	plate width
c, k	constants
$e = (E/E_s) - 1$	
$n = s + \theta qr$	
p	number of waves (used in section entitled "Exact Theory")
$P_y$	equivalent load, including influence of twisting moments, transferred by plate to beams
$q = \alpha_1^2 - (B\lambda^2/D)$	in plastic range (used in section entitled "Exact Theory")
$q = \alpha_1^2 - \nu\lambda^2$	in elastic range (used in section entitled "Exact Theory")
$r = \alpha_2^2 + (B\lambda^2/D)$	in plastic range (used in section entitled "Exact Theory")
$r = \alpha_2^2 + \nu\lambda^2$	in elastic range (used in section entitled "Exact Theory")
r	radius of gyration
$r_o$	polar radius of gyration about shear center
$s_{1,2} = \frac{\lambda^2}{EID} (B_{1,2}\lambda^2 - A_{1,2}\sigma_{cr})$	in plastic range

$$s_{1,2} = \frac{\lambda^2}{N} (B_{1,2} \lambda^2 - A_{1,2} \sigma_{cr}) \quad \text{in elastic range}$$

t	plate thickness
$u = S - \theta r^2$	(used in section entitled "Exact Theory")
$v = S - \theta q^2$	(used in section entitled "Exact Theory")
w	deflection
x,y,z	coordinates
$y_0$	distance between shear center and center of gravity
A,B,D,F,G,H,K	constants in theory of plastic plate buckling (used in section entitled "Exact Theory")
$A_{1,2}$	cross section of beams (used in section entitled "Exact Theory")
$A_c$	total cross section of columns
$A_w$	total cross section of webs situated perpendicular to direction of buckling
$A_f$	total cross section of flanges situated perpendicular to direction of buckling
$B_{1,2}$	flexural rigidities of beams (used in section entitled "Exact Theory")
$C_1, C_2, C_3, C_4$	constants
$C_w$	warping constant
D	deflecting force in method of split rigidities
E	modulus of elasticity
$E_s$	secant modulus
$E_t$	tangent modulus
G	modulus of rigidity
I	moment of inertia

$I_p$	polar moment of inertia about shear center
$I_t$	Saint Venant torsion constant
$M$	bending or torsional moment
$N$	plate flexural rigidity
$Q$	transverse shear
$R$	resisting force in method of split rigidities
$S$	shear center
$V$	energy
$X, Y, Z$	coordinate axes
$\alpha_{1,2}, \alpha'_{1,2}$	given by equations (8), (11), (27), and (28)
$\beta$	ratio between half wave length $a$ and plate width $b$
$\alpha, \gamma, \epsilon, \eta, \eta_3, \theta, \mu, \phi$	coefficients in method of split rigidities
$\bar{\eta}$	reduction coefficient for plasticity
$\lambda = p\pi/L$	(used in section entitled "Exact Theory")
$\nu$	Poisson's ratio
$\sigma$	normal stress
$\tau = q + r$	(used in section entitled "Exact Theory")
$\psi = b\sqrt{t\sigma_{cr}/N}$	(used in section under "Buckling of I-Section in Direction Perpendicular to Plane of Web" entitled "Comparison with Exact Theory")
$\psi = I_{pw}/I_p$ , where $I_p$	is polar moment of inertia of web about shear center (used in section under "Buckling of Columns with T-Section" entitled "Critical Stress for T-Section with Fixed Shear Center Axis")
$\Psi$	reciprocal spring constant of restraining plate (used in section entitled "Exact Theory")

$\theta = EID\psi$  (used in section entitled "Exact Theory")

$\phi = \sqrt{t\sigma_{cr}/EI}$  (used in section entitled "Exact Theory")

## T H E O R E T I C A L I N V E S T I G A T I O N

### E X A C T T H E O R Y

The exact general theory of elastic as well as plastic buckling of plate assemblies was published by the first author (references 2 and 3). It will be summarized here to the extent that it is used in this paper.

Consider an asymmetric column, consisting of a web plate with width  $b$  and thickness  $t$ , which is supported at both unloaded edges by flanges of different width  $2b'$  and thickness  $t'$  (fig. 4(a)). Let the web plate be the "buckling" plate which is restrained at both edges by the flanges, the "restraining" plates.

The X-axis is chosen in the longitudinal direction of the column, while for the buckling plate the Y- and Z-directions are chosen as shown in figure 4. Hence the differential equation for the buckling plate is, for the general case of plastic buckling (references 3 and 4),

$$EI \left[ A \frac{\partial^4 w}{\partial x^4} + 2(B + 2F) \frac{\partial^4 w}{\partial x^2 \partial y^2} + D \frac{\partial^4 w}{\partial y^4} \right] + t\sigma_{cr} \frac{\partial^2 w}{\partial x^2} = 0 \quad (1)$$

where  $I = t^3/12$  and  $\sigma_{cr}$  is the buckling stress  $\sigma_x$ . For pure compression, as occurs here,  $A$ ,  $B$ ,  $D$ , and  $F$ , if expressed in terms of the secant modulus  $E_s$ , the tangent modulus  $E_t$ , and Poisson's ratio  $\nu$ , are (reference 4):

$$\begin{aligned}
 A &= \psi_1/\psi_4 \\
 B &= \psi_2/\psi_4 \\
 D &= \psi_3/\psi_4 \\
 \psi_1 &= 1 + 3(E_t/E_s) \\
 \psi_2 &= 2 - 2(1 - 2\nu)(E_t/E) \\
 \psi_3 &= 4 \\
 \psi_4 &= (5 - 4\nu + 3e) - (1 - 2\nu)^2(E_t/E) \\
 F &= 1/(2 + 2\nu + 3e) \\
 e &= (E/E_s) - 1
 \end{aligned}
 \tag{2}$$

With  $\nu = 0.5$  these values reduce to those used by Stowell (reference 5):

$$\begin{aligned}
 A &= (1/3)(E_s/E) + (E_t/E) \\
 B &= (2/3)(E_s/E) \\
 D &= (4/3)(E_s/E) \\
 F &= (1/3)(E_s/E)
 \end{aligned}$$

In the elastic domain in equations (2)  $e = 0$  and  $E_s = E_t = E$ , so that equations (2) yield:

$$\begin{aligned}
 A &= D = 1/(1 - \nu^2) \\
 B &= \nu/(1 - \nu^2) \\
 F &= 1/[2(1 + \nu)]
 \end{aligned}
 \tag{3}$$

With sufficiently long members and a plate length  $L$  it may be assumed that

$$w = Y \sin(p\pi x/L) \tag{4}$$

in which  $Y$  is a function of  $y$  only and  $p$  is the number of half waves in the  $X$ -direction. Insertion of equation (4) in equation (1) yields

$$D \frac{d^4 Y}{dy^4} - 2(B + 2F)\lambda^2 \frac{d^2 Y}{dy^2} + (A\lambda^2 - \phi^2)\lambda^2 Y = 0 \quad (5)$$

in which

$$\left. \begin{aligned} \lambda &= p\pi/L \\ \phi^2 &= t\sigma_{cr}/EI \end{aligned} \right\} \quad (6)$$

With  $Y = e^{\alpha y}$  this leads to

$$w = (C_1 \cosh \alpha_1 y + C_2 \sinh \alpha_1 y + C_3 \cos \alpha_2 y + C_4 \sin \alpha_2 y) \cos \frac{p\pi x}{a} \quad (7)$$

with

$$\alpha_{1,2} = \sqrt{\pm G\lambda^2 + \lambda\sqrt{H\lambda^2 + K\phi^2}} \quad (8)$$

in which

$$\left. \begin{aligned} G &= \frac{B + 2F}{D} \\ H &= \frac{(B + 2F)^2 - AD}{D^2} \\ K &= \frac{1}{D} \end{aligned} \right\} \quad (9)$$

On the other hand for the restraining plates, with thickness  $t'$ , a similar equation such as equation (1) also applies. Considering, for example, the lower half of a flange, as sketched in figure 5, this leads, analogous to equation (7), to the general equation of the deflection surface

$$w' = (C_1' \cosh \alpha_1' y' + C_2' \sinh \alpha_1' y' + C_3' \cos \alpha_2' y' + C_4' \sin \alpha_2' y') \cos\left(\frac{p\pi x}{L}\right) \quad (10)$$

with

$$\alpha_{1,2}' = \sqrt{\pm G\lambda^2 + \lambda\sqrt{H\lambda^2 + K(\phi')^2}} \quad (11)$$

in which  $(\phi')^2 = t'\sigma_{cr}/EI'$  and  $I' = (t')^3/12$ .

Since the buckling and restraining plates are rigidly connected,  $\lambda = p\pi/L$  has, of course, to be the same for all plates.

Dealing first with the restraining plates, for the sections dealt with in this report it is only necessary to consider the case of figure 5. Let the buckling plate exert a moment  $M_y' = M \cos(p\pi x/L)$  on the restraining plate. In the plastic domain the bending and twisting moments in the restraining plate are (references 3 and 4)

$$\left. \begin{aligned} M_x' &= -EI' \left[ A \frac{\partial^2 w'}{\partial x^2} + B \frac{\partial^2 w'}{(\partial y')^2} \right] \\ M_y' &= -EI' \left[ B \frac{\partial^2 w'}{\partial x^2} + D \frac{\partial^2 w'}{(\partial y')^2} \right] \\ M_{yx}' &= -2EI' F \frac{\partial^2 w'}{\partial x \partial y'} \\ &= -M_{xy}' \end{aligned} \right\} \quad (12)$$

Hence at  $y' = 0$ , where  $w' = 0$  and  $\partial^2 w'/\partial x^2 = 0$ , the boundary conditions are, from equations (12),

$$w' = 0 \quad (13a)$$

and

$$M_y' = -EI'D \frac{\partial^2 w'}{(\partial y')^2} = M \cos \frac{p\pi x}{L} \quad (13b)$$

At  $y' = b'$  (fig. 5) the plate is free, so that  $M_y' = 0$  and the so-called equivalent load  $p_y' = 0$ . Choosing the positive directions in the same way as in reference 6, figure 160, page 295, and using the equation for the transverse shear from reference 6, page 297,

$$p_y' = -Q_y' - \frac{\partial M_{yx}'}{\partial x} = -\frac{\partial M_y'}{\partial y'} + \frac{\partial M_{xy}'}{\partial x} - \frac{\partial M_{yx}'}{\partial x}$$

or from equations (12)

$$p_y' = EI' \left[ D \frac{\partial^3 w'}{(\partial y')^3} + (B + 4F) \frac{\partial^3 w'}{\partial x^2 \partial y'} \right] \quad (14)$$

Hence from equations (12) and (14) at  $y' = b'$  the boundary conditions  $M_y' = 0$  and  $p_y' = 0$  are

$$B \frac{\partial^2 w'}{\partial x^2} + D \frac{\partial^2 w'}{(\partial y')^2} = 0 \quad (13c)$$

$$D \frac{\partial^3 w'}{(\partial y')^3} + (B + 4F) \frac{\partial^3 w'}{\partial x^2 \partial y'} = 0 \quad (13d)$$

Inserting equation (10) in the four boundary conditions (13a) to (13d) yields the constants  $C_1'$ ,  $C_2'$ ,  $C_3'$ , and  $C_4'$  in equation (10), so that the angular rotation at  $y' = 0$  can be computed from equation (10),

$$\begin{aligned} \frac{\partial w'}{\partial y'} &= (C_2' \alpha_1' + C_4' \alpha_2') \cos \frac{p\pi x}{L} \\ &= (M_y')_{y'=0} \psi \end{aligned} \quad (15)$$

The value  $1/\psi = (M_y')_{y'=0} / (\partial w' / \partial y')_{y'=0}$  may be called the spring constant of the restraining plate. Hence

$$\begin{aligned} \theta &= EID\psi \\ &= EID(\partial w' / \partial y') / M_y' \end{aligned} \quad (16)$$

which value will be used in the boundary conditions of the buckling plate, may be computed, yielding (reference 3, equation (56), p. 60)

$$\theta = \left(\frac{t}{t'}\right)^3 \frac{[(\alpha_1')^2(r')^2 - (\alpha_2')^2(q')^2] \sinh \alpha_1' b' \sin \alpha_2' b' - \alpha_1' \alpha_2' [(q')^2 + (r')^2] \cosh \alpha_1' b' \cos \alpha_2' b' - 2\alpha_1' \alpha_2' q' r'}{[(\alpha_1')^2 + (\alpha_2')^2] [\alpha_1' (r')^2 \cosh \alpha_1' b' \sin \alpha_2' b' - \alpha_2' (q')^2 \sinh \alpha_1' b' \cos \alpha_2' b']}$$
 (17)

where

$$\left. \begin{aligned} q' &= (\alpha_1')^2 - (B\lambda^2/D) \\ r' &= (\alpha_2')^2 + (B\lambda^2/D) \\ \lambda &= p\pi/L \end{aligned} \right\} \quad (18)$$

If  $\alpha_2'$  becomes imaginary, with  $\alpha_1' = \alpha_1''$  and  $\alpha_2' = i\alpha_2''$ ,

$$\theta = \left(\frac{t}{t'}\right)^3 \frac{[(\alpha_1'')^2(r'')^2 + (\alpha_2'')^2(q'')^2] \sinh \alpha_1'' b' \sinh \alpha_2'' b' - \alpha_1'' \alpha_2'' [(q'')^2 + (r'')^2] \cosh \alpha_1'' b' \cosh \alpha_2'' b' - 2\alpha_1'' \alpha_2'' q'' r''}{[(\alpha_1'')^2 - (\alpha_2'')^2] [\alpha_1'' (r'')^2 \cosh \alpha_1'' b' \sinh \alpha_2'' b' - \alpha_2'' (q'')^2 \sinh \alpha_1'' b' \cosh \alpha_2'' b']}$$
 (17a)

where

$$\left. \begin{aligned} q'' &= (\alpha_1'')^2 - B\lambda^2/D \\ r'' &= -(\alpha_2'')^2 + B\lambda^2/D \end{aligned} \right\} \quad (18a)$$

If more than one restraining plate like that of figure 5 meets at  $y' = 0$  the total spring constant

$$\frac{1}{\psi_t} = \sum \frac{1}{\psi} \quad (19)$$

so that for a symmetrical flange  $1/\psi_t = 2/\psi$  and  $\psi_t = \psi/2$ , or from equation (16)

$$\theta_t = (1/2)\theta \quad (20)$$

Considering now the buckling plate (fig. 4(b)), the restraining plates are at the same time the "beams" by which the buckling plate is supported. At  $y = 0$  (fig. 4(b)) the difference between the transverse shearing forces acting on an element  $dx$  of the left beam will have to be in equilibrium with the equivalent load  $p_y$  transmitted by the buckling plate and the resultant of the compressive forces  $A_1\sigma_{cr}$  acting on the beam element  $dx$ . Here  $A_1$  is the cross section of the left beam. The pertinent equilibrium condition is given by the equation (reference 6, p. 346):

$$B_1 \frac{\partial^4 w}{\partial x^4} = p_y - A_1\sigma_{cr} \frac{\partial^2 w}{\partial x^2} \quad (21)$$

in which  $B_1$  is the flexural rigidity of the left beam about its major axis. At  $y = 0$

$$\begin{aligned} p_y &= Q_y + \frac{\partial M_{yx}}{\partial x} \\ &= \frac{\partial M_y}{\partial y} - \frac{\partial M_{xy}}{\partial x} + \frac{\partial M_{yx}}{\partial x} \end{aligned}$$

or, from equations (12),

$$p_y = -EI \left[ D \frac{\partial^3 w}{\partial y^3} + (B + 4F) \frac{\partial^3 w}{\partial x^2 \partial y} \right] \quad (22)$$

so that from equation (21) one of the boundary conditions of the buckling plate at  $y = 0$  is (reference 3, equation (I), p. 61)

$$B_1 \frac{\partial^4 w}{\partial x^4} + EI \left[ D \frac{\partial^3 w}{\partial y^3} + (B + 4F) \frac{\partial^3 w}{\partial x^2 \partial y} \right] + A_1\sigma_{cr} \frac{\partial^2 w}{\partial x^2} = 0$$

The other boundary condition at  $y = 0$  follows from equation (15). Figures 4(b) and 5 show that for a one-sided flange  $M_{y1} = (M_y')_{y'=0}$

and  $(\partial w / \partial y)_{y=0} = (\partial w' / \partial y')_{y'=0}$ , so that equation (15) becomes

$$\frac{\partial w}{\partial y} = M_{y1} \psi_1 \quad (23)$$

From figure 4(b)  $M_{y1}$  is a negative moment. By equation (16)  $\psi_1$  may be expressed in terms of  $\theta_1$ . For a symmetrical flange  $\theta_1$  is given by  $\theta_t$  in equation (20), where  $\theta$  follows from equations (17) or (17a). The subscript 1 refers to the left flange (fig. 4(a)). Hence from equations (12) and (16) equation (23) yields as second boundary condition for  $y = 0$  (reference 3, equation (II), p. 61)

$$\frac{\partial w}{\partial y} - \theta_1 \left( \frac{B}{D} \frac{\partial^2 w}{\partial x^2} + \frac{\partial^2 w}{\partial y^2} \right) = 0$$

In the same way the boundary conditions for  $y = b$  become

$$B_2 \frac{\partial^4 w}{\partial x^4} - EI \left[ D \frac{\partial^3 w}{\partial y^3} + (B + 4F) \frac{\partial^3 w}{\partial x^2 \partial y} \right] + A_2 \sigma_{cr} \frac{\partial^2 w}{\partial x^2} = 0$$

$$\frac{\partial w}{\partial y} + \theta_2 \left( \frac{B}{D} \frac{\partial^2 w}{\partial x^2} + \frac{\partial^2 w}{\partial y^2} \right) = 0$$

The subscript 2 refers to the right flange. Insertion of equation (7) in the four boundary conditions for the buckling plate leads to four linear homogeneous equations, which yield only values of the constants different from zero if the denominator determinant vanishes. This leads to the general buckling condition (reference 3, equation (61), p. 62)

$$\begin{aligned}
& \left\{ \alpha_1^2 \left[ s_1 s_2 - \alpha_2^2 \tau^2 - (\theta_1 s_2 + \theta_2 s_1) r^2 + \theta_1 \theta_2 r^4 \right] - \right. \\
& \left. \alpha_2^2 \left[ s_1 s_2 - (\theta_1 s_2 + \theta_2 s_1) q^2 + \theta_1 \theta_2 q^4 \right] + \theta_1 \theta_2 s_1 s_2 \tau^2 \right\} \sinh \alpha_1 b \sin \alpha_2 b - \\
& \alpha_1 \alpha_2 \left[ 2 s_1 s_2 - (\theta_1 + \theta_2) (s_1 + s_2) \tau^2 + 2 (\theta_1 s_2 + \theta_2 s_1) q r + \right. \\
& \left. 2 \theta_1 \theta_2 q^2 r^2 \right] \cosh \alpha_1 b \cos \alpha_2 b + \alpha_2 \tau \left\{ \alpha_1^2 \left[ s_1 + s_2 - (\theta_1 + \theta_2) r^2 \right] - \right. \\
& \left. (\theta_1 + \theta_2) s_1 s_2 + \theta_1 \theta_2 (s_1 + s_2) q^2 \right\} \sinh \alpha_1 b \cos \alpha_2 b + \alpha_1 \tau \left\{ \alpha_2^2 \left[ s_1 + s_2 - \right. \right. \\
& \left. \left. (\theta_1 + \theta_2) q^2 \right] + (\theta_1 + \theta_2) s_1 s_2 - \theta_1 \theta_2 (s_1 + s_2) r^2 \right\} \cosh \alpha_1 b \sin \alpha_2 b + \\
& 2 \alpha_1 \alpha_2 \left[ s_1 s_2 + (\theta_1 s_2 + \theta_2 s_1) q r + \theta_1 \theta_2 q^2 r^2 \right] = 0 \tag{24}
\end{aligned}$$

in which

$$\left. \begin{aligned}
q &= \alpha_1^2 - (B\lambda^2/D) \\
r &= \alpha_2^2 + (B\lambda^2/D) \\
\tau &= q + r \\
&= \alpha_1^2 + \alpha_2^2 \\
&= 2\lambda \sqrt{H\lambda^2 + K\phi^2} \\
s_{1,2} &= \frac{\lambda^2}{EID} (B_{1,2}\lambda^2 - A_{1,2}\sigma_{cr})
\end{aligned} \right\} \tag{25}$$

For the elastic range A, B, D, and F are given by equations (3), so that from equations (9)

$$\left. \begin{aligned} G &= 1 \\ H &= 0 \\ K &= 1 - \nu^2 \end{aligned} \right\} \quad (26)$$

The same buckling condition (24) obtains here, in which, consequently,

$$\left. \begin{aligned} \alpha_{1,2} &= \sqrt{\pm\lambda^2 + \lambda\sqrt{t\sigma_{cr}/N}} \\ q &= \alpha_1^2 - \nu\lambda^2 \\ r &= \alpha_2^2 + \nu\lambda^2 \\ \tau &= 2\lambda\sqrt{t\sigma_{cr}/N} \\ s_{1,2} &= \frac{\lambda^2}{N}(B_{1,2}\lambda^2 - A_{1,2}\sigma_{cr}) \\ N &= \frac{EI}{1 - \nu^2} \end{aligned} \right\} \quad (27)$$

while in equation (17)

$$\left. \begin{aligned} \alpha_{1,2}' &= \sqrt{\pm\lambda^2 + \lambda\sqrt{t'\sigma_{cr}/N'}} \\ q' &= (\alpha_1')^2 - \nu\lambda^2 \\ r' &= (\alpha_2')^2 + \nu\lambda^2 \\ N' &= \frac{EI'}{1 - \nu^2} \end{aligned} \right\} \quad (28)$$

For an I- or H-section where both flanges are alike  $\theta_1 = \theta_2 = \theta$  and  $s_1 = s_2 = s$  by which equation (24) transforms to

$$\begin{aligned}
& (\alpha_1^2 u^2 - \alpha_2^2 v^2 - \alpha_1^2 \alpha_2^2 \tau^2 + \theta^2 s^2 \tau^2) \sinh \alpha_1 b \sin \alpha_2 b - \\
& 2\alpha_1 \alpha_2 (w^2 - 2\theta s \tau^2) \cosh \alpha_1 b \cos \alpha_2 b + \\
& 2\alpha_2 \tau (\alpha_1^2 u - \theta s v) \sinh \alpha_1 b \cos \alpha_2 b + \\
& 2\alpha_1 \tau (\alpha_2^2 v + \theta s u) \cosh \alpha_1 b \sin \alpha_2 b + 2\alpha_1 \alpha_2 n^2 = 0
\end{aligned} \tag{29}$$

in which

$$\left. \begin{aligned}
u &= s - \theta r^2 \\
v &= s - \theta q^2 \\
n &= s + \theta q r
\end{aligned} \right\} \tag{30}$$

while  $\theta$  is given by  $\theta_t$  from equations (20) and (17).

If the deflections of the beams (the flanges) in their own plane are neglected, so that  $s = \infty$ , equation (29) reduces to (reference 3, pp. 59 and 63):

$$\alpha_1 \tanh(\alpha_1 b/2) + \alpha_2 \tan(\alpha_2 b/2) + \theta \tau = 0 \tag{31}$$

This condition applies for any symmetrical rotational restraint of the web. In reference 3 the pertinent expressions for  $\theta$  were derived for several cases. For I- or H-sections  $\theta$  is given by  $\theta_t$  from equations (20) and (17).

With relatively narrow and thin flanges, the rotational restraint exerted by the flanges on the web may be neglected, so that  $\theta = \infty$  and equation (29) transforms to

$$\begin{aligned}
& (\alpha_1^2 r^4 - \alpha_2^2 q^4 - s^2 \tau^2) \sinh \alpha_1 b \sin \alpha_2 b - 2\alpha_1 \alpha_2 q^2 r^2 (\cosh \alpha_1 b \cos \alpha_2 b - 1) + \\
& 2\alpha_2 q^2 s \tau \sinh \alpha_1 b \cos \alpha_2 b - 2\alpha_1 r^2 s \tau \cosh \alpha_1 b \sin \alpha_2 b = 0
\end{aligned} \tag{32}$$

For a T-section, where the web may be considered as the buckling plate, at the free edge of the web  $s_2 = 0$  and  $\theta_2 = \infty$ . Denoting  $s_1$

and  $\theta_1$ , which refer to the restrained edge, by  $s$  and  $\theta$ , equation (24) transforms to (reference 2, equation (34))

$$\begin{aligned} & (\alpha_1^2 r^2 u - \alpha_2^2 q^2 v) \sinh \alpha_1 b \sin \alpha_2 b - \alpha_1 \alpha_2 (q^2 u + r^2 v) \cosh \alpha_1 b \cos \alpha_2 b + \\ & \alpha_2 \tau (\alpha_1^2 r^2 - \theta s q^2) \sinh \alpha_1 b \cos \alpha_2 b + \\ & \alpha_1 \tau (\alpha_2^2 q^2 + \theta s r^2) \cosh \alpha_1 b \sin \alpha_2 b - 2\alpha_1 \alpha_2 q r n = 0 \end{aligned} \quad (33)$$

where  $\theta$  is given by equations (20) and (17).

For an angle with equal legs the legs may be assumed to transfer no bending moments  $M_y$  to each other, so that  $\theta = \infty$ . Consequently from equation (33) the buckling condition for each flange becomes (reference 7, equation (40)):

$$\begin{aligned} & (\alpha_1^2 r^4 - \alpha_2^2 q^4) \sinh \alpha_1 b \sin \alpha_2 b - 2\alpha_1 \alpha_2 q^2 r^2 (\cosh \alpha_1 b \cos \alpha_2 b - 1) + \\ & \alpha_2 q^2 s \tau \sinh \alpha_1 b \cos \alpha_2 b - \alpha_1 r^2 s \tau \cosh \alpha_1 b \sin \alpha_2 b = 0 \end{aligned} \quad (34)$$

In case of a T-stiffener or a column of a section as given by figure 6, at edge 1  $s_1 = \infty$  and  $\theta_1 = \infty$ , so that, denoting  $s_2$  and  $\theta_2$  at edge 2 as  $s$  and  $\theta$ , equation (24) transforms to

$$\begin{aligned} & \theta s \tau^2 + \alpha_1 \alpha_2 \tau^2 \coth \alpha_1 b \cot \alpha_2 b + \\ & \alpha_2 \tau (\theta q^2 - s) \cot \alpha_2 b - \alpha_1 \tau (\theta r^2 - s) \coth \alpha_1 b = 0 \end{aligned} \quad (35)$$

This case was completely worked out in reference 8, chapter 2.2. It was found that in case of a T-shaped steel sheet stiffener, which buckles at the yield stress, the interaction between the two modes of buckling, that is, torsional and local buckling, was negligible.

DERIVATION OF INTERACTION FORMULAS BY METHOD OF  
SPLIT RIGIDITIES

The method of split rigidities divides the elastic or elasto-plastic behavior of a composite structure into its component parts. After the individual buckling stresses for these component parts are calculated, an interaction formula, which combines the individual critical stresses, gives the actual critical stress of the composite structure.

This method was previously applied to the calculation of the critical stresses of built-up columns (references 8 and 9) and to flexural and torsional buckling of angles (references 7, 8, and 10) and open sections in general (reference 10) as well as to the calculation of critical stresses in sandwich plates (references 1 and 11). The application to sandwich plates was very extensively explained in reference 1. In its application to the interaction of column and local buckling the method has to be used in a more generalized form. If two or more modes of deformation are involved in the buckling process, such as column buckling on the one hand and plate buckling of the web on the other in the case of an I-section, these two types, denoted as cases (1) and (2), respectively, are first considered separately. While one type is considered, the rigidity against the deformation of the other type is assumed temporarily to be infinite.

In considering cases (1) or (2) separately, an equation may be established between the internal reactions and external actions. For case (1) above, for example, it is appropriate to compare the internal and external bending moments. In other cases, for example, case (2) above, it is convenient to establish an equation between the restraining and deflecting forces acting on a small element of the plate. In general for each case the most appropriate internal and external actions should be compared, which may, for other cases, differ from those mentioned above. For each separate case the external actions (bending moment, deflecting force, or otherwise) are directly proportional to the buckling stress for that case ( $\sigma_1$  or  $\sigma_2$  for cases (1) or (2), respectively) and to the deflection with buckling ( $w_1$  or  $w_2$ , respectively). Hence these external actions may be expressed in these values:  $\sigma_1, w_1$  or  $\sigma_2, w_2$ . Since during incipient buckling the internal actions are equal to the external ones, the former are also expressed in  $\sigma_1, w_1$  and  $\sigma_2, w_2$  for cases (1) and (2), respectively.

For the actual combined case, with buckling stress  $\sigma_{cr}$  and deflection  $w = w_1 + w_2$ , the deflections  $w_1$  and  $w_2$  are of form similar to those for the separate cases or are assumed to be so. Consequently the

internal actions caused by these deflections are assumed to be also equal to those for the separate cases. Hence the total internal action may be expressed in terms of  $\sigma_1$ ,  $\sigma_2$ ,  $w_1$ , and  $w_2$ .

On the other hand the total external action with actual combined buckling is proportional to the actual buckling stress  $\sigma_{cr}$  and may be expressed in terms of  $\sigma_{cr}$  and of a linear function of the deflections  $w_1$  and  $w_2$ . Writing down the equalities of internal and external actions, firstly for the particular actions considered in case (1) (in the chosen example the bending moments) and secondly for those considered in case (2) (here the restraining and deflecting forces acting on a small element) two homogeneous linear equations in  $w_1$  and  $w_2$  are obtained, from which the buckling condition is found by equating the denominator determinant of these equations to zero. Since this determinant contains  $\sigma_1$ ,  $\sigma_2$ , and  $\sigma_{cr}$  this gives a formula which expresses  $\sigma_{cr}$  in terms of the known individual buckling stresses  $\sigma_1$  and  $\sigma_2$ .

In order to show more directly how this method is applied, the explicit case of an I-section column will be considered first. In the section entitled "General Case of Columns with One or Two Planes of Symmetry" the general case of sections which are symmetrical with one or two axes will then be dealt with. In the sections entitled "Buckling of Tubes with Square Cross Section" and "Buckling of Columns with H-Shaped Cross Sections" cases of special sections, that is, tubes and H-sections which show some special features, are examined. It follows that for all these sections the interaction is in general negligible.

The interaction is important only if the web that is perpendicular to the direction of column buckling is simply supported or elastically restrained at one side and free at the other side, so that a combination of flexural and torsional buckling occurs. This case occurs with T-section columns and with angles. These sections are dealt with in the sections entitled "Buckling of Columns with T-Sections" and "Buckling of Angles with Equal Legs."

#### Buckling of I-Section Column in Direction Perpendicular

##### to Plane of Web

Derivation of interaction formula.- First an I-section with comparatively narrow and thin flanges is considered (fig. 7(a)) so that, when the web buckles, practically no rotational restraints are exerted on it by the flanges.

If the column buckles in a direction perpendicular to the plane of the web, its deformation may be split into two parts: (1) Buckling as a

column, without distortion of the cross section (fig. 7(b)) and (2) distortion of the cross section (fig. 7(c)).

If only case (1) occurs with buckling in a half wave of length  $a$  the buckling stress is

$$\sigma_1 = \frac{\pi^2 E_t}{(a/r)^2} \quad (36)$$

where  $E_t$  is the tangent modulus and  $r$  is the radius of gyration of the cross section. In the elastic range,  $E_t = E$ .

With a deformation according to case (2) alone, where, as stated above, the web is practically simply supported at the unloaded edges, for the same half wave length  $a$  the buckling stress would be (reference 3, equation (37) or reference 1, equation (34))

$$\sigma_2 = \frac{\pi^2 EI}{b^2 t} \left[ (A/\beta^2) + 2(B + 2F) + D\beta^2 \right] \quad (37)$$

or in the elastic domain

$$\sigma_2 = \frac{\pi^2 N}{b^2 t} \left( \frac{1}{\beta} + \beta \right)^2 \quad (38)$$

where

$$\beta = a/b \quad (39)$$

In order to obtain the interaction formula, an equation will first be derived which expresses the equality between the external moments and the internal moments in the cross sections of the column.

If only a deformation according to case (1) occurs, involving at an arbitrary point a deflection  $w_1$  (figs. 7(a) and 7(b)) it follows from the equality of internal and external moments denoted by  $M_i$  and  $M_e$ , respectively, that  $M_i = M_e$  or

$$M_{i1} = P_1 w_1 = A_c \sigma_1 w_1 \quad (40)$$

in which  $A_c$  is the cross-sectional area of the column. This equation holds in all cases where the deformation  $w_1$  has the shape of a sine wave, no matter whether it is produced by an actual critical load  $P_1$  or by some other agent which causes the member to deflect in this shape. This is so because the internal moment is merely a function of the curvature. For the case of sine-wave deflection this curvature is proportional to the deflection itself at all points, so that internal moments are given by equation (40), no matter what the cause of the sine-wave deflection.

This will also hold true for the plastic range, if  $P_1$  or  $\sigma_1$  are calculated from equation (36) by using the tangent modulus corresponding to the actual axial stress  $\sigma_{cr}$  in the column.

Assume now that a complete deformation according to figure 7(a) occurs by buckling with a half wave length  $a$ . Then by the deformation according to case (1) the internal moment is given by equation (40). By the deformation according to case (2) (fig. 7(a)) the deflection of the web will vary in the Y-direction according to a curve which may be approximated sufficiently accurately by a sine wave. (This would actually hold true for  $w_1 = 0$ .) Hence the average deflection of the web from case (2) is about  $(2/\pi)w_2$ . With concentric cylindrical buckling of the single web with a half wave length  $a$  the buckling stress for the elastic range would be

$$\begin{aligned}\sigma_{2c} &= \frac{\pi^2 N}{a^2 t} \\ &= \frac{\pi^2 N}{b^2 t} \frac{b^2}{a^2} \\ &= \frac{\pi^2 N}{b^2 t} \frac{1}{\beta^2}\end{aligned}\tag{41}$$

or from equation (38)

$$\begin{aligned}\sigma_{2c} &= \left[ \frac{1/\beta}{\left(\frac{1}{\beta}\right) + \beta} \right]^2 \sigma_2 \\ &= \frac{1}{(1 + \beta^2)^2} \sigma_2 \\ &= \eta \sigma_2\end{aligned}\tag{42}$$

Hence, in the same way as shown above, it follows from the equality of internal and external moments that, with a cylindrical deflection  $w_{2c}$ ,  $M_i = M_e$  or

$$\begin{aligned} M_i &= A_w \sigma_{2c} w_{2c} \\ &= A_w \eta \sigma_2 w_{2c} \end{aligned} \quad (43)$$

where  $A_w$  is the cross-sectional area of the web. Therefore the average deflection  $(2/\pi)w_2$  from case (2) causes an internal moment

$$M_{i2} = \frac{2}{\pi} A_w \eta \sigma_2 w_2 \quad (44)$$

Consequently with buckling according to figure 7(a) the total internal moment is, from equations (40) and (44)  $M_i = M_{i1} + M_{i2}$  or

$$M_i = A_c \left( \sigma_1 w_1 + \frac{2}{\pi} \frac{A_w}{A_c} \eta \sigma_2 w_2 \right) \quad (45)$$

From equation (42)

$$\eta = 1 / (1 + \beta^2)^2 \quad (46)$$

With the additional notation

$$\phi = \frac{2}{\pi} \frac{A_w}{A_c} \quad (47)$$

Equation (45) becomes

$$\begin{aligned} M_i &= M_{i1} + M_{i2} \\ &= A_c \left( \sigma_1 w_1 + \eta \phi \sigma_2 w_2 \right) \end{aligned} \quad (48)$$

If the actual critical stress is  $\sigma_{cr}$ , deflection  $w_1$  from case (1) causes an external moment  $M_{e1} = A_c \sigma_{cr} w_1$  while deflection  $w_2$  from case (2) causes an external moment  $M_{e2} = A_w \sigma_{cr} \frac{2}{\pi} w_2$ . Hence the total external moment is

$$\begin{aligned}
 M_e &= M_{e1} + M_{e2} \\
 &= A_c \sigma_{cr} w_1 + A_w \sigma_{cr} \frac{2}{\pi} w_2
 \end{aligned} \tag{49}$$

or, using equation (47),

$$M_e = A_c \sigma_{cr} (w_1 + \phi w_2) \tag{50}$$

Since  $M_e$  and  $M_1$  have to be equal, equations (48) and (50) yield, since  $A_c$  cancels,

$$\sigma_{cr} (w_1 + \phi w_2) = \sigma_1 w_1 + \eta \phi \sigma_2 w_2 \tag{51}$$

which gives one equation for finding the interaction formula. Another equation can be obtained by expressing the equality of the deflecting and restraining forces acting on a small element of the web.

If only a deformation according to case (2) occurs (fig. 7(c)), that is, if  $w_1$  in figure 7(a) were zero, the critical stress in the elastic domain is  $\sigma_2$  from equation (38). For the equilibrium shape of the middle plane in case (2) at an arbitrary point P of the plate the deflecting force acting on a small element  $t \, dx \, dy$  is  $D_2 = -t \sigma_2 \, dx \, dy (\partial^2 w / \partial x^2)$ .

Since for the same shape of the middle plane at that particular point P the second derivative  $\partial^2 w / \partial x^2$  is proportional to the maximum deflection  $w_2$  of the plate,  $D_2$  is proportional to  $\sigma_2$  and to  $w_2$  and hence it may be denoted by  $c \sigma_2 w_2$ . Here  $c$  is a proportionality factor which is a constant only for the given point P and for the same shape of the deflection surface, but is different for different points of the plate. Since the restraining force  $R_2$  acting on the element and caused by the transverse shear stresses is equal to the deflecting force  $D_2$  it follows from the equation

$$R_2 = D_2$$

that

$$R_2 = c \sigma_2 w_2 \tag{52}$$

In the elastic domain the restraining force depends only on the shape of the middle plane of the plate. In the plastic range the ratio

of internal moment to curvature depends on the modulus and thus on the magnitude of the average compressive stress. Hence equation (52) remains true in the plastic domain even if the compressive stress differs from  $\sigma_2$ , provided that in calculating  $\sigma_2$  from equation (37), values A, B, D, and F are calculated for the actual compressive stress  $\sigma_{cr}$ .

Considering again the actual deformation of the column during buckling according to figure 7(a), it follows that the deflection  $w_2$  from case (2) causes a restraining force  $R_2$  according to equation (52). The deflection  $w_1$  from case (1) causes a cylindrical bending of the web. If only this cylindrical bending occurs, the buckling stress of the web is equal to  $\sigma_{2c}$  from equation (42). In that case the average deflection force  $D_1$  acting on various elements of the web would be greater than  $c\sigma_{2c}w_1$  because the proportionality factor  $c$  for a given point P of the web, as stated above, applies to a shape of the deflection surface similar to that of  $w_2$  (fig. 7(a)). The influence of the deflecting forces is the greater the greater the distance of the elements on which they act is from the edges of the web. Hence their influence may be expressed fairly well by comparing it with that of continuously distributed loads (proportional to  $w_1$  or  $w_2$ ) on the bending moment in the middle of a simply supported beam with span  $b$ . For a uniform load  $q$  representing a distribution like  $w_1$ , in the middle ( $y = 0$  in fig. 7(a)) this bending moment is  $\frac{1}{8}qb^2$ . It is  $\frac{1}{\pi^2}qb^2$  for sinusoidal distribution like  $w_2$ . Therefore as an average the deflecting force  $D_1$  on an element in case only deflection  $w_1$  occurs may be expressed as  $D_1 = (\pi^2/8)c\sigma_{2c}w_1$ . With the notation

$$\gamma = \pi^2/8 \quad (53)$$

it follows then from the equality of restraining and deflecting forces, or  $R_1 = D_1$ , that

$$R_1 = c\gamma\sigma_{2c}w_1 \quad (54)$$

Consequently the total restraining force acting on an element of the web with buckling according to figure 7(a) is, from equations (52) and (54),  $R = R_2 + R_1$  or

$$R = c\sigma_2w_2 + c\gamma\sigma_{2c}w_1 \quad (55)$$

or, using equation (42),

$$R = c\sigma_2(w_2 + \eta\gamma w_1) \quad (56)$$

With the actual critical stress  $\sigma_{cr}$  deflection  $w_2$  causes a deflecting force  $c\sigma_{cr}w_2$  while deflection  $w_1$  causes a deflecting force  $c\gamma\sigma_{cr}w_1$ . Hence the total deflecting force is

$$D = c\sigma_{cr}(w_2 + \gamma w_1) \quad (57)$$

Equating this deflecting force to the restraining force from equation (56) yields, since  $c$  cancels,

$$\sigma_{cr}(w_2 + \gamma w_1) = \sigma_2(w_2 + \eta\gamma w_1) \quad (58)$$

Equations (51) and (58) are two equations with three unknowns,  $\sigma_{cr}$ ,  $w_1$ , and  $w_2$ . This is necessary and sufficient, since  $w_1$  and  $w_2$  have a common arbitrary factor, so that only the ratio  $w_2/w_1$  has to be known. Writing equations (51) and (58) as follows:

$$\left. \begin{aligned} (\sigma_1 - \sigma_{cr})w_1 - \phi(\sigma_{cr} - \eta\sigma_2)w_2 &= 0 \\ \gamma(\sigma_{cr} - \eta\sigma_2)w_1 - (\sigma_2 - \sigma_{cr})w_2 &= 0 \end{aligned} \right\} \quad (59)$$

the buckling condition is obtained by equating the denominator determinant of these equations to zero, yielding

$$\sigma_{cr} = \frac{1}{2(1 - \gamma\phi)} \left\{ \sigma_1 + (1 - 2\gamma\phi\eta)\sigma_2 - \sqrt{[\sigma_1 + (1 - 2\gamma\phi\eta)\sigma_2]^2 - 4(1 - \gamma\phi)(\sigma_1 - \gamma\phi\eta^2\sigma_2)\sigma_2} \right\} \quad (60)$$

in which, from equations (46), (47), and (53)

$$\eta = \frac{1}{(1 + \beta^2)^2} \quad (46)$$

$$\phi = \frac{2}{\pi} \frac{A_w}{A_c} \quad (47)$$

$$\gamma = \frac{\pi^2}{8} \quad (53)$$

so that

$$\gamma\phi = \frac{\pi}{4} \frac{A_w}{A_c} = 0.78 \frac{A_w}{A_c} \quad (61)$$

while  $\sigma_1$  and  $\sigma_2$  are given by equations (36) and (37) or (38).

Comparison with exact theory. - In order to check the accuracy of equation (60) its results will be compared with those of the exact calculation, according to which the buckling condition for this case is given by equation (32). It is given also, though in different notations, by equation (t), page 347 of reference 6. For several channel sections with narrow flanges figure 182, page 348, of the same reference gives values of  $\psi$  against the ratios  $a/b = \beta$ . With the notations of the present report

$$\psi = b \sqrt{\frac{t\sigma_{cr}}{N}} \quad (62)$$

A check of this graph shows, however, that the moment of inertia of the supporting beams, the flanges, with a width  $d$  and a thickness  $t$ , has been erroneously assumed for these channels to be equal to  $\frac{1}{12} td^3$  instead of to half of that of the entire cross section with respect to the axis of inertia parallel to the web. Hence the curves actually apply to I-section columns with flanges of width  $d$  rather than to channels. The curves for  $d = 4$  inches and  $d = 2$  inches are reproduced here in figure 8, where also the pertinent cross section is given. The Euler curves for the same I-sections, plotting  $\sigma_1$  according to equation (36) with  $E_t = E$ , are given in figure 8 by the dashed curves. All curves refer to the elastic range.

Although the web width  $b$  should theoretically be measured between the middle planes of the flanges by which it is supported, for a correct comparison it will be measured here between the inner faces of the flanges, as was done in the exact calculation in reference 6. According to equations (36) and (38), with  $E_t = E$  and for a flange width  $d = 4$ ", a web width  $b = 15 \frac{3}{4}$ ", a plate thickness  $t = 5/16$ ", and Poisson's ratio  $\nu = 1/4$ .

$$\sigma_1/E = 4.50/a^2 \quad (63)$$

$$\sigma_2/E = 0.000345 \left( \beta + \frac{1}{\beta} \right)^2 \quad (64)$$

while from equation (61)

$$\gamma\phi = 0.52 \quad (65)$$

For several ratios  $\beta = a/b$  values of  $\eta$ ,  $\sigma_1/E$ , and  $\sigma_2/E$  have been calculated from equations (46), (63), and (64), respectively. Hence  $\sigma_{cr}/E$  is computed from the approximate interaction equation (60). The results for  $d = 4$  inches are given in the table below. Corresponding approximate values  $\psi$  from equation (62) have been computed and inserted in the table as  $\psi_{cr}$ . These values have to be compared with the exact values  $\psi_{ex}$  according to figure 182 of reference 6 or figure 8 of this report, which values are also given in the table.

d (in.)	$\beta = \frac{a}{b}$	$\eta$	$\sigma_1/E$	$\sigma_2/E$	$\sigma_{cr}/E$	$\psi_{cr}$	$\psi_{ex}$	Percent error
4	1	0.25	0.0181	0.00138	0.001338	6.20	6.20	0
	2	.04	.00452	.00215	.00166	6.90	6.90	0
	2.5	.019	.00289	.00290	.001706	6.99	7.00	-.14
	3	.01	.00201	.00383	.001522	6.60	6.70	-1.50
	3.5	(.0057)	.00148	.00495	.001246	5.98	6.05	-1.15
	6	(.0007)	.00050	.01312	.000469	3.67	3.72	-1.35

It follows that equation (60), derived by the method of split rigidities, is very accurate and deviates but slightly to the safe side.

For an I-section with  $d = 2$  inches, according to equations (36) and (38),

$$\sigma_1/E = 0.73/a^2 \quad (66)$$

$$\sigma_2/E = 0.000345 \left( \beta + \frac{1}{\beta} \right)^2 \quad (67)$$

while from equation (61)

$$\gamma\phi = 0.62 \quad (68)$$

For this cross section the pertinent values have been calculated in the same way and are given in the table below. Values of  $\psi_{ex}$  have been obtained from figure 182 of reference 6 or figure 8 of this report.

d (in.)	$\beta = \frac{a}{b}$	$\eta$	$\sigma_1/E$	$\sigma_2/E$	$\sigma_{cr}/E$	$\psi_{cr}$	$\psi_{ex}$	Percent error
2	1	0.25	0.00294	0.00138	0.001147	5.73	5.85	-2.2
	2	.04	.000735	.00215	.000611	4.18	4.08	2.5
	4	(.0035)	.000184	.00624	.000176	2.24	2.24	0

Here, too, the agreement between  $\psi_{cr}$  and  $\psi_{ex}$  is very satisfactory. In figure 8 values  $\psi_{cr}$  from equation (60) are given by circles showing the excellent agreement with the curves. The cross section of figure 8 is unusual, since the moment of inertia with respect to the minor axis is very low as compared with the cross-sectional area.

Simplified, more approximate interaction formula.- For normal I-sections or channels the values of  $\sigma_1$ ,  $\sigma_2$ , and  $\sigma_{cr}$ , if plotted against the ratio  $\beta = a/b$  of half wave length  $a$  to web width  $b$ , will vary as in figure 1. The buckling stress is governed by the horizontal line AB for ratios  $\beta$  between  $\beta_1$  and  $\beta_2$  and by the curve for  $\sigma_{cr}$  for about  $\beta > \beta_2$ . At A, for  $\beta = \beta_1$ ,  $\sigma_1$  is very high as compared with  $\sigma_2$ . For  $\beta \geq \beta_2$ , on the other hand,  $\sigma_2$  is very high with regard to  $\sigma_1$ . Equation (60) may be written as

$$\sigma_{cr} = \frac{\sigma_1 + (1 - 2\gamma\phi\eta)\sigma_2}{2(1 - \gamma\phi)} \left\{ 1 - \sqrt{1 - \frac{4(1 - \gamma\phi)(\sigma_1 - \gamma\phi\eta^2\sigma_2)\sigma_2}{[\sigma_1 + (1 - 2\gamma\phi\eta)\sigma_2]^2}} \right\} \quad (69)$$

If now  $\sigma_1$  is much higher than  $\sigma_2$ , such as is the case for  $\beta = \beta_1$ , the last term under the radical is very much smaller than unity. Denoting this term by  $\epsilon$ , the term in the braces can be written as follows:

$$\begin{aligned} 1 - \sqrt{1 - \epsilon} &= 1 - \left( 1 - \frac{1}{2} \epsilon - \frac{1}{8} \epsilon^2 - \dots \right) \\ &= \frac{1}{2} \epsilon \left( 1 + \frac{1}{4} \epsilon + \dots \right) \end{aligned} \quad (70)$$

in which

$$\epsilon = \frac{4(1 - \gamma\phi)(\sigma_1 - \gamma\phi\eta^2\sigma_2)\sigma_2}{[\sigma_1 + (1 - 2\gamma\phi\eta)\sigma_2]^2} \quad (71)$$

From the derivation of equation (69) it follows that conservative values for  $\sigma_{cr}$  are obtained if  $\eta$  is equated to zero, so that from equation (71)

$$\epsilon \approx \frac{4(1 - \gamma\phi)\sigma_1\sigma_2}{(\sigma_1 + \sigma_2)^2} \quad (72)$$

Hence from equations (69), (70), and (72)

$$\sigma_{cr} \approx \frac{\sigma_2}{\sigma_1 + \sigma_2} \left[ \sigma_1 + \frac{(1 - \gamma\phi)\sigma_1^2\sigma_2}{(\sigma_1 + \sigma_2)^2} \right] \quad (73)$$

Since  $\sigma_1 \gg \sigma_2$ , in the last term in the brackets  $\sigma_1^2/(\sigma_1 + \sigma_2)^2$  may be equated to unity, so that equation (73) reduces to

$$\begin{aligned} \sigma_{cr} &\approx \left( 1 - \gamma\phi \frac{\sigma_2}{\sigma_1 + \sigma_2} \right) \sigma_2 \\ &= \frac{\sigma_1 + (1 - \gamma\phi)\sigma_2}{\sigma_1 + \sigma_2} \sigma_2 \end{aligned} \quad (74)$$

In the same way at  $\beta \geq \beta_2$ , where as a rule  $\sigma_2 \gg \sigma_1$ , it is found that

$$\begin{aligned} \sigma_{cr} &\approx \left( 1 - \gamma\phi \frac{\sigma_1}{\sigma_1 + \sigma_2} \right) \sigma_1 \\ &= \frac{\sigma_2 + (1 - \gamma\phi)\sigma_1}{\sigma_2 + \sigma_1} \sigma_1 \end{aligned} \quad (75)$$

Since  $\gamma\phi$  is always smaller than unity, this yields for  $\beta = \beta_1$  as well as for  $\beta \geq \beta_2$  the conservative values

$$\begin{aligned}\sigma_{cr} &= \frac{\sigma_1 \sigma_2}{\sigma_1 + \sigma_2} \\ &= \left( \sigma_1^{-1} + \sigma_2^{-1} \right)^{-1}\end{aligned}\quad (76)$$

Criterion for range of negligible interaction. - From equation (74) for  $\beta = \beta_1$  the decrease of  $\sigma_{cr}$  with respect to  $\sigma_2$  due to interaction is

$$\begin{aligned}(\Delta\sigma)_2 &= \sigma_2 - \sigma_{cr} \\ &= \frac{\gamma\phi\sigma_2}{\sigma_1 + \sigma_2} \sigma_2\end{aligned}\quad (77)$$

From equation (75) for  $\beta = \beta_2$  the decrease of  $\sigma_{cr}$  with respect to  $\sigma_1$  is

$$\begin{aligned}(\Delta\sigma)_1 &= \sigma_1 - \sigma_{cr} \\ &= \frac{\gamma\phi\sigma_1}{\sigma_2 + \sigma_1} \sigma_1\end{aligned}\quad (78)$$

At  $\beta = \beta_1$  value  $\sigma_2$  is equal to  $\sigma_1$  for  $\beta = \beta_2$  (fig. 1), so that from equation (77)

$$(\Delta\sigma)_2 = \frac{\gamma\phi(\sigma_1)_{\beta=\beta_2}}{(\sigma_1)_{\beta=\beta_1} + (\sigma_1)_{\beta=\beta_2}} \sigma_2\quad (79)$$

From equation (36), since  $\beta = a/b$

$$(\sigma_1)_{\beta=\beta_1} = \left( \frac{\beta_2}{\beta_1} \right)^2 (\sigma_1)_{\beta=\beta_2}\quad (80)$$

It should be noted that this equation, as well as equation (36), neglects the influence of shear deformations, as is customary. However, for such small buckling lengths as considered here (for  $\beta = \beta_1$  the buckling length  $a \approx b$ ) the shear deformations may substantially decrease the buckling stress  $\sigma_1$ . It was shown in an unpublished paper that this does not influence the resulting governing interaction as expressed in equation (93). From equations (79) and (80)

$$(\Delta\sigma)_2 = \frac{\gamma\phi}{(\beta_2/\beta_1)^2 + 1} \sigma_2 \quad (81)$$

On the other hand, at  $\beta = \beta_2$  the value  $\sigma_1$  is equal to  $\sigma_2$  for  $\beta = \beta_1$  (fig. 1), so that from equation (78)

$$(\Delta\sigma)_1 = \frac{\gamma\phi(\sigma_2)_{\beta=\beta_1}}{(\sigma_2)_{\beta=\beta_2} + (\sigma_2)_{\beta=\beta_1}} \sigma_1 \quad (82)$$

From equation (38)

$$(\sigma_2)_{\beta=\beta_2} = \left[ \frac{(1/\beta_2) + \beta_2}{(1/\beta_1) + \beta_1} \right]^2 (\sigma_2)_{\beta=\beta_1} \quad (83)$$

so that from equation (82)

$$(\Delta\sigma)_1 = \frac{\gamma\phi}{\left[ \frac{(1/\beta_2) + \beta_2}{(1/\beta_1) + \beta_1} \right]^2 + 1} \sigma_1 \quad (84)$$

The stress  $\sigma_2$  from equation (38) is minimum for  $\beta = \beta_1 = 1$ . Assuming, for an example, the rather low ratio  $\beta_2/\beta_1 = 10$ , so that  $\beta_2 = 10$ , and using equation (61), equation (81) for  $\beta = \beta_1$  yields

$$\begin{aligned} (\Delta\sigma)_2 &= \frac{0.78A_w/A_c}{101} \sigma_2 \\ &= 0.0077 \frac{A_w}{A_c} \sigma_2 \end{aligned} \quad (85)$$

Equation (84), for  $\beta = \beta_2$ , gives

$$\begin{aligned} (\Delta\sigma)_1 &= \frac{0.78A_w/A_c}{26.5} \sigma_1 \\ &= 0.030 \frac{A_w}{A_c} \sigma_1 \end{aligned} \quad (86)$$

With  $A_w/A_c = 1/3$  or  $2/3$ , equations (85) and (86) give decreases  $(\Delta\sigma)_2$  and  $(\Delta\sigma)_1$  of  $0.0026\sigma_2$  or  $0.0052\sigma_2$  and  $0.01\sigma_1$  or  $0.02\sigma_1$ , respectively, and thus maximums of 1/2 and 2 percent, respectively. From equations (81) and (84) the interaction is the smaller the greater the ratio  $\beta_2/\beta_1$ , so that for  $\beta_2/\beta_1 \geq 10$  it is negligible. In the elastic range  $\beta_2$  is determined by the condition (fig. 1):

$$(\sigma_1)_{\beta=\beta_2} = (\sigma_2)_{\beta=\beta_1} \quad (87)$$

From equation (38), since  $\sigma_2$  is minimum for  $\beta = \beta_1 = 1$ , with  $\nu = 0.3$

$$\begin{aligned} (\sigma_2)_{\beta=\beta_1} &= 4 \frac{\pi^2 N}{b^2 t} \\ &= 3.62E \left(\frac{t}{b}\right)^2 \end{aligned} \quad (88)$$

so that from equations (87) and (36)

$$\left(\frac{\pi^2 E}{(a/r)^2}\right)_{\beta=\beta_2} = 3.62E \left(\frac{t}{b}\right)^2 \quad (89)$$

or

$$(a/r)_{\beta=\beta_2} = 1.65b/t \quad (90)$$

or

$$\begin{aligned}
 \beta_2/\beta_1 &= \beta_2 \\
 &= (a/b)_{\beta=\beta_2} \\
 &= 1.65r/t
 \end{aligned}
 \tag{91}$$

Hence, since for  $\beta_2/\beta_1 \geq 10$  the interaction is negligible, it is also negligible for

$$r/t > \frac{10}{1.65} > 6 \tag{92}$$

Approximate formula for maximum amount of interaction.- If  $\beta_2/\beta_1$  is of the order of magnitude of 10, it is seen from equations (81) and (84) that for other ratios  $\beta_2/\beta_1$  than 10 the discrepancies  $(\Delta\sigma)_2$  and  $(\Delta\sigma)_1$  will vary practically proportionally to  $(\beta_1/\beta_2)^2$  or, from equation (91), to  $(t/r)^2$ . From equations (85), (86), and (92) for  $\beta_2/\beta_1 = 10$  or  $r/t = 6$  the governing discrepancy  $\Delta\sigma$  is  $3(A_w/A_c)$  percent. Hence in general the maximum decrease of  $\sigma_1$  or  $\sigma_2$  by interaction will be

$$(\Delta\sigma)_i \approx 3 \frac{A_w}{A_c} \left( \frac{6}{r/t} \right)^2 \text{ percent} \tag{93}$$

It was assumed above that the rotational restraints offered by the flanges to the web could be neglected. It may be shown, however, that equation (93) remains valid if the web is substantially rotationally restrained. From the derivation of equations (51) and (58) it is evident that these equations and hence the resulting buckling condition (60) and its further elaboration apply for that case as well. Only  $\phi$ ,  $\gamma$ , and  $\eta$  change in value in that case. But even equation (61) for  $\gamma\phi$  remains practically the same. Indeed, the restraints cause a decrease of  $\phi$  but an increase of  $\gamma$ , so that a calculation shows  $\gamma\phi$  to be practically independent of the rotational restraints. Even for negative restraints (see the section entitled "Buckling of Columns with H-Shaped Cross Section") and also for the quite different case of the web of a T-section (see section entitled "Buckling of Columns with H-Shaped Cross Section")  $\gamma\phi$  from equations (118) and (176) is  $0.8A_w/A_c$  and  $0.75A_w/A_c$ , respectively, and thus practically equal to  $\gamma\phi = 0.78A_w/A_c$  from equation (61). In calculating the individual buckling stress  $\sigma_2$  of the webs the

restraints at their unloaded edges have, of course, to be taken into account. In this case  $\eta$  will have a value different from that of equation (46). However,  $\eta$  may always sufficiently accurately be equated to zero, as was done from equation (72) on.

Finally equation (93) is based on equations (86) and (92). To see whether equation (92) remains valid for rotationally restrained web edges the most extreme case of built-in web will be considered. For this case (reference 6) the minimum value of  $\sigma_2$  is

$$\begin{aligned} (\sigma_2)_{\beta=\beta_1} &= 7 \frac{\pi^2 N}{b^2 t} \\ &= 6.32E \left(\frac{t}{b}\right)^2 \end{aligned}$$

and occurs for  $a/b = \beta_1 = 0.7$ . Hence now, instead of equation (89)

$$\left[ \frac{\pi^2 E}{(a/r)^2} \right]_{\beta=\beta_2} = 6.32E \left(\frac{t}{b}\right)^2 \quad (94)$$

or

$$(a/r)_{\beta=\beta_2} = 1.25b/t$$

or

$$\beta_2 = (a/b)_{\beta=\beta_2} = 1.25r/t \quad (95)$$

With  $r/t = 6$  equation (95) yields  $\beta_2 = 7.5$ , so that  $\beta_2/\beta_1 = 7.5/0.7 = 10.7$ , and hence it is but slightly higher than  $\beta_2/\beta_1 = 10$  for  $r/t = 6$  and simply supported web edges.

Furthermore, for a given ratio  $\beta_2/\beta_1$ ,  $(\Delta\sigma)_2/\sigma_2$  from equations (79) and (36) is independent of the rotational restraints of the web. On the other hand  $(\Delta\sigma)_1/\sigma_1$  from equation (82) will decrease with increasing restraint. From reference 12 for fully clamped edges

$$\sigma_2 = \left[ \frac{1}{\beta^2} + 2.5 + 5\beta^2 \right] \frac{\pi^2 N}{b^2 t} \quad (96)$$

Hence for  $r/t = 6$ ,  $\beta_2 = 7.5$  and  $\beta_1 = 0.7$ , and, using equation (61), equation (82) yields

$$(\Delta\sigma)_1 = \frac{0.78A_w/A_c}{41.6} = 0.019 \frac{A_w}{A_c} \sigma_1 \quad (97)$$

Consequently from equations (86) and (97) for  $r/t = 6$  the governing discrepancy  $\Delta\sigma = (\Delta\sigma)_1$  for varying amounts of web restraint will vary between  $3(A_w/A_c)$  percent and  $1.9(A_w/A_c)$  percent, so that for any positive rotation restraints equation (93) yields safe results. Apparently with negative web restraints, such as occur in H-sections, for  $r/t = 6$ ,  $\Delta\sigma$  may be larger than  $3(A_w/A_c)$  percent, so that equation (93) errs on the low side. This will also become apparent from the section entitled "Buckling of Columns with H-Shaped Cross Section."

If  $\sigma_{cr}$  is in the plastic range, for simply supported web edges from equations (87), (36), and (37) one has, instead of equation (89),

$$\left[ \frac{\pi^2 E_t}{(a/r)^2} \right]_{\beta=\beta_2} = 3.62 \bar{\eta} E \left( \frac{t}{b} \right)^2$$

or, instead of equation (91),

$$\beta_2 = 1.65 \frac{E_t}{\bar{\eta} E} \frac{r}{t} \quad (98)$$

Here  $E_t$  is the tangent modulus and  $\bar{\eta}$  is the reduction coefficient for plastic plate buckling (references 3 and 4), both referring to the actual buckling stress  $\sigma_{cr}$ . Since  $E_t/E$  is smaller than  $\bar{\eta}$ , for equal ratios  $r/t$  the value of  $\beta_2$  is smaller than in the elastic range. However,  $\beta_1$  is likewise smaller than its value  $\beta_1 = 1$  in the elastic domain (reference 3). Nevertheless,  $\beta_2/\beta_1$  may be somewhat smaller than in the elastic domain.

Equations (79) and (82) apply also to the plastic domain, where  $\sigma_1$  and  $\sigma_2$  are given by equations (36) and (37), respectively. Equations (80) and (81) also remain valid so that for the same ratio  $\beta_2/\beta_1$  the ratio  $(\Delta\sigma)_2/\sigma_2$  for  $\beta = \beta_1$  is the same as in the elastic domain.

Because in equation (37) factors  $(B + 2F)$  and  $D$  are always higher than factor  $A$ , the ratio between the values of  $\sigma_2$  for  $\beta = \beta_2$  and  $\beta = \beta_1$ , for the same ratio  $\beta_2/\beta_1$ , is even higher than that expressed by equation (83) for the elastic domain. Hence for equal ratio  $\beta_2/\beta_1$  the ratio  $(\Delta\sigma)_1/\sigma_1$  from equation (82) is still smaller than in the elastic domain.

Moreover all discrepancies between  $\sigma_{cr}$  and  $\sigma_1$  or  $\sigma_2$  are greatly reduced in the plastic range because with decreasing  $\sigma_{cr}$  the pertinent plastic values  $E_t$ ,  $A$ ,  $B$ ,  $D$ , and  $F$  increase. This may reduce  $(\Delta\sigma)_i$  from equation (93) many times, in the same way as a relative difference in elastic buckling stress may be reduced many times in the plastic range. For steel columns or plates of which the buckling stress is, for example, at the yield stress (in the sense that the tangent modulus is zero) an increase in the elastic buckling stress by 100 percent will result in no increase in the actual plastic buckling stress.

Therefore in the plastic domain equation (93) will yield safe values for  $(\Delta\sigma)_i$ .

#### General Case of Columns with One or Two Planes of Symmetry

From the preceding derivations for columns with an I-section it is evident that it makes no difference whether the symmetrical support of the web is effected by symmetrical flanges or otherwise. Therefore formula (93) applies in general for any column of which the pertinent web is symmetrically supported and positively rotationally restrained at both unloaded edges and which buckles in the plane of symmetry and in a direction perpendicular to that web. Examples are columns with an I-section, channels, and box sections. In the latter case (fig. 9), which will be dealt with more extensively in the section entitled "Buckling of Tubes with Square Cross Section" in the case of buckling in the mode of figure 10,  $A_w$  refers to the joint cross section of the two horizontal webs, which buckle individually in the same direction as the entire column.

Moreover, from the derivation of the interaction formulas (74), (75), and (76) it follows that they apply as well for columns which buckle in the plane of the web, and which are symmetrical with respect to that web. Examples of this kind are H- and T-sections. The plate buckling stress  $\sigma_2$  in the above-mentioned formulas refers here to the buckling stress of a plate which is clamped at one unloaded side and free at the other. For this case  $\gamma\phi$  follows from equations (157), (160), (166), (167), and (175) and is equal to  $0.69A_f/A_c$  where  $A_f$  is

the total cross section of the flanges. For these cases too the interaction between column and plate buckling is generally negligible.

The interaction is important only if the pertinent web, that is, that perpendicular to the direction of column buckling, is elastically restrained at one side and free at the other, so that a combination of flexural and torsional buckling occurs. This case is dealt with in the section entitled "Buckling of Columns with T-Section."

#### Buckling of Tubes with Square Cross Section

In the square tube the four plates act as if they are simply supported at the unloaded sides, so that their buckling stress in the elastic domain, from equations (38) and (88), is

$$\sigma_2 = 4 \frac{\pi^2 N}{b^2 t} = 3.62E \left( \frac{t}{b} \right)^2 \quad (88)$$

In this case condition (92) is certainly satisfied so that the interaction will be very small. However, in connection with the tests on these sections reported later herein, they will be studied in some more detail.

The following two cases will be discussed separately: (a) The plates buckle at about  $\sigma_2$ . One has then to investigate whether such plate buckling induces column deflections and consequent interaction. (b) The member buckles by column deflection at about  $\sigma_1$ , that is, at  $\beta \geq \beta_2$  in figure 1. In this case one has to investigate whether such column buckling induces plate deflections and, if so, what their effect is on interaction.

(a) The plates buckle symmetrically with respect to the vertical and horizontal axes of inertia of the tube (fig. 11), so that the total equivalent load  $p_y$  which they transfer to the column as a whole is zero, in the vertical as well as in the horizontal direction. Hence no bending of the column as a whole is induced by local buckling of the plates. It is as if the column were infinitely rigid against bending, so that in figure 1 at  $\beta = \beta_1 = 1$  the situation is the same as if  $\sigma_1$  were infinite. Hence at  $\beta = \beta_1$  in figure 1  $\sigma_{cr}$  is not smaller than  $\sigma_2$  so that

$$\sigma_{cr} = \sigma_2 = 3.62E \left( \frac{t}{b} \right)^2 \quad (99)$$

and no interaction occurs. (Of course, a very slight deflection of the unloaded edges of, for example, the horizontal plates occurs because the vertical plates in figure 11 will compress very slightly in the transverse (vertical) direction by the loads transferred to them by the buckling (horizontal) plates, but the resulting deformations may be neglected.)

At  $\beta = \beta_2$  (fig. 1) likewise the buckling stress  $\sigma_1$  of the column is not diminished by a buckling of the cross section according to figure 11 because this does not change the position of the center of gravity of the cross section. Hence it does not cause an extra external moment. Neither does it cause a change of the internal moment. Consequently it does not affect the buckling stress of the column, so that at  $\beta = \beta_2$

$$\sigma_{cr} = \sigma_1 = \frac{\pi^2 E}{(a/r)^2} \quad (100)$$

and no interaction occurs.

Interaction may occur, though, with buckling of the webs according to figure 12. Here, however,  $\sigma_2$  is much higher than according to equation (88). The plate buckling stress in this case is the same as for a section according to figure 12 with  $b' = b/2$ . The buckling stress for this case was calculated (reference 3) from equation (31), where, as was derived in reference 3

$$\theta = \theta_a = \left(\frac{t}{t'}\right)^3 \frac{\alpha_1' \coth \alpha_1' b' - \alpha_2' \cot \alpha_2' b'}{(\alpha_1')^2 + (\alpha_2')^2}$$

and  $\alpha_1'$  and  $\alpha_2'$  are given by equation (11) above. The ratio  $b/t$  at which the horizontal plate buckles at a given stress is expressed in terms of those ratios  $(b/t)_{FF}$  and  $(b/t)_{SS}$  at which plates with both sides fixed or both sides simply supported, respectively, would buckle at the same stress. This relation is expressed in reference 3 by equation (62)

$$\frac{b}{t} = \left(\frac{b}{t}\right)_{FF} - \left[ \left(\frac{b}{t}\right)_{FF} - \left(\frac{b}{t}\right)_{SS} \right] \gamma_1 \quad (101)$$

where  $\gamma_1$  for several ratios  $\mu = \frac{tb'}{t'b}$  is given in figure 13 of that reference. It follows from equation (88) that

$$\left(\frac{b}{t}\right)_{SS} = \sqrt{3.62 \frac{E}{\sigma_2}} = 1.90 \sqrt{\frac{E}{\sigma_2}} \quad (102)$$

For a plate with both unloaded sides fixed from equation (94)

$$\left(\frac{b}{t}\right)_{FF} = \sqrt{6.32 \frac{E}{\sigma_2}} = 2.52 \sqrt{\frac{E}{\sigma_2}} \quad (103)$$

Hence from equation (101)

$$\frac{b}{t} = (2.52 - 0.62\gamma_1) \sqrt{\frac{E}{\sigma_2}} \quad (104)$$

or

$$\sigma_2 = (2.52 - 0.62\gamma_1)^2 E \left(\frac{t}{b}\right)^2 \quad (105)$$

For the section of figure 12, with  $t' = t$  and  $b' = b/2$ ,  $\mu = tb'/t'b = 0.5$ , whence from figure 13 of reference 3 one finds  $\gamma_1 = 0.52$ . Thus equation (105) yields

$$\sigma_2 = 4.84E \left(\frac{t}{b}\right)^2 \quad (106)$$

Since the factor  $\gamma_1$  for the horizontal plate in figure 12 is about midway between those for simply supported ( $\gamma_1 = 1$ ) and for fully clamped plates ( $\gamma_1 = 0$ ), the optimum half wave length will be about the same as for a plate with one side clamped and the other simply supported, namely,  $0.80b$ . Hence here  $\beta_1$  in figure 1 is  $0.80$ .

For a square tube (fig. 9) the moment of inertia and the cross-sectional area are  $I = \frac{1}{12}(B^4 - A^4)$  and  $A_c = B^2 - A^2$ , respectively, so that the radius of inertia is

$$r = \sqrt{\frac{1}{12} \frac{B^4 - A^4}{B^2 - A^2}} = \sqrt{\frac{B^2 + A^2}{12}} \quad (107)$$

To take an example, with  $B = 2.5$  inches and  $t = 0.062$  inch,  $A = 2.376$  inches and  $r^2 = 0.991$  square inch. With  $a = 0.80b = 0.80(B - t) = 0.80 \times 2.438$  inches = 1.952 inches, equation (36) yields

$$\sigma_1 = \frac{\pi^2}{(1.952)^2/0.991} E = 2.56E$$

While from equation (106)

$$\sigma_2 = 4.84 \left( \frac{0.062}{2.438} \right)^2 E = 0.00314E$$

Since equations (74) and (76) from the section entitled "Buckling of I-Section in Direction Perpendicular to Plane of Web" apply in the present case, from the more conservative equation (76) at  $\beta = \beta_1$

$$\sigma_{cr} = \frac{2.56}{2.563} 0.00314E = 0.003136E \quad (108)$$

It is apparent that the interaction is negligible even for the mode of figure 12. Moreover, since for the mode of figure 11  $\sigma_{cr}$  from equation (99) is smaller than for that of figure 12, buckling according to figure 12 will not occur in the first place and  $\sigma_{cr}$  is given by equation (99), resulting in

$$\sigma_{cr} = 3.62 \left( \frac{0.062}{2.438} \right)^2 E = 0.00235E \quad (109)$$

(b) With buckling as a column at  $\beta = \beta_2$  the deflection  $w_1$  of the column causes deflective forces  $-t\sigma\partial^2w/\partial x^2$  (fig. 10) which cause a similar deformation of the cross section as in figure 12. For an equally distributed vertical load  $q$  on the horizontal plates of figure 10 the moments  $M$  in the corners  $C$  follow from the equation

$$\frac{qb^3}{24N} = \frac{Mb}{2N} + \frac{Mb'}{3N} = \frac{2}{3} \frac{Mb}{N}$$

yielding

$$M = \frac{1}{16} qb^2$$

or 3/4 times the clamping moments for a fully clamped plate. Hence a conservative value for the buckling stress is obtained by using the average of a simply supported and a fully clamped plate. Thus from equations (38) and (96)

$$\sigma_2 = \left[ \left( 1/\beta^2 \right) + 2.25 + 3\beta^2 \right] \frac{\pi^2 N}{b^2 t} \quad (110)$$

At  $\beta = \beta_2$  the value of  $\sigma_1$  is equal to  $\sigma_2$  for  $\beta = \beta_1$  so that from equations (88), (89), and (90)

$$\frac{a}{r} = 1.65 \frac{b}{t}$$

and

$$\beta = a/b = 1.65 \frac{r}{t} \quad (111)$$

As  $A = b - t$  and  $B = b + t$ , from equation (107), since  $t/b$  is small,  $r = 0.41b$ , so that from equation (111)

$$\beta_2 = 0.678 \frac{b}{t} \quad (112)$$

or with the dimensions given above

$$\beta_2 = 0.678 \frac{2.438}{0.062} = 26.6$$

Hence from equation (110), for  $\beta = \beta_2$

$$\sigma_2 = 2129.25 \frac{\pi^2}{2.438^2 \times 0.062} N = 1.244E$$

In figure 1 at  $\beta = \beta_2$ , from equations (88) and (109)

$$\sigma_1 = (\sigma_2)_{\beta=\beta_1} = 0.00235E$$

so that from equation (76) a conservative value for  $\sigma_{cr}$  at  $\beta = \beta_2$  is

$$\sigma_{cr} = \frac{1.244}{1.24635} 0.00235E = 0.002346E$$

Hence the effect of interaction is here less than 0.2 percent. According to the more accurate equation (75), since  $\gamma\phi$  is here about  $0.75A_w/A_c = 0.75 \times 0.5 = 0.38$

$$\sigma_{cr} = \frac{1.24545}{1.24635} 0.00235E = 0.002348E$$

Hence the more accurate effect of the interaction is only 0.1 percent.

The approximate formula (93) yields an effect of

$$\frac{3}{2} \left( \frac{6}{0.41b/t} \right)^2 \text{ percent} = \frac{3}{2} \left( \frac{6}{1/0.062} \right)^2 \text{ percent} = 0.2 \text{ percent}$$

This formula gives values which are too high because the mode which yields the minimum value  $\sigma_2$ , that is, plate buckling according to figure 11, does not govern the interaction in this case of buckling according to figure 10.

Thus for concentric buckling the effect of the interaction between column and local buckling in square tubes may be neglected.

#### Buckling of Columns with H-Shaped Cross Section

Somewhat more-pronounced interaction between column and plate buckling may occur in H-sections where the width of the flanges is such that they are rotationally restrained from buckling by the web (fig. 13). In that case the optimum half wave length of buckling will be larger than the width  $b$  of the web, so that in figure 1  $\beta_1 > 1$ . Thus the ratio  $\beta_2/\beta_1$  on which the interaction depends may be smaller here than if the web were simply supported or elastically rotationally restrained by the flanges and therefore more interaction may occur.

Let the H-section have the dimensions given in figure 13, so that  $b = A - t = 2.875$  inches,  $b' = 0.5B = 2.3125$  inches, and  $t = 1/8$  inch. The buckling condition is given by equation (29), but it may more easily be obtained by using equations (74) and (75), which, according to the section entitled "Buckling of I-Section Column in Direction Perpendicular to Plane of Web," apply here.

The plate buckling stress  $\sigma_2$  follows from reference 13 from the condition

$$\Sigma S = S^{IV} + 2S^{III} = 0$$

which, using the pertinent tables (reference 14), is satisfied for a minimum stress

$$\sigma_2 = 0.002008E = 21,500 \text{ psi} \quad (113)$$

for a half wave length  $a = 2b = 5.75$  inches. Thus here  $\beta_1 = 2$  (fig. 1). The radius of gyration of this section with respect to the middle plane of the web (fig. 13) is given by

$$r^2 = \frac{I}{A_c} = \frac{\frac{1}{6} tB^3 + \frac{1}{12} At^3 - \frac{1}{6} t^4}{(2B + A - 2t)t} \approx \frac{1}{6} \frac{B^3}{2B + A - 2t}$$

or numerically  $r^2 = 1.375$  square inches, so that  $\frac{a^2}{r^2} = \frac{(5.75)^2}{1.375} = 24$ . Hence from equation (36), with  $E_t = E$ , at  $\beta = \beta_1$  (fig. 1)

$$\sigma_1 = \frac{\pi^2 E}{(a/r)^2} = 0.411E \quad (114)$$

The same value  $\gamma\phi$  as found in equation (61) for the case of figure 7 will approximately apply here, so that

$$\gamma\phi \approx 0.78 \frac{A - t}{2B + A - 2t} = 0.185$$

Hence equation (74) yields

$$\begin{aligned} \sigma_{cr} &= \frac{0.411 + 0.815 \times 0.002}{0.413} \sigma_2 \\ &= \frac{0.41263}{0.413} 0.002008E \\ &= 0.002006E \end{aligned} \quad (115)$$

so that at  $\beta = \beta_1$  the interaction is negligible.

At  $\beta = \beta_2$

$$\sigma_1 = \frac{\pi^2 E}{(a/r)^2} = (\sigma_2)_{\beta=\beta_1} = 0.002008E \quad (116)$$

so that, with  $r^2 = 1.375$  square inches, from equation (116)

$$a = \sqrt{4920r^2} = 82.3 \text{ in.}$$

Hence

$$\beta_2 = \frac{a}{b} = \frac{82.3}{2.875} = 28.6$$

$$\beta_2' = \frac{a}{b'} = \frac{82.3}{2.3125} = 35.6$$

Since for these high  $\beta$  values tables are not available, the plate buckling stress  $\sigma_2$  for  $\beta = \beta_2$ , and hence for the case where the deflections of the beams are neglected, was calculated directly from the pertinent equation (31)

$$\alpha_1 \tanh(\alpha_1 b/2) + \alpha_2 \tan(\alpha_2 b/2) + \theta \tau = 0 \quad (31)$$

in which  $\theta$  is given by  $\theta_t$  from equations (20) and (17),

$$\theta = \frac{1}{2} \left( \frac{t}{t'} \right)^3 \frac{(\alpha_1'^2 r'^2 - \alpha_2'^2 q'^2) \sinh \alpha_1' b' \sin \alpha_2' b' - \alpha_1' \alpha_2' (q'^2 + r'^2) \cosh \alpha_1' b' \cos \alpha_2' b' - 2\alpha_1' \alpha_2' q' r'}{(\alpha_1'^2 + \alpha_2'^2) (\alpha_1' r'^2 \cosh \alpha_1' b' \sin \alpha_2' b' - \alpha_2' q'^2 \sinh \alpha_1' b' \cos \alpha_2' b')}$$

By trial and error it was found that equation (31) is satisfied for  $\sigma_2 = 0.0675E$ .

Moreover, this case may also be calculated by the method of split rigidities. This method yields a buckling stress of  $0.0665E$ . Assuming thus

$$\sigma_2 = 0.0675E \quad (117)$$

the actual critical stress can be calculated from equation (75). Since with the assumed large half wave length in the X-direction the web is bent approximately according to a parabola by the moments  $M_y$  exerted on it by the more unstable flanges, it follows from the derivation of equations (47) and (53) that here

$$\phi = \frac{2}{3} A_w/A_c = 0.16$$

$$\gamma = 1.2$$

$$\gamma\phi = 0.8 A_w/A_c = 0.192 \quad (118)$$

Hence from equations (75), (116), and (117),

$$\begin{aligned} \sigma_{cr} &= \frac{\sigma_2 + (1 - \gamma\phi)\sigma_1}{\sigma_2 + \sigma_1} \sigma_1 \\ &= \frac{0.0675 + (0.808)(0.002)}{0.0695} \sigma_1 \\ &= 0.001996E \end{aligned}$$

Even here the interaction diminishes  $\sigma_1$  only by 0.5 percent. Since here  $A_w/A_c = 0.24$  and  $r/t = \sqrt{1.375}/0.125 = 9.4$  a rough estimate from equation (93) would yield a decrease of  $3 \frac{A_w}{A_c} \left(\frac{6}{r/t}\right)^2$  percent = 0.3 percent.

That equation in the section entitled "Buckling of I-Section in Direction Perpendicular to Plane of Web" was derived for webs with no restraints or with positive rotational restraints only. It was already remarked there that for negative web restraints it will give values for  $(\Delta\sigma)_i$  which are too small. In the present case, however, the order of magnitude is correctly indicated by equation (93).

## Buckling of Columns with T-Section

In the stability of such sections it is best to distinguish two cases: (a) The flange has a relatively small torsional rigidity or is not significantly more stable than the web (fig. 14) or, more generally, the web is not substantially rotationally restrained by the flange, and (b) the flange has a relatively large torsional rigidity and is much more stable than the web, so that the web is substantially rotationally restrained.

On the basis of a numerical example it will first be shown that in case (a) the interaction from cross-sectional distortion is practically nil. Case (b) will then be discussed in greater detail.

(a) If the ratio  $b/t$  of the web is not much greater than the ratio  $b'/t'$  of the flange and the flange is relatively weak (fig. 14), so that the web is only slightly rotationally restrained by the flange, both web and flange remain practically straight in cross section; that is, the cross section is not distorted during buckling. Hence in that case a column with T-section buckles approximately in the way that it is assumed to buckle in the analysis of flexural and torsional buckling. The interaction formula for the buckling stress for this case was derived by Kappus (reference 15) from three simultaneous different equations of the fourth order and also by Lundquist and Fligg (reference 16). It was also derived by the first author according to this method of split rigidities (reference 10). The exact solution for this problem was given by the first author in references 2 and 3, including the influence of distortion of section, while in the present report it is given by equation (33).

In reference 10 the buckling stress for a steel column with an effective length  $L$  of 700 centimeters and with the cross section of figure 15 was calculated from the interaction formula of flexural and torsional buckling (without regard to cross-sectional distortion) as well as from the exact equation (33). The corresponding buckling stresses were 948 and 942 kilograms per square centimeter, respectively. (In reference 10 the first stress is also given as 942 kg/cm<sup>2</sup>, which value was due to a computational error.) Hence in this case the exact buckling stress is only 2/3 percent less than that found from the assumption that the cross sections of the plates do not bend.

It was stated in reference 10 that this is due to the high value of the critical stress of a plate which is clamped at one unloaded side and free at the other for a half wave length of many times its width, as compared with the buckling stress of the T-section. The additional influence of this plate buckling stress can be taken into account in the following manner: The torsional-flexural buckling stress  $\sigma_{1-2}$  is first

computed according to the interaction formula for this case. If, in analogy to the derivation of equation (76) in the section entitled "Buckling of I-Section in Direction Perpendicular to Plane of Web," this mode with  $\sigma_{1-2}$  is regarded as case (1), case (2) is represented by the above buckling of the web clamped at one unloaded side and free at the other, with a corresponding buckling stress  $\sigma_3$ . This is true because such buckling is the only deformation which could occur if the column were infinitely rigid against the deformation of case (1). The transverse bending of the flange may be neglected. Hence, as will be shown in detail later, an interaction formula results which is again approximated conservatively by a formula similar to equation (76). The actual combined buckling stress is then given by

$$\sigma_{cr} = \frac{\sigma_3}{\sigma_3 + \sigma_{1-2}} \sigma_{1-2} \quad (119)$$

in which  $\sigma_{1-2} = 948$  kilograms per square centimeter = 13,460 psi and  $\sigma_3$  is the buckling stress of a plate that is clamped at one unloaded side and free at the other (reference 12).

$$\sigma_3 = \frac{\pi^2 N}{b^2 t} \left[ \left( \frac{1}{\beta^2} \right) + 0.125\beta^2 + 0.57 \right] \quad (120)$$

where  $\beta = a/b = L/b$ . In this example the width  $b$  of the web, which is actually supported in the middle plane of the flange, is 30.5 centimeters, (fig. 15), so that  $\beta = 700/30.5 = 22.9$ , yielding, with  $\nu = 0.3$ ,

$$\begin{aligned} \sigma_3 &= \left( \frac{1}{527} + 0.57 + \frac{527}{8} \right) \frac{\pi^2 N}{b^2 t} = 66.472 \frac{\pi^2 N}{b^2 t} \\ &= 66.472 \frac{\pi^2 E t^3}{12(1 - \nu^2) b^2 t} = 0.0645E \\ &= 0.0645 \times 2,100,000 \text{ kg/cm}^2 = 135,500 \text{ kg/cm}^2 \\ &= 1,925,000 \text{ psi} \end{aligned}$$

Hence from equation (119)

$$\sigma_{cr} = \frac{135,500}{135,500 + 948} 948 \text{ kg/cm}^2 = 941 \text{ kg/cm}^2 = 13,360 \text{ psi}$$

which checks the exact buckling stress of 942 kilograms per square centimeter = 13,375 psi found from equation (33).

It is seen that for this particular example: (1) The interaction formula, equation (119), is accurate within about 1/10 percent, and (2) the interaction between torsional-flexural and plate buckling amounts to about 2/3 percent, that is, is negligible.

(b) If the flange has a relatively large torsional rigidity and is much more stable than the web, as, for example, for the dimensions of figure 16, the web is rather strongly constrained rotationally by the flange. In this case the influence of plate buckling, with a buckling stress  $\sigma_3$ , is more pronounced, especially for small half wave lengths. At the extreme, with a flange which is infinitely rigid, only pure plate buckling could occur.

The deflection of the cross section consists here of a translation  $w_1$ , a rotation with respect to the shear center  $S$ , denoted by the deflection  $w_2$  at the lower side of the web and a plate buckling of the web with a maximum deflection  $w_3$  (fig. 17). The shear center may be assumed sufficiently accurately to be situated at the intersection of the middle planes of flange and web. Again, the transverse bending of the flange is negligible.

If only the deflection  $w_1$  occurs, that is, flexural buckling only, the critical stress is

$$\sigma_1 = \frac{\pi^2 E_t}{(a/r_y)^2} \quad (121)$$

or in the elastic domain

$$\sigma_1 = \frac{\pi^2 E}{(a/r_y)^2} \quad (122)$$

This case will be called case (1). If only the deflection  $w_2$  occurs (case (2)), the critical stress is (reference 10)

$$\sigma_2 = \frac{1}{I_p} \left( E F I_t + E_t C_w \frac{\pi^2}{a^2} \right) \quad (123)$$

or in the elastic domain (reference 17)

$$\sigma_2 = \frac{1}{I_p} \left( G I_t + E C_w \frac{\pi^2}{a^2} \right) \quad (124)$$

where  $I_p$ ,  $GI_t$ , and  $EC_w$  are the polar moment of inertia about  $S$ , the torsional rigidity, and the warping rigidity, respectively. Equation (123) follows directly from equation (124) since in the plastic domain, if during buckling infinitesimal shear stresses  $\tau_{xy}'$  are superimposed on pure compressive stresses, the ratio  $\tau_{xy}'/\gamma_{xy}'$  between excess shear stresses and excess shear strains, which is  $G$  in the elastic domain, is replaced by  $EF$  (reference 3). Furthermore, in equation (124) the elastic modulus  $E$  refers to excess bending stresses, so that in the plastic domain it changes to the tangent modulus  $E_t$ .

The deflection of the web with a maximum  $w_3$  (case (3)) would, if the column were infinitely rigid with respect to the other deflections, correspond to a critical stress in the plastic domain:

$$\sigma_3 = \frac{\pi^2 EI}{b^2 t} \left( \frac{A}{\beta^2} + 0.125 D \beta^2 + 1.84 F - 0.25 B \right) \quad (125)$$

In the elastic range equation (125) reduces to equation (120). The critical stress in the plastic domain according to equation (125) may be found by the energy method of equating the internal work  $V_i$  to the external work  $V_e$ , hence

$$V_i = V_e \quad (126)$$

in which (reference 3)

$$V_i = \frac{1}{2} EI \iint \left[ A \left( \frac{\partial^2 w}{\partial x^2} \right)^2 + 2B \frac{\partial^2 w}{\partial x^2} \frac{\partial^2 w}{\partial y^2} + D \left( \frac{\partial^2 w}{\partial y^2} \right)^2 + 4F \left( \frac{\partial^2 w}{\partial x \partial y} \right)^2 \right] dx dy \quad (127)$$

and

$$V_e = \frac{1}{2} t \sigma_3 \iint \left( \frac{\partial w}{\partial x} \right)^2 dx dy \quad (128)$$

Assuming

$$w = w_3 [1 - \cos(\pi y/2b)] \sin(\pi x/a) \quad (129)$$

equations (126), (127), and (128) yield

$$\sigma_3 = \frac{\pi^2 EI}{b^2 t} \left( \frac{A}{\beta^2} + 0.138 D \beta^2 + 2.2 F - 0.3 B \right) \quad (130)$$

This gives for the elastic domain, where, from equations (3),  
 $A = D = 1/(1 - \nu^2)$ ,  $B = \nu/(1 - \nu^2)$ , and  $F = 1/\sqrt{2(1 + \nu)}$ ,  
 with  $\nu = 0.3$ ,

$$\sigma_3 = \frac{\pi^2 N}{b^2 t} \left( \frac{1}{\beta^2} + 0.138\beta^2 + 0.68 \right) \quad (131)$$

instead of the more-accurate value from equation (120). This is due to the fact that the energy method yields values which are too high. Hence equation (130) may be improved by adjusting it to the more-accurate known value in the elastic range. This is done by multiplying the coefficients of  $D$  by  $0.125/0.138$  and those of  $B$  and  $F$  by  $0.57/0.68$ . This is how equation (125) was obtained.

Some years ago the first author derived the interaction formula for the critical stress  $\sigma_{cr}$  as expressed in terms of the critical stresses  $\sigma_1$ ,  $\sigma_2$ , and  $\sigma_3$  for the component modes. This was done by considering successively (1) the equilibrium between external and internal bending moments, (2) that between external and internal torsional moments, for the entire column, and (3) the equilibrium between external and internal torsional moments acting on the web alone. This leads to a system of three linear homogeneous equations in  $w_1$ ,  $w_2$ , and  $w_3$ , from which the buckling condition follows by equating the determinant of the system to zero, yielding a cubic equation in  $\sigma_{cr}$ .

In order to check this equation, during the summer of 1948 Mr. C. D. Maussart, the first author's assistant at the Institute of Technology at Delft, Holland, calculated  $\sigma_{cr}$  exactly for the elastic range from equation (33), where  $\alpha_1$  and  $\alpha_2$  are given by equations (27), for the T-section of figure 16 with  $b = 31$  centimeters,  $b' = 15$  centimeters,  $t = 1$  centimeter, and  $t' = 2$  centimeters. The freely supported length was assumed to be 700 centimeters and  $\sigma_{cr}$  was calculated for elastic buckling in 1, 2, 4, 8, and 12 half waves and hence for half wave lengths  $a$  of 700, 350, 175, 87.5, and 58.33 centimeters, respectively. The exact critical stresses  $\sigma_{cr}$  in pounds per square inch thus found are plotted in figure 3 against the half wave length  $a$ . In table 1 they are given in kilograms per square centimeter as well as in pounds per square inch under the column heading " $\sigma_{cr}$  from equation (33)."

The stresses  $\sigma_1$ ,  $\sigma_2$ , and  $\sigma_3$  from equations (122), (124), and (120) for the component cases (1), (2), and (3) are likewise given in figure 3 and table 1. The above-mentioned cubic interaction formula in  $\sigma_{cr}$  was found to yield results which deviate less than 1 percent from the exact values. This proved the accuracy of the method, but did not yet provide a simple and direct way of computation, since the coefficients of the cubic equation are rather involved.

In the following discussion simpler interaction formulas are derived for this type of buckling and are checked against the accurate values from equation (33).

In order to find explicit interaction formulas for the specific case of  $\beta = \beta_1$  (fig. 1), the critical stress  $\sigma_{2-3}$  will first be calculated for  $w_1 = 0$ , that is, for fixed shear-center axis, so that  $\sigma_{2-3}$  follows directly from a quadratic equation like equation (60) in the section entitled "Buckling of I-Section in Direction Perpendicular to Plane of Web." Since  $\sigma_1$  is here very large (in fig. 3 for  $a = 60$  cm), so that  $\sigma_{cr}$  will be only slightly smaller than  $\sigma_{2-3}$ , it will subsequently be sufficiently accurate to express the interaction of  $\sigma_{2-3}$  and  $\sigma_1$  in a simple formula of the type of equation (76). On the other hand, at  $\beta = \beta_2$  (fig. 1), hence, in figure 3 at  $a \approx 600$  centimeters,  $w_3$  is first assumed to be zero, so that the critical stress  $\sigma_{1-2}$  for flexural and torsional buckling is obtained as interaction of cases (1) and (2). Subsequently the small interaction between  $\sigma_{1-2}$  and the very high plate buckling stress  $\sigma_3$  may again be expressed by a formula of the type of equation (76).

Critical stress for T-section with fixed shear-center axis.- Although actually the shear center is situated slightly below the middle plane of the flange it is sufficiently accurate to assume the shear-center axis at the intersection of the middle planes of flange and web.

In a similar way to that done in the section entitled "Buckling of I-Section in Direction Perpendicular to Plane of Web" the entire section is considered first. Since, however, twisting about the shear axis occurs here instead of free bending, no equilibrium between bending moments can be considered. The best procedure is to compare the moments about the shear-center axis  $S$  of the deflecting and restraining forces acting on a small slice of length  $dx$  of the column (fig. 18).

Assume first a deformation according to case (2) to occur which corresponds to  $w_2$ . At buckling the deflecting force  $-t\sigma_2(\partial^2 w/\partial x^2)dx dy$  acting on a small element  $t dx dy$  of the slice in the web is proportional to  $\sigma_2$  and to  $w$ , so that it may be denoted by  $c\sigma_2 w t dy$ . Since  $t dy$  represents a small element  $dA_c$  of the cross section of the column, the deflecting forces on elements in the web as well as the flange may be denoted by  $c\sigma_2 w dA_c$ .

Hence, since from figure 18 for case (2) the displacement  $w$  of any point of the cross section is  $\frac{r}{b} w_2$ , if  $r$  is its distance from  $S$ ,

the total moment about  $S$  of the deflecting forces acting on the slice  $A_c dx$  is

$$\begin{aligned} M_{d2} &= \int c \sigma_2 w r \, dA_c \\ &= \frac{c}{b} \sigma_2 w_2 \int r^2 \, dA_c \\ &= \frac{c}{b} \sigma_2 w_2 I_p \end{aligned} \quad (132)$$

where  $I_p$  is the polar moment of inertia about  $S$ .

Consequently the moment  $M_r$  about  $S$  of the restraining forces acting on the slice, that is, of the transverse shearing stresses acting in its end cross sections, is likewise

$$M_{r2} = \frac{c}{b} \sigma_2 w_2 I_p \quad (133)$$

Assume now a deformation according to case (3) alone (corresponding to  $w_3$ , fig. 18) or, in other words, assume the column to be infinitely rigid against a deformation of case (2). Since here the web alone deforms, if this deformation were of the same shape as in case (2) the deflecting moment about  $S$  would be given in equation (132), where  $I_p$  would be replaced by the polar moment of inertia  $I_{pw}$  of the web about  $S$  and  $\sigma_2 w_2$  by  $\sigma_3 w_3$ . However, since with equal deflection at  $y = b$  the deflection at other points is less in case (3) than in case (2), the deflecting moment is also less, so that here

$$M_{d3} = \alpha \frac{c}{b} \sigma_3 w_3 I_{pw} \quad (134)$$

where  $\alpha < 1$ . The restraining forces are exerted here by shearing stresses in both end sections of the slice but also by the bending moment  $M_y$  exerted by the flange on the web at its built-in unloaded edge. This is an internal moment so that it does not add to the restraining forces acting on the slice as a whole. In equation (120) for  $\sigma_3$ ,  $M_y$  is accounted for by the factor  $0.125\beta^2$ . Omitting it for

the reasons just stated, the restraining moment for this case is

$$M_{r3} = \alpha \frac{c}{b} \eta_3 I_{pw} \sigma_3 w_3 \quad (135)$$

in which, from equation (120),

$$\eta_3 = \frac{(1/\beta^2) + 0.57}{(1/\beta^2) + 0.125\beta^2 + 0.57} \quad (136)$$

Hence, with both cases (2) and (3) occurring simultaneously, the restraining moment about S is

$$\begin{aligned} M_r &= M_{r2} + M_{r3} \\ &= \left( \sigma_2 w_2 + \alpha \eta_3 \frac{I_{pw}}{I_p} \sigma_3 w_3 \right) \frac{c}{b} I_p \end{aligned} \quad (137)$$

At the moment of buckling, with a buckling stress  $\sigma_{2-3}$ , the deflecting moment about S follows from equations (132) and (134) by replacing  $\sigma_2$  and  $\sigma_3$  by  $\sigma_{2-3}$ , so that

$$\begin{aligned} M_d &= M_{d2} + M_{d3} \\ &= \sigma_{2-3} \left( w_2 + \alpha \frac{I_{pw}}{I_p} w_3 \right) \frac{c}{b} I_p \end{aligned} \quad (138)$$

Hence from equations (137) and (138) the condition of buckling  $M_d = M_r$  is given by the equation

$$\sigma_{2-3} \left( w_2 + \alpha \frac{I_{pw}}{I_p} w_3 \right) = \sigma_2 w_2 + \alpha \frac{I_{pw}}{I_p} \eta_3 \sigma_3 w_3 \quad (139)$$

In order to obtain a second equation in  $w_2$  and  $w_3$  the equilibrium of a slice  $bt \, dx$  of the web alone is considered by comparing again the moments of deflecting and restraining forces about S.

If a deformation according to case (2) alone occurs, the critical stress of the web is, analogous to equation (124) for the entire section,

$$\sigma_{2w} = \frac{1}{I_{pw}} \left( GI_{tw} + EC_{ww} \frac{\pi^2}{a^2} \right) \quad (140)$$

where the second subscript  $w$  refers to the web. The deflecting moment, using the same proportionality factor as in equation (132), would be

$$M_{d2w} = \frac{c}{b} \sigma_{2w} w_2 I_{pw} \quad (141)$$

which follows directly from equation (132) by replacing  $\sigma_2$  and  $I_p$  by  $\sigma_{2w}$  and  $I_{pw}$ . Hence the restraining moment in this case is likewise

$$M_{r2w} = \frac{c}{b} \sigma_{2w} w_2 I_{pw} \quad (142)$$

With a deformation according to case (3) alone the deflecting moment is already given by equation (134). Since at this stage the equilibrium of the web is considered, the restraining moment  $M_y$  exerted by the flange must also be taken into account, so that now the moment about  $S$  of the restraining forces acting on a slice  $bt \, dx$  of the web is equal to  $M_{d3}$  in equation (134)

$$M_{r3w} = \alpha \frac{c}{b} \sigma_3 w_3 I_{pw} \quad (143)$$

whence the total restraining moment

$$\begin{aligned} M_{rw} &= M_{r2w} + M_{r3w} \\ &= \left( \sigma_{2w} w_2 + \alpha \sigma_3 w_3 \right) \frac{c}{b} I_{pw} \end{aligned} \quad (144)$$

At the moment of buckling, with a buckling stress  $\sigma_{2-3}$ , the deflecting moment about  $S$  follows from equations (142) and (143) by replacing  $\sigma_{2w}$  and  $\sigma_3$  by  $\sigma_{2-3}$ , so that

$$\begin{aligned}
 M_{dw} &= M_{d2} + M_{d3} \\
 &= \sigma_{2-3}(w_2 + \alpha w_3) \frac{c}{b} I_{pw}
 \end{aligned} \tag{145}$$

Hence the condition of buckling

$$M_{dw} = M_{rw}$$

is here

$$\sigma_{2-3}(w_2 + \alpha w_3) = \sigma_{2w} w_2 + \alpha \sigma_3 w_3 \tag{146}$$

Collecting terms in  $w_2$  and  $w_3$ , equations (139) and (146) become

$$\left. \begin{aligned}
 (\sigma_2 - \sigma_{2-3})w_2 + (\eta_3 \sigma_3 - \sigma_{2-3})\psi \alpha w_3 &= 0 \\
 (\sigma_{2w} - \sigma_{2-3})w_2 + (\sigma_3 - \sigma_{2-3})\alpha w_3 &= 0
 \end{aligned} \right\} \tag{147}$$

where

$$\psi = I_{pw}/I_p \tag{148}$$

The buckling condition is obtained by equating the determinant of equations (147) to zero, from which

$$\begin{aligned}
 \sigma_{2-3} &= \frac{1}{2(1 - \psi)} \left\{ \sigma_2 + \sigma_3 - \psi(\sigma_{2w} + \eta_3 \sigma_3) - \right. \\
 &\quad \left. \sqrt{[\sigma_2 + \sigma_3 - \psi(\sigma_{2w} + \eta_3 \sigma_3)]^2 - 4(1 - \psi)\sigma_3(\sigma_2 - \psi\eta_3\sigma_{2w})} \right\} \tag{149}
 \end{aligned}$$

where for the elastic range  $\sigma_2$ ,  $\sigma_3$ ,  $\sigma_{2w}$ ,  $\eta_3$ , and  $\psi$  are given by equations (124), (120), (140), (136), and (148), respectively. The stress  $\sigma_{2-3}$  has been calculated for the T-section of figure 16 for several half wave lengths  $a$ . The result is given in table 1 and

figure 3. It follows clearly from figure 3 that  $\sigma_{2-3}$  approaches  $\sigma_2$  for larger wave lengths, where  $\sigma_3$  is very high.

Buckling stress of column with T-section for  $\beta \approx \beta_1$  (fig. 1).-

In order to find the real buckling stress  $\sigma_{cr}$  the influence of a deflection  $w_1$  of the column (fig. 17) has still to be considered. Since for  $\beta = \beta_1$  (fig. 1)  $\sigma_1$  is very high, this influence is rather small. The stress  $\sigma_{cr}$  will be calculated from the interaction of case (1) with deflection  $w_1$  (fig. 17) and the combined case (2-3), considered in the previous section, with a buckling stress  $\sigma_{2-3}$  and a deflection  $w_{2-3}$  (fig. 19).

This case is similar to that of the I-beam in the section entitled "Buckling of I-Section in Direction Perpendicular to Plane of Web." Considering first the equilibrium between external and internal moments analogous to equation (40) the internal moment from the deflection  $w_1$  from case (1) is here

$$M_{i1} = A_c \sigma_1 w_1 \quad (150)$$

Analogous to equations (43) and (44) the internal moment from the deflection  $w_{2-3}$  of the web would be found here as

$$M_{i(2-3)} = A_w \eta \sigma_{2-3} \mu w_{2-3} \quad (151)$$

in which

$$\eta = \frac{\sigma_{2c}}{\sigma_{2-3}} \quad (152)$$

where  $\sigma_{2c}$  is given by equation (41). The average deflection of the web from case (2-3) is  $\mu w_{2-3}$ . However, this internal moment  $M_{i(2-3)}$  is somewhat ambiguous. In case (2), where a pure rotation of the section with respect to the shear center occurs, according to the definition of the shear center no internal bending moments will originate. But equation (151) indicates internal moments for this case. This is a consequence of the fact that the center of shear  $S$  was assumed at the intersection of the middle planes of flange and web, while in reality it is slightly lower. Therefore it is better and safe to neglect  $M_{i(2-3)}$  here, the more so since it is extremely small in comparison with  $M_{i1}$  from equation (150). Hence

$$M_i = M_{i1} = A_c \sigma_1 w_1 \quad (153)$$

With actual combined buckling the external moment resulting from  $w_1$  is

$$M_{ei} = A_c \sigma_{cr} w_1 \quad (154)$$

From  $w_{2-3}$  analogous to equation (151)

$$M_{e(2-3)} = A_w \sigma_{cr} \mu w_{2-3} \quad (155)$$

To find  $\mu$  it is noted that for a deflection of the web from case (2), where the cross section remains straight, the average deflection  $\mu w_2 = 0.5 w_2$ , so that  $\mu_2 = 0.5$ . For case (3) the cross-sectional distortion of the web may sufficiently accurately be approximated by that of a cantilever beam with uniform load  $q$  (fig. 20). Thus

$$\begin{aligned} M &= -\frac{1}{2} q(b-y)^2 \\ w &= -\iint M \, dy \, dy \\ &= \frac{q}{24EI} (y^4 - 4by^3 + 6b^2y^2) \end{aligned}$$

so that  $w_3 = (w)_{y=b} = \frac{q}{8EI} b^4$  and

$$w = \frac{y^4 - 4by^3 + 6b^2y^2}{3b^4} w_3 \quad (156)$$

Hence

$$\mu_3 = \frac{\int_0^b w \, dy}{bw_3} = 0.4 \quad (157)$$

Thus in equation (155)

$$0.5 > \mu > 0.4 \quad (158)$$

From equations (154) and (155) the total external moment is

$$\begin{aligned} M_e &= M_{e1} + M_{e(2-3)} \\ &= A_c \sigma_{cr} \left( w_1 + \mu \frac{A_w}{A_c} w_{2-3} \right) \end{aligned} \quad (159)$$

or with the notation

$$\phi = \mu A_w / A_c \quad (160)$$

$$M_e = A_c \sigma_{cr} (w_1 + \phi w_{2-3}) \quad (161)$$

Hence from equations (153) and (161), since  $M_e = M_1$

$$\sigma_{cr} (w_1 + \phi w_{2-3}) = \sigma_1 w_1 \quad (162)$$

Next, in the same way as in the section entitled "Buckling of I-Section in Direction Perpendicular to Plane of Web," a second relation is obtained by considering deflecting and restraining forces acting on an element  $t \, dx \, dy = dA_w \, dx$  of the web. If only case (2-3) occurs the deflecting force may be written as  $c \sigma_{2-3} w_{2-3}$  so that, analogous to equation (52), the restraining force in that case is also

$$R_2 = c \sigma_{2-3} w_{2-3} \quad (163)$$

If only deflection  $w_1$  occurs, the deflecting force is  $c \gamma \sigma_{2c} w_1$ , where  $\gamma$  accounts for the fact that with equal maximum deflection at  $y = b$ , a larger average deflecting force results with  $w = w_1 = \text{Constant}$  than with a variation of  $w$  with  $y$  as in case (2-3). A good measure of this influence is the moment of the deflecting forces with respect to  $S$ . As a matter of fact, this means that the moments about  $S$  of the deflecting and restraining forces acting on a slice  $bt \, dx$  of the web are considered and equated. Denoting the deflecting forces on an element  $dA_w \, dx$  by  $k \omega \, dA_w$ , the deflecting moment is for case (1)

$$\begin{aligned} M_1 &= k \sigma \int_0^b w_1 y \, dA_w \\ &= 0.5 k b^2 t \omega w_1 \end{aligned} \quad (164)$$

For case (2), where  $w = \frac{y}{b} w_2$ ,

$$\begin{aligned} M_2 &= k\sigma \int_0^b wy \, dA_w \\ &= 0.333kb^2 t\sigma w_2 \end{aligned} \quad (165)$$

For case (3), where  $w$  is approximately given by equation (156),

$$\begin{aligned} M_3 &= k\sigma \int_0^b wy \, dA_w \\ &= 0.289kb^2 t\sigma w_3 \end{aligned} \quad (166)$$

Hence from equations (164), (165), and (166)

$$\frac{0.5}{0.289} > \gamma > \frac{0.5}{0.333}$$

or

$$1.73 > \gamma > 1.5 \quad (167)$$

Thus analogous to equation (54), the restraining force  $R_1 = D_1$  or

$$R_1 = c\gamma\sigma_{2c}w_1 \quad (168)$$

so that the total restraining force is, from equations (163) and (168),  
 $R = R_2 + R_1$  or

$$R = c\sigma_{2-3}w_{2-3} + c\gamma\sigma_{2c}w_1 \quad (169)$$

or from equation (152)

$$R = c\sigma_{2-3}(w_{2-3} + \eta\gamma w_1) \quad (170)$$

With actual combined buckling the deflecting force is  $c\sigma_{cr}w_{2-3}$  for case (2-3) and  $c\gamma\sigma_{cr}w_1$  for case (1), so that its total is

$$D = c\sigma_{cr}(w_{2-3} + \gamma w_1) \quad (171)$$

Hence from the equality of D and R

$$\sigma_{cr}(w_{2-3} + \gamma w_1) = \sigma_{2-3}(w_{2-3} + \eta \gamma w_1) \quad (172)$$

Collecting terms with  $w_1$  and  $w_{2-3}$  in equations (162) and (172), they become

$$\left. \begin{aligned} (\sigma_1 - \sigma_{cr})w_1 - \phi \sigma_{cr} w_{2-3} &= 0 \\ \gamma(\sigma_{cr} - \eta \sigma_{2-3})w_1 - (\sigma_{2-3} - \sigma_{cr})w_{2-3} &= 0 \end{aligned} \right\} \quad (173)$$

These equations are nearly identical with equations (59). The only difference is that here  $w_{2-3}$  occurs instead of  $w_2$ , and that in the first of equations (173)  $\eta$  has been equated to zero because  $M_{i(2-3)}$  from equation (151) is negligible. From equations (173)

$$\sigma_{cr} = \frac{1}{2(1 - \gamma\phi)} \left\{ \sigma_1 + (1 - \gamma\phi\eta)\sigma_{2-3} - \sqrt{[\sigma_1 + (1 - \gamma\phi\eta)\sigma_{2-3}]^2 - 4(1 - \gamma\phi)\sigma_1\sigma_{2-3}} \right\} \quad (174)$$

Here  $\eta$  is given by equations (152), (41), and (149), while from equations (158), (160), and (167) one can only conclude

$$0.75 \frac{A_w}{A_c} > \gamma\phi > 0.69 \frac{A_w}{A_c} \quad (175)$$

To decide which value  $\gamma\phi$  to use it is noted that  $\sigma_{cr}$  is the smaller the larger  $\gamma\phi$ . (The quantity  $\gamma\phi$  is an interaction factor, which is equal, for example, to unity in the case of sandwich plates). Hence a safe and only slightly conservative value is

$$\gamma\phi = 0.75 \frac{A_w}{A_c} \quad (176)$$

In the same way as was stated in elaborating equation (60), conservative and sufficiently accurate values of  $\sigma_{cr}$  are obtained if  $\eta$  is equated to zero. With  $\eta = 0$  equation (174) is identical in form with equation (60), if  $\sigma_2$  is replaced by  $\sigma_{2-3}$ . Hence, for the

particular case of  $\beta = \beta_1$ , that is, for very large  $\sigma_1$  (fig. 1) equation (174) may be written, in analogy to equation (74), as

$$\sigma_{cr} = \frac{\sigma_1 + (1 - \gamma\phi)\sigma_{2-3}}{\sigma_1 + \sigma_{2-3}} \sigma_{2-3} \quad (177)$$

or more simply and conservatively, analogous to equation (76), as

$$\sigma_{cr} = \frac{\sigma_1}{\sigma_1 + \sigma_{2-3}} \sigma_{2-3} \quad (178)$$

Here  $\sigma_1$  is given by equation (122),  $\sigma_{2-3}$  by equation (149) and  $\gamma\phi$  by equation (176). For the particular section of figure 16  $\gamma\phi = 0.75 \frac{30}{90} = 0.25$ . (Comparing equations (177) and (178) it follows that the sandwich-plate formula (reference 1) is indeed obtained if the interaction factor  $\gamma\phi = 1$ .)

In table 1,  $\sigma_{cr}$  is computed for the T-section of figure 16 from equation (177) as well as from equation (178) and given under the headings " $\sigma_{cr}$  from equation (177)" and " $\sigma_{cr}$  from equation (178)," respectively. Comparing these values of  $\sigma_{cr}$  with the exact values obtained by using equation (33), it is seen that the governing value of  $\sigma_{cr}$ , that is, for  $\beta = \beta_1$  (fig. 1), corresponding here to a value  $a$  of about 58.33 centimeters, may be computed more accurately from the simpler formula (178). The results from equation (178) for  $a = 58.33$  and  $a = 62$  centimeters are indicated in figure 3 by circles, and are seen to fit almost exactly the exact curve for  $\sigma_{cr}$ . For  $a = 87.5$  and  $a = 135$  centimeters, the more-accurate equation (177) has to be used, since here the difference between  $\sigma_{cr}$  and  $\sigma_{2-3}$  becomes more important. However, in these cases  $\sigma_{cr}$  for buckling in one half wave has no practical value, since buckling in more than one half wave results in smaller buckling stresses. The resulting values are indicated in figure 3 by crosses. The agreement with the exact curve is excellent.

Computation of critical stress  $\sigma_{1-2}$  for flexural and torsional buckling of T-section. - Although the more general derivation of  $\sigma_{1-2}$  according to the method of split rigidities was given in reference 10, the pertinent critical stress for the special case of a T-section will be derived here directly. In a computation of flexural and torsional buckling it is assumed that no distortion of the cross section takes place. Hence only deformations according to cases (1) and (2) occur, while in an approximate sense the column is supposed to be infinitely rigid against a deformation from case (3).

The bending with respect to the Y-axis is considered first. If only case (1) occurred, a deflection  $w_1$  would cause an external moment  $A_c \sigma_1 w_1$ , so that this deflection entails an internal moment

$$M_{i1} = A_c \sigma_1 w_1 \quad (179)$$

Since it is a property of the shear center  $S$  that a rotation with respect to  $S$  yields a torsional moment only and no flexural moments, the internal flexural moment from case (2) is zero. Hence the total internal flexural moment is

$$M_i = M_{i1} = A_c \sigma_1 w_1 \quad (180)$$

The external flexural moment is found by multiplying the critical thrust  $A_c \sigma_{1-2}$  for flexural and torsional buckling by the displacement  $CC'$  of the center of gravity  $C$ . From figure 21 this is equal to  $w_1 + \frac{y_0}{b} w_2$ , so that

$$M_e = A_c \sigma_{1-2} \left( w_1 + \frac{y_0}{b} w_2 \right) \quad (181)$$

Equating  $M_e$  and  $M_i$  yields the condition

$$\sigma_{1-2} \left( w_1 + \frac{y_0}{b} w_2 \right) = \sigma_1 w_1 \quad (182)$$

Torsion with respect to the center of shear  $S$  is next considered. Here a slice of length  $dx$  of the column is considered, as under the section entitled "Critical Stress for T-Section with Fixed Shear-Center Axis," where it was found in equation (133) that for case (2) the moment with respect to  $S$  of the restraining forces acting on the slice  $dx$  can be represented by the formula

$$M_{r2} = \frac{c}{b} \sigma_2 w_2 I_p$$

Again, from the definition of the center of shear it follows that the deflection  $w_1$  from case (1) causes no internal torsional moments, so that the resisting moment as above defined, for the combined cases (1) and (2), is

$$M_r = M_{r2} = \frac{c}{b} \sigma_2 w_2 I_p \quad (183)$$

From equations (132) or (183) it follows directly that at the critical stress  $\sigma_{1-2}$  the deflecting forces from the deflection  $w_2$  cause a moment

$$M_{d2} = \frac{c}{b} \sigma_{1-2} w_2 I_p \quad (184)$$

From the second member of equation (132) the deflecting moment from  $w_1$  is found as

$$\begin{aligned} M_{d1} &= \int c \sigma_{1-2} w_1 r \, dA_c \\ &= c \sigma_{1-2} w_1 A_c y_o \end{aligned} \quad (185)$$

so that the total deflecting moment is

$$\begin{aligned} M_d &= M_{d1} + M_{d2} \\ &= c \sigma_{1-2} \left( A_c y_o w_1 + \frac{I_p}{b} w_2 \right) \end{aligned} \quad (186)$$

Equating  $M_d$  and  $M_r$  yields

$$\sigma_{1-2} \left( y_o w_1 + \frac{r_o^2}{b} w_2 \right) = \sigma_2 \frac{r_o^2}{b} w_2$$

or

$$\sigma_{1-2} \left( \frac{b y_o}{r_o^2} w_1 + w_2 \right) = \sigma_2 w_2 \quad (187)$$

Collecting terms in equations (182) and (187),

$$\left. \begin{aligned} (\sigma_1 - \sigma_{1-2}) w_1 - \frac{y_o}{b} \sigma_{1-2} w_2 &= 0 \\ \frac{b y_o}{r_o^2} \sigma_{1-2} w_1 - (\sigma_2 - \sigma_{1-2}) w_2 &= 0 \end{aligned} \right\} \quad (188)$$

from which

$$\sigma_{1-2} = \frac{1}{2 \left[ 1 - (y_0^2/r_0^2) \right]} \left[ \sigma_1 + \sigma_2 - \sqrt{(\sigma_1 - \sigma_2)^2 + 4\sigma_1\sigma_2 y_0^2/r_0^2} \right] \quad (189)$$

where  $y_0$  is the distance between the centers of gravity and shear and  $r_0$  is the polar radius of gyration about S, while  $\sigma_1$  and  $\sigma_2$  are given by equations (122) and (124). For the T-section of figure 16  $\sigma_{1-2}$  is given in table 1 and by the curve  $\sigma_{1-2}$  in figure 3.

Buckling stress of column with T-section for  $\beta \geq \beta_2$  (fig. 1).-

For  $\beta \geq \beta_2$  the critical stress  $\sigma_3$  for case (3) is very high (fig. 3), so that the exact critical stress  $\sigma_{cr}$  will be only slightly lower than  $\sigma_{1-2}$ . Hence it may be expected that the sandwich formula, where 100-percent interaction is involved, provides a sufficiently accurate and safe approximation, so that  $\sigma_{cr}$  may be calculated from the formula

$$\sigma_{cr} = \frac{\sigma_3}{\sigma_3 + \sigma_{1-2}} \sigma_{1-2} \quad (119)$$

Indeed for  $a = 700$  centimeters, where from equation (33) the exact value of the buckling stress is 1880 kilograms per square centimeter = 26,700 psi, equation (119) yields  $\sigma_{cr} = 1883$  kilograms per square centimeter = 26,740 psi. This value as well as that for  $a = 620$  centimeters is also given in table 1, while in figure 3 both values are indicated by circles and fit the theoretical curve of  $\sigma_{cr}$  exactly.

To check the method of calculation in general,  $\sigma_{cr}$  will be calculated more accurately. Considering first the bending moments in the column with respect to the Y-axis, according to equation (153) in the subsection entitled "Buckling Stress of Column with T-Section for  $\beta \approx \beta_1$  (fig. 1)" the total internal moment is

$$M_i = A_c \sigma_1 w_1 \quad (190)$$

The total external moment by deformation according to cases (1) and (2) is, analogous to equation (181),

$$M_{e(1-2)} = A_c \sigma_{cr} \left( w_1 + \frac{y_0}{b} w_2 \right) \quad (191)$$

In equation (157) in the subsection mentioned above it was found that in case (3) the average deflection of the web is

$$\mu_3 w_3 = \frac{\int_0^b w \, dy}{b} = 0.4w_3$$

so that for case (3)

$$M_{e3} = A_w \sigma_{cr} (0.4) w_3 \quad (192)$$

yielding a total external moment

$$\begin{aligned} M_e &= M_{e(1-2)} + M_{e3} \\ &= A_c \sigma_{cr} \left( w_1 + \frac{y_0}{b} w_2 + 0.4 \frac{A_w}{A_c} w_3 \right) \end{aligned} \quad (193)$$

In order to limit to two the number of unknown deflections and thus the necessary number of equations and the degree of the buckling condition, it is observed that from equation (182) of the preceding subsection

$$w_1 + \frac{y_0}{b} w_2 = \frac{\sigma_1}{\sigma_{1-2}} w_1 \quad (194)$$

so that, with the notations

$$\left. \begin{aligned} \alpha &= \frac{\sigma_1}{\sigma_{1-2}} \\ \theta &= \frac{A_w}{A_c} \end{aligned} \right\} \quad (195)$$

equation (193) becomes

$$M_e = A_c \sigma_{cr} (\alpha w_1 + 0.4\theta w_3) \quad (196)$$

Hence from equations (190) and (196)

$$\sigma_{cr} (\alpha w_1 + 0.4\theta w_3) = \sigma_1 w_1 \quad (197)$$

Next a slice  $bt dx$  of the web is considered. From equations (164), (165), and (166) of the subsection entitled "Buckling stress of a column with T-section for  $\beta \approx \beta_1$  (fig. 1)" the moments about  $S$  of the deflecting forces acting on the slice may be represented as

$$M_1 = 0.5kb^2t\sigma w_1 \quad (164)$$

$$M_2 = 0.333kb^2t\sigma w_2 \quad (165)$$

$$M_3 = 0.289kb^2t\sigma w_3 \quad (166)$$

for cases (1), (2), and (3), respectively. The internal moment originating from a deflection  $w_1$  of the web is negligible for the large half wave length at  $\beta \geq \beta_2$ . If only  $w_2$  occurs, the buckling stress is  $\sigma_{2w}$  from equation (140), while with  $w_3$  alone, it is  $\sigma_3$  from equation (120). These stresses result in deflecting moments, which, from equations (165) and (166), may be denoted as

$$M_{d2w} = 0.333c\sigma_{2w}w_2 \quad (198)$$

and

$$M_{d3w} = 0.289c\sigma_3w_3 \quad (199)$$

respectively. Hence the total restraining moment is

$$\begin{aligned} M_{rw} &= M_{r2w} + M_{r3w} \\ &= M_{d2w} + M_{d3w} \end{aligned}$$

or

$$M_{rw} = c(0.333\sigma_{2w}w_2 + 0.289\sigma_3w_3) \quad (200)$$

Similarly from equations (164), (165), and (166) the total deflecting moment with actual buckling may be represented as

$$M_{dw} = c\sigma_{cr}(0.5w_1 + 0.333w_2 + 0.289w_3) \quad (201)$$

so that from equations (200) and (201)

$$(0.5w_1 + 0.333w_2 + 0.289w_3)\sigma_{cr} = 0.333\sigma_{2w}w_2 + 0.289\sigma_3w_3 \quad (202)$$

From equations (194) and (195)

$$w_2 = (\alpha - 1)\frac{b}{y_0} w_1 \quad (203)$$

On the other hand, the position of the center of gravity C (fig. 21) is determined by the equation

$$A_w \frac{b}{2} = A_c y_0$$

so that from equation (195)

$$\frac{b}{y_0} = 2 \frac{A_c}{A_w} = \frac{2}{\theta} \quad (204)$$

and from equation (203)

$$w_2 = 2 \frac{\alpha - 1}{\theta} w_1 \quad (205)$$

Hence from equation (202)

$$\sigma_{cr} \left[ \left( 0.5 + 0.667 \frac{\alpha - 1}{\theta} \right) w_1 + 0.289w_3 \right] = 0.667 \frac{\alpha - 1}{\theta} \sigma_{2w} w_1 + 0.289\sigma_3 w_3 \quad (206)$$

Collecting terms in  $w_1$  and  $w_3$ , equations (197) and (206) become

$$\left. \begin{aligned} (\sigma_1 - \alpha\sigma_{cr})w_1 - 0.4\theta\sigma_{cr}w_3 &= 0 \\ \left\{ 1.33(\alpha - 1)\sigma_{2w} - [\theta + 1.33(\alpha - 1)]\sigma_{cr} \right\} w_1 + 0.578\theta(\sigma_3 - \sigma_{cr})w_3 &= 0 \end{aligned} \right\} \quad (207)$$

from which

$$\sigma_{cr} = \frac{1}{2(1.33 + 0.11\alpha - \theta)} \left\{ 1.44\alpha(\sigma_{1-2} + \sigma_3) - 1.33(\alpha - 1)\sigma_{2w} - \sqrt{[1.44\alpha(\sigma_{1-2} + \sigma_3) - 1.33(\alpha - 1)\sigma_{2w}]^2 - 5.76\sigma_1\sigma_3(1.33 + 0.11\alpha - \theta)} \right\} \quad (208)$$

in which  $\alpha$  and  $\theta$  are given by equation (195). Using, in equation (70) the first term only, equation (208) simplifies to

$$\sigma_{cr} = \frac{\sigma_3}{\sigma_3 + \sigma_{1-2} - 0.925\sigma_{2w} \left[ 1 - (\sigma_{1-2}/\sigma_1) \right]} \sigma_{1-2} \quad (209)$$

which results conservatively in equation (119) as given before; that is,

$$\sigma_{cr} = \frac{\sigma_3}{\sigma_3 + \sigma_{1-2}} \sigma_{1-2} \quad (119)$$

The stress  $\sigma_{cr}$  has been calculated from equations (208) and (119) for  $a = 350, 620,$  and  $700$  centimeters, respectively, and is denoted in table 1 by " $\sigma_{cr}$  from equation (208)" and " $\sigma_{cr}$  from equation (119)," respectively. It is seen that for  $a = 620$  and  $700$  centimeters, where  $\sigma_{cr}$  is the governing stress, equation (119) yields even more exact results than equation (208). Its values are indicated in figure 3 by circles. For  $a = 350$  centimeters, where the difference between  $\sigma_{1-2}$  and  $\sigma_{cr}$  is much larger, equation (208) gives accurate results, while equation (119) is somewhat too conservative, as could be expected. The value for  $\sigma_{cr}$  from equation (208) for  $a = 350$  centimeters is indicated by a cross in figure 3.

#### Buckling of Angles with Equal Legs

For reasons of symmetry the legs do not rotationally restrain each other, so that the exact buckling condition for this case is given by equation (34). On the other hand the buckling stress for flexural and torsional buckling (reference 10) is given by equation (189). To illustrate the use of the interaction formula, the exact and the approximate buckling stresses will be computed for a specific example.

Assuming a steel angle with a length  $L = 40$  inches, a width  $b = 2$  inches, and a thickness  $t = 0.1$  inch,  $b/t = 20$ , so that it

buckles in the elastic domain. The flexural rigidity  $B$  of a flange against bending in its own plane, for use in equation (27), is here  $Eb^3t/3$  instead of  $Eb^3t/12$ , since the axial strain  $\epsilon_x$  from the deformation by bending, which results in the deflection  $w_1$  (fig. 22), is here zero for the fibers at the shear center axis  $S$ . By trial and error equation (34) yields the exact buckling stress  $\sigma_{cr} = 0.000875E$  (references 7 and 8).

In the approximate equation (189), as applied to this case,  $\sigma_1$  is the critical stress for flexural buckling about the Y-axis (fig. 22), since with torsional buckling of the section the center of gravity displaces in the direction of the Z-axis, resulting in bending about the Y-axis. The stress  $\sigma_2$  is given by equation (124).

Since the flanges are not rotationally restrained, they remain practically straight in cross section, so that, in contradistinction to the case of the T-section in the section entitled "Buckling of Columns with T-Section," case (3) does not occur here.

For an angle,  $y_0 = b/(2\sqrt{2})$  and  $I_p = 2tb^3/3$ , so that  $r_0^2 = I_p/(2bt) = b^2/3$  and  $y_0^2/r_0^2 = 3/8$ . Hence equation (189) for the case of an angle reduces to

$$\sigma_{cr} = 0.8 \left[ \sigma_1 + \sigma_2 - \sqrt{(\sigma_1 - \sigma_2)^2 + 1.5\sigma_1\sigma_2} \right] \quad (210)$$

With  $I_y = (1/12)(t\sqrt{2})(b\sqrt{2})^3 = (1/3)b^3t$  and  $r_y^2 = (1/6)b^2$ , from equation (122) for the particular angle quoted above, with  $a = L$ ,

$$\sigma_1 = \frac{\pi^2 E}{(a/r_y)^2} = 0.00411E$$

From equation (124), with  $I_t = \frac{2}{3}bt^3$ , while the last term is negligible,

$$\sigma_2 = G \frac{I_t}{I_p} = \frac{E}{2.6} \left( \frac{t}{b} \right)^2 = 0.0009625E$$

so that from equation (210)  $\sigma_{cr} = 0.000879E$ . This is in close agreement with the exact result  $\sigma_{cr} = 0.000875E$  from equation (34).

Buckling according to the considered mode governs only if it yields smaller critical stresses than for buckling of the angle with respect to its minor axis. For the latter mode the interaction is negligible and the pertinent moment of inertia is

$$\frac{1}{12}(2t\sqrt{2})\left(\frac{b}{\sqrt{2}}\right)^3 = \frac{1}{12} b^3 t$$

and hence  $I_y/4$ , so that the column buckling stress is  $\sigma_1/4 = 0.00103E$ . Since this value is higher than that previously computed for torsional buckling,  $\sigma_{cr} = 0.000879E$  governs.

### THEORETICAL RESULTS

Comparison between the exact and approximate methods of calculations leads to the conclusion that the interaction between column and local buckling may be computed very accurately by the method of split rigidities in the following manner:

(a) For columns where the web plates are supported at both unloaded sides, such as columns with I-, H-, or box sections or with channels, for buckling in a direction perpendicular to the web or webs the interaction between column and local buckling is always practically negligible. As a way of estimating roughly the effect of the interaction, formula (93) may be used, which states that  $\sigma_{cr}$  is at most about  $3(A_w/A_c) [6/(r/t)]^2$  percent less than the column or plate buckling stress,  $\sigma_1$  or  $(\sigma_2)_{min}$ , whichever is smaller. The total cross section of the web or webs located perpendicular to the direction of buckling is  $A_w$ . The total cross section of the column is denoted by  $A_c$ . The radius of gyration referring to the above-mentioned direction of buckling is  $r$ , while  $t$  is the web thickness.

The critical stress  $\sigma_{cr}$  may be calculated from equations (74) and (75) more directly. For  $\beta = \beta_1$  (fig. 1)

$$\sigma_{cr} = \frac{\sigma_1 + (1 - \gamma\phi)\sigma_2}{\sigma_1 + \sigma_2} \sigma_2 \quad (74)$$

where  $\sigma_1$  and  $\sigma_2$  are the column and plate buckling stresses, respectively, for the considered half wave length of buckling. This half wave length has to be chosen such as to make  $\sigma_{cr}$  a minimum. It can practically always be taken equal to the half wave length that makes  $\sigma_2$

minimum. The value  $(\sigma_{cr})_{\min}$  thus obtained governs as long as  $\beta$  is smaller than about  $\beta_2$  (fig. 1).

For  $\beta \geq \beta_2$

$$\sigma_{cr} = \frac{\sigma_2 + (1 - \gamma\phi)\sigma_1}{\sigma_2 + \sigma_1} \sigma_1 \quad (75)$$

where both  $\sigma_1$  and  $\sigma_2$  have to be calculated for a half wave length equal to the effective length of the column. The value of  $\gamma\phi$  is about  $0.75A_w/A_c$ . More conservatively, in general

$$\begin{aligned} \sigma_{cr} &= \frac{\sigma_1 \sigma_2}{\sigma_1 + \sigma_2} \\ &= \left( \sigma_1^{-1} + \sigma_2^{-1} \right)^{-1} \end{aligned} \quad (76)$$

Equations (74), (75), and (76) obtain also for the plastic domain, if the plastic values  $E_t/E$ ,  $A$ ,  $B$ ,  $D$ , and  $F$  from equations (36) and (2) are calculated for the actual buckling stress  $\sigma_{cr}$ . Moreover, equations (74), (75), and (76) apply for buckling in the plane of the web for columns which are symmetrical with respect to the web, as for example H- and T-sections. In that case  $\sigma_2$  refers to the plate buckling stress of the flanges which, for the considered direction of buckling, behave as plates which are free at one unloaded side and clamped at the other. In this case  $\gamma\phi$  is about  $0.7A_f/A_c$ , where  $A_f$  is the total cross section of the flanges.

In all above-mentioned cases the interaction is practically always negligible.

(b) The interaction between column and plate buckling is important, however, if the pertinent plate subtends a significant angle to the direction of buckling and is elastically rotationally restrained at one side and free at the other side, such as in T-sections and angles. In this case a combination of column buckling and twisting occurs. This follows directly from the conservative formula (76), because in this case both the flexural and torsional buckling stresses  $\sigma_1$  and  $\sigma_2$  have their smallest value for the largest possible half wave length, that is, the effective length of the column. For many practical sections these two stresses are of the same order of magnitude. For example, with  $\sigma_1 = \sigma_2$ , equation (76), though too conservative in this case, yields  $\sigma_{cr} = 0.5\sigma_1 = 0.5\sigma_2$ , which shows how significant interaction can become.

If the plates do not restrain each other significantly rotationally, as in T-sections with rather weak flanges or in angles, the interaction is rather accurately accounted for by the formulas for flexural (column) and torsional (plate) buckling. Then

$$\sigma_{cr} = \frac{1}{2 \left[ 1 - \left( y_o^2 / r_o^2 \right) \right]} \left[ \sigma_1 + \sigma_2 - \sqrt{(\sigma_1 - \sigma_2)^2 + \left( 4\sigma_1\sigma_2 y_o^2 / r_o^2 \right)} \right]$$

where  $\sigma_1$  and  $\sigma_2$  are the column and torsional buckling stresses, respectively, both calculated for a half wave length  $a$  equal to the column length  $L$ . The stress  $\sigma_1$  refers here to buckling in the Z-direction (figs. 17 and 22). In particular, in the elastic range

$$\sigma_1 = \frac{\pi^2 E}{(a/r_y)^2} \quad (122)$$

and

$$\sigma_2 = \frac{1}{I_p} \left( GI_t + EC_w \frac{\pi^2}{a^2} \right) \quad (124)$$

where  $I_p$ ,  $GI_t$ , and  $EC_w$  are the polar moment of inertia about the shear center  $S$ , the torsional rigidity, and the warping rigidity, respectively.

In the plastic range

$$\sigma_1 = \frac{\pi^2 E_t}{(a/r_y)^2} \quad (121)$$

and

$$\sigma_2 = \frac{1}{I_p} \left( EF I_t + E_t C_w \frac{\pi^2}{a^2} \right) \quad (123)$$

where  $F$  is given by equation (2) and  $E_t$  is the tangent modulus.

Values  $r_o$  and  $y_o$  in the above equation for  $\sigma_{cr}$  are the polar radius of gyration about the shear center  $S$  and the distance between shear center

and center of gravity, respectively (figs. 21 and 22). This buckling stress  $\sigma_{cr}$  governs only if it is smaller than the column buckling stress for buckling in the Y-direction (figs. 17 and 22), for which case the interaction is practically always negligible.

If the web of a T-section is substantially rotationally restrained by the flange the critical stress has to be calculated from equations (178), (149), (119), and (189). For  $\beta = \beta_1$  (fig. 1)

$$\sigma_{cr} = \frac{\sigma_1}{\sigma_1 + \sigma_{2-3}} \sigma_{2-3} \quad (178)$$

where

$$\sigma_{2-3} = \frac{1}{2(1 - \psi)} \left\{ \sigma_2 + \sigma_3 - \psi(\sigma_{2w} + \eta_3 \sigma_3) - \sqrt{\left[ \sigma_2 + \sigma_3 - \psi(\sigma_{2w} + \eta_3 \sigma_3) \right]^2 - 4(1 - \psi)\sigma_3(\sigma_2 - \psi\eta_3\sigma_{2w})} \right\} \quad (149)$$

while

$$\sigma_1 = \frac{\pi^2 E}{(a/r_y)^2} \quad (122)$$

$$\sigma_2 = \frac{1}{I_p} \left( GI_t + EC_w \frac{\pi^2}{a^2} \right) \quad (124)$$

$$\sigma_{2w} = \frac{1}{I_{pw}} \left( GI_{tw} + EC_{ww} \frac{\pi^2}{a^2} \right) \quad (140)$$

$$\sigma_3 = \frac{\pi^2 N}{b^2 t} \left( \frac{1}{\beta^2} + 0.125\beta^2 + 0.57 \right) \quad (120)$$

$$\eta_3 = \frac{(1/\beta^2) + 0.57}{(1/\beta^2) + 0.125\beta^2 + 0.57} \quad (136)$$

$$\psi = I_{pw}/I_p \quad (148)$$

The second subscript w in equations (140) and (148) refers to the web alone.

In the plastic domain

$$\sigma_1 = \frac{\pi^2 E_t}{(a/r_y)^2} \quad (121)$$

$$\sigma_2 = \frac{1}{I_p} \left( E F I_t + E_t C_w \frac{\pi^2}{a^2} \right) \quad (123)$$

$$\sigma_3 = \frac{\pi^2 E I}{b^2 t} \left( \frac{A}{\beta^2} + 0.125 D \beta^2 + 1.84 F - 0.25 B \right) \quad (125)$$

while instead of equations (140) and (136)

$$\sigma_{2w} = \frac{1}{I_{pw}} \left( E F I_{tw} + E_t C_{ww} \frac{\pi^2}{a^2} \right)$$

$$\eta_3 = \frac{(A/\beta^2) + 1.84F - 0.25B}{(A/\beta^2) + 0.125D\beta^2 + 1.84F - 0.25B}$$

All plastic values  $E_t$ ,  $A$ ,  $B$ ,  $D$ , and  $F$  refer to the actual buckling stress  $\sigma_{cr}$ . The latter four values are given in equations (2).

The stress  $\sigma_{cr}$  from equation (178) has to be calculated for that half wave length  $a = \beta b$  for which it is minimum. This is practically the half wave length for which  $\sigma_{2-3}$  is minimum. The value  $(\sigma_{cr})_{\min}$  thus obtained governs up to about a value  $\beta = a/b = \beta_2$  (fig. 1). For  $\beta \geq \beta_2$

$$\sigma_{cr} = \frac{\sigma_3}{\sigma_3 + \sigma_{1-2}} \sigma_{1-2} \quad (119)$$

where

$$\sigma_{1-2} = \frac{1}{2[1 - (y_0^2/r_0^2)]} \left[ \sigma_1 + \sigma_2 - \sqrt{(\sigma_1 - \sigma_2)^2 + (4\sigma_1\sigma_2y_0^2/r_0^2)} \right] \quad (189)$$

while  $\sigma_1$ ,  $\sigma_2$ , and  $\sigma_3$  are given by equations (122), (124), and (120) or equations (121), (123), and (125), for the elastic or plastic domain, respectively, and are calculated for  $a = L$ . The symbols  $r_0$  and  $y_0$  are the polar radius of gyration about the shear center  $S$  and the distance between shear center and center of gravity, respectively (fig. 21).

## EXPERIMENTAL INVESTIGATION

### STRESS-STRAIN TESTS

#### Description of Specimens

Square tube specimens used for this series of tests are 61S-T6 aluminum alloy with the following nominal dimensions:

2 by 2 inches by 0.063 inch	designated "B"
$2\frac{1}{2}$ by $2\frac{1}{2}$ inches by 0.047 inch	designated "D"

All tubes are special drawings of the Aluminum Company of America with square corners and slight thickening of the walls on the inside near the corners.

Deviations from flatness, straightness, and squareness are well within tolerable limits, increasing as expected with wall width and diminishing wall thickness. The "D" tubes, in particular, show maximum deviation from squareness of about  $5^\circ$ , from flatness equal to the wall thickness, and a twist not exceeding  $5^\circ$  per 15 feet of length. One-third of the specimens are thus affected. Deviation from straightness is negligible. Variation from nominal wall thickness for all tubes is 0.0010 to -0.0040 inch.

#### Instrumentation

In order to determine the compressive stress-strain characteristics of the tube material, it was necessary to prevent premature local buckling

of the tube wall. The walls were supported by blocking inside and outside, such that the unsupported portion of wall had a  $b/t$  ratio not exceeding 12.5. Ascertainable buckling was prevented at least as far as a strain corresponding to a secant modulus of 0.7E.

The external blocking arrangement consisted of three square clamping frames which held vertical steel supporting blocks one against each face of the tube, as shown in figure 23.

Small internal clearance of the tubes made it necessary to design a special expanding fixture operable from the ends of the specimens. The device, consisting of two supporting blocks and the screw-driven wedge system, is shown in figures 24 and 25. The range of expansion is about  $1/4$  inch, requiring the use of auxiliary blocks for the larger tubes. Figure 23 shows the expander as applied to a specimen.

Strain measurements were made with SR-4 electrical resistance strain gages, type A-1, in connection with standard Wheatstone bridge strain recorders of both Baldwin and Young manufacture. Eight gages were used, two to a face outside the supporting blocks, located near the corners at the midlength of the specimen.

#### Test Procedure

All stress-strain specimens were 8 inches long to avoid end effects and to provide a convenient size for handling. Nearly perfect flatness of ends was obtained by squaring and sanding of the sawed specimens on a disk sander, followed by hand-lapping on a surface plate with oil and emery.

The internal expander, slightly shorter than the specimen, was inserted first with necessary auxiliary blocking, and centered on the length of the tube. All block surfaces contacting the tube were lubricated with medium-weight cup grease to avoid frictional restraints.

The external blocking was next applied. The steel supporting blocks, lubricated with cup grease, were centered vertically and laterally, supported at the base on sponge-rubber pads, and held in place by the center clamping frame. All blocking was then drawn up to the tube, a light seating load was applied, and the other two clamping frames set in place.

Preliminary tests were made to check the effect of varying clamping pressures. On the basis of these tests, it was decided that slight clamping pressure corresponding to a quarter-turn tight on all screws would not be detrimental. More than this showed definite gage "lag" in repeated load cycles, while less resulted in premature local buckling. The pressure so selected was used in all tests.

Centering the specimen, that is, providing uniform stress distribution, was perhaps the most difficult and persistent problem encountered in this series of tests. To correct for nonparallelism of ends and/or machine heads, use was made of tissue paper shims 0.0015 inch thick slipped between the upper machine head and the corners of a hardened-steel bearing block on the upper end of the specimen. Shims were applied or relocated until strain readings on the eight gages showed a total high-to-low deviation of less than 3 percent. Usually it was possible to hold this to less than  $1\frac{1}{2}$  percent at each of three widely separated loads in the elastic range.

Beyond this point no unusual problems were encountered. During the stress-strain tests precautions were taken to observe closely beginning of buckling and adequacy of the blocking and to keep a running load-strain curve.

#### Summary of Stress-Strain Data

Eight stress-strain specimens involving the two sizes of tube have been tested. Representative stress-strain curves are presented in figure 26. Comparison of the test results showed consistent and similar characteristics for the two sizes of tube, with negligible deviation from the average for each series, a yield stress of about 44,000 psi, and an elastic modulus of  $10.7 \times 10^6$  psi.

In the course of testing, 23 stress-strain tests on three other sizes of similar tubing were run, and they gave results completely consistent with those of the "B" and "D" series.

As a further check on consistency of results, the Ramberg-Osgood formula (reference 18) was used for comparison with the experimental data and found to agree almost exactly with the average of the "B" and "D" series. In addition, the curves of worst deviation from the average were calculated and compared with the group average for stress-strain characteristics, tangent modulus, and secant modulus. In all cases the agreement was quite favorable.

#### COLUMN TESTS

##### Description of Specimens

The two sizes of square tube specimens used for this program are described under "Stress-Strain Tests" and were chosen so as to have the

critical plate buckling stress fall in the plastic range for one series ("B") and in the elastic range for the other ("D"). Specimens were selected to cover a wide range of  $L/r$  ratio, encompassing the interaction specimens; that is, those specimens for which the critical plate-buckling stress and primary column-buckling stress are identical. The interaction specimens in this instance are those designated I in tables 2 to 4 and have a ratio  $L/r = 45.95$  for the "B" series and  $L/r = 85.80$  for the "D" series. Including duplicate and triplicate specimens, 14 "B" columns and 7 "D" columns were tested, as given in tables 2 to 4.

### Procedure for Determining Effective Length of Interaction

#### Column with Box Section

(1) For series "D" specimens for which plate buckling stress  $\sigma_2$  is in the elastic range: For the interaction column,

$$\frac{\pi^2 E_t}{(L/r)^2} = 3.62 \left(\frac{t}{b}\right)^2$$

from whence  $L/r = 1.65b/t$  where  $b$  is the plate width center-to-center of adjacent plates.

(2) For series "B" specimens for which plate buckling stress  $\sigma_2$  is in plastic range: The length of the interaction specimen should be such that

$$\sigma_1 = \frac{\pi^2 E_t}{(L/r)^2} = \sigma_2$$

(a) Given the stress-strain curve, compute the curve for plastic buckling stress  $\sigma_{2p}$  as follows. Assume several values of  $\sigma_{2p}$  and for each calculate the parameters  $E_t$ ,  $E_s$ , and

$\sigma_{2p}/\sigma_{2e} = 0.455(\sqrt{AD} + B + 2F)$ , where  $\sigma_{2e}$  is the elastic plate buckling stress. (See reference 4, table 5.) The parameters A, D, B, and F are given by equations (2). Further, compute for each selected value of  $\sigma_{2p}$  the corresponding value of  $\sigma_{2e}/E$  according to the relationship

$$\frac{\sigma_{2e}}{E} = \frac{\sigma_{2p}}{(\sigma_{2p}/\sigma_{2e})E}$$

$\sigma_{2p}$  against  $\sigma_{2e}/E$  for each value of  $\sigma_{2p}$  selected.

(b) Having found the curve for  $\sigma_{2p}$ , calculate

$$\frac{\sigma_{2e}}{E} = 3.62 \left( \frac{t}{b} \right)^2$$

With this value as abscissa, pick the corresponding  $\sigma_{2p}$  from the curve, and the corresponding  $E_t$  to the stress-strain curve at that stress. Then calculate the required  $L/r$  ratio as defined above.

(c) The curve for  $\sigma_{2p}$  may be plotted on the same coordinate system as the stress-strain curve, as shown in figure 27.

It will be noted that  $E_t$  and  $\sigma_{2p}$  are interdependent, which necessitates the trial-and-error procedure as given in order to find the values satisfying the interaction criterion.

Since  $\sigma_{2e}/E$  is immediately known and the curve for  $\sigma_{2p}$  is usually near to the stress-strain curve, it is necessary to select only the values of  $\sigma_{2p}$  that narrowly encompass the stress corresponding to this value of  $\sigma_{2e}/E$ .

(d) The specimen length may be determined by correcting the effective length just computed for the particular end-support conditions used.

#### Instrumentation

In order to study properly the interaction of local and Euler buckling, it was necessary to develop means of measuring separately the two types of buckling. It was felt that electrical resistance strain gages on the column faces would not accomplish this by virtue of difficulty in "sorting out" the proportionate effects of the two types of deformation. In terms of mechanical gages, it was recognized that a device to measure plate deflections due to local buckling must be attached to and "ride" with the column during primary deflection in order to exclude the effects of the latter. The primary column deflections are measurable by any one of several simple devices referred to the ends of the column.

A collar to fit on the column and carry a local buckling gage without affecting the local buckling characteristics has been developed.

The local buckling gage developed for these tests shown in figure 28 is based in principle on the type of gage described in reference 20 and

has the advantage of being independent of buckle location. It makes use of a suspended blade in contact with the column face and measures the blade movement resulting from buckle formation by means of dial gages. (The gages were Federal No. C21 with 0.0001-in. divisions and 0.3-in. range and were full-jeweled.) The blade suspension is 1/2 by 0.002-inch stainless spring steel, combining high resistance to breakage and negligible blade restraint.

Gages of this type were applied (at two different levels) on the column faces parallel to direction of primary buckling in order to avoid effect of primary curvature of the column.

Euler deflections were measured by means of 0.001-inch dial gages at midlength and both quarter points, in combination with a 0.01-inch division scale at midlength read simultaneously for correlation with reset readings of the dial gages and for large deflections beyond the range of the dial gages.

Columns were supported at the ends by knife edges, with appropriate adjustment for centering. Carbonyl knife edges, with corresponding flat bearing surfaces, were loaned by the National Bureau of Standards.

A general view of the testing arrangement is given in figure 29.

#### Test Procedure

The ends of all columns were squared, sanded, and hand-lapped in a manner similar to that for the stress-strain specimens.

The centering procedure made use of both strain readings and lateral-deflection readings. Eight Tuckerman optical strain gages were applied to the corners of the column at two stations, generally 12 to 15 inches outside the upper and lower quarter points, and always at a distance from the ends of at least twice the plate width to avoid end effects. The two sets of strain readings made a simple matter of determining required centering adjustments and in particular of deciding whether eccentricities of the column ends were in the same or opposite directions.

Final centering, at about two-thirds of the predicted critical load, was done by adjusting the column ends until lateral deflections at midlength and both quarter-points were negligible, and then making a final check of strain distribution. Centering by deflection proved to be considerably more accurate than strain readings for the final adjustment. Differences in the average strain on opposite faces of the column were held to a maximum of 1 percent in the direction of primary buckling and two percent in the other less critical direction.

Local buckling gages were then applied to the centered column, and the test proceeded by reading local and Euler deflections at each load increment to failure.

#### Evaluation of Experimental Data

Ultimate stress for each column is given in tables 3 and 4 and also is plotted in relation to the tangent-modulus column curves in figures 30 and 31.

The method of obtaining the tangent modulus from the stress-strain curve may be of interest here. A semitransparent mirror with a one-to-one transmission-reflection ratio was used. It was placed perpendicular to the curve at the desired point and perpendicularity was checked by casting the reflected image of a short portion of curve in front of the mirror onto a short portion of the curve seen through the mirror. A line - the normal to the curve - was then scribed along the face of the mirror. The method proved to be more accurate than drawing the tangent by eye, especially in the sense that several operators with little experience could obtain precisely the same value of modulus.

Local buckling data were evaluated by means of the "top-of-the-knee" method as developed by the NACA (reference 19) and critical plate-buckling stresses thus obtained are plotted on the "D"-series column curve, figure 31. Typical curves of load against local deflection for the "D"-series columns are shown in figure 32. No local buckling data were obtainable for the "B" series, since the critical plate stress was in the plastic range with the result that beginning of plate buckling was immediately followed by complete collapse of the column. Consequently, the ultimate load for the column coincided with the plate buckling stress, and no postbuckling strength was indicated. This observation is in accordance with results given in reference (21). In contrast, the "D"-series columns had considerable postbuckling strength as shown in table 4 and figure 31.

#### C O N C L U D I N G R E M A R K S

The following results were observed from an investigation made to determine the interaction of column and local buckling in compression members.

1. The test results do not show any noticeable interaction effect for the square tubes tested. This seems to substantiate the theory, which shows the order of stress reduction due to interaction effect to be so small that it cannot be differentiated experimentally from the

reduction of concentric buckling stress occurring as a result of inherent eccentricities.

2. The interaction effect is negligible for box sections, as indicated by both theory and experiment. As stated in the paper, the same conclusion applies to the common sizes of I-, H-, and channel sections, but not to sections for which torsional instability is an important factor, such as T and angle shapes.

3. Tests confirm the known fact that appreciable postbuckling strength beyond the critical plate stress is possible when the latter is well within the elastic range. Conversely, when the critical plate stress is in the plastic range, complete collapse of the column accompanies beginning of plate buckling.

Cornell University  
Ithaca, N. Y., March 23, 1951

## R E F E R E N C E S

1. Bijlaard, P. P.: Analysis of the Elastic and Plastic Stability of Sandwich Plates by the Method of Split Rigidities. Preprint No. 259, Sherman M. Fairchild Pub. Fund, Inst. Aero Sci., Jan. 1950.
2. Bijlaard, P. P.: Afleiding van eenvoudige gebruiksformules en grafieken ter bepaling van het plooiagevaar van de wanden van vloeistalen staafprofielen. De Ingenieur Ned. Indie, vol. 6, no. 10, 1939, pp. I.239-I.256.
3. Bijlaard, P. P.: Theory of the Plastic Stability of Thin Plates. Pub. Int. Assoc. Bridge and Structural Eng., vol. 6, 1940-41, pp. 45-69.
4. Bijlaard, P. P.: Theory and Tests on the Plastic Stability of Plates and Shells. Jour. Aero. Sci., vol. 16, no. 9, Sept. 1949, pp. 529-541.
5. Stowell, Elbridge Z.: A Unified Theory of Plastic Buckling of Columns and Plates. NACA Rep. 898, 1948. (Formerly NACA TN 1556.)
6. Timoshenko, S.: Theory of Elastic Stability. First ed., McGraw-Hill Book Co., 1936.
7. Bijlaard, P. P.: Nauwkeurige berekening van de plooispanning van hoekstalen, zowel voorhet elastische als voor het plastische gebied. De Ingenieur Ned. Indie, vol. 6, no. 3, 1939, pp. I.35-I.45.
8. Bijlaard, P. P.: Some Contributions to the Theory of Elastic and Plastic Stability. Pub. Int. Assoc. Bridge and Structural Eng., vol. 8, 1947, pp. 17-80.
9. Bijlaard, P. P.: Berekening van de knikspanning van gekoppelde profielen volgens een nieuwe methode. De Ingenieur Ned. Indie, vol. 6, no. 3, 1939, pp. I.45-I.46.
10. Bijlaard, P. P.: On the Torsional and Flexural Stability of Thin Walled Open Sections. Verhand. Kon. Ned. Akad. Wetensch. (Amsterdam), vol. LI, no. 3, 1948, pp. 314-321.
11. Bijlaard, P. P.: On the Elastic Stability of Sandwich Plates. I. Verhand. Kon. Akad. Wetensch. (Amsterdam), vol. L, no. 1, 1947, pp. 79-87.  
On the Elastic Stability of Sandwich Plates. II. Verhand. Kon. Akad. Wetensch. (Amsterdam), vol. L, no. 2, 1947, pp. 186-193.

12. Bleich, F.: Theorie und Berechnung der eisernen Brücken. Julius Springer (Berlin), 1924.
13. Lundquist, Eugene E., Stowell, Elbridge Z., and Schuette, Evan H.: Principles of Moment Distribution Applied to Stability of Structures Composed of Bars or Plates. NACA Rep. 809, 1945. (Formerly NACA ARR 3K06.)
14. Kroll, W. D.: Tables of Stiffness and Carry-Over Factor for Flat Rectangular Plates under Compression. NACA ARR 3K27, 1943.
15. Kappus, Robert: Twisting Failure of Centrally Loaded Open-Section Columns in the Elastic Range. NACA TM 851, 1938.
16. Lundquist, Eugene E., and Fligg, Claude M.: A Theory for Primary Failure of Straight Centrally Loaded Columns. NACA Rep. 582, 1937.
17. Niles, A. S., and Newell, J. S.: Airplane Structures. Vol. II. John Wiley & Sons, Inc., 1943.
18. Ramberg, Walter, and Osgood, William R.: Description of Stress-Strain Curves by Three Parameters. NACA TN 902, 1943.
19. Hu, Pai C., Lundquist, Eugene E., and Batdorf, S. B.: Effect of Small Deviations from Flatness on Effective Width and Buckling of Plates in Compression. NACA TN 1124, 1946.
20. Pride, Richard A., and Heimerl, George J.: Plastic Buckling of Simply Supported Compressed Plates. NACA TN 1817, 1949.
21. Heimerl, George J.: Determination of Plate Compressive Strengths. NACA TN 1480, 1947.

TABLE 1.- VALUES OF  $\sigma$  FROM THEORETICAL INVESTIGATION

a (cm)	$\sigma_1$	$\sigma_2$	$\sigma_3$	$\sigma_{2w}$	$\sigma_{1-2}$	$\sigma_{2-3}$	$\sigma_{cr}$ from equation (33)	$\sigma_{cr}$ from equation (177)	$\sigma_{cr}$ from equation (178)	$\sigma_{cr}$ from equation (208)	$\sigma_{cr}$ from equation (119)	Unit
50							2,440 34,650					kg/cm <sup>2</sup> psi
58.33	304,670 4,325,000	6,030 85,600	2,553 36,220	1,323 18,800		2,410 34,240	2,375 33,750	2,405 34,170	2,391 33,950			kg/cm <sup>2</sup> psi
62	269,800 3,830,000	5,917 84,000	2,607 37,000	1,267 18,000	5,889 83,600	2,427 34,460		2,421 34,380	2,405 34,150			kg/cm <sup>2</sup> psi
87.5	135,580 1,925,000	5,483 77,900	3,333 47,350	1,042 14,800	5,444 77,250	2,755 39,120	2,755 39,120	2,741 38,920	2,700 38,350			kg/cm <sup>2</sup> psi
135	56,900 807,500	5,230 74,300	5,907 84,000	910 12,910		3,533 50,200		3,477 49,400	3,326 47,220			kg/cm <sup>2</sup> psi
175	33,870 480,400	5,156 73,300	9,043 128,300		4,961 70,500		3,855 54,750					kg/cm <sup>2</sup> psi
350	8,467 120,100	5,067 72,000	32,600 463,000	830 11,790	4,289 60,900	4,613 65,500	4,030 57,250		4,019 57,100	3,790 53,850		kg/cm <sup>2</sup> psi
620	2,699 38,300	5,052 71,800	99,800 1,417,200	819 11,630	2,341 33,250				2,325 33,000	2,287 32,500		kg/cm <sup>2</sup> psi
700	2,117 30,050	5,050 71,800	127,000 1,804,000	817 11,600	1,911 27,170	4,925 70,000	1,880 26,700		1,904 27,040	1,883 26,750		kg/cm <sup>2</sup> psi



TABLE 2.- PROPERTIES OF TUBE SPECIMENS

[Series "B" tubes are 2 by 2 by 0.062 in. with av. r = 0.792 in.; series "D" tubes are  $2\frac{1}{2}$  by  $2\frac{1}{2}$  by 0.047 in. with av. r = 1.001 in.]

Tube	Column	Cut length (in.)	Weight (grams)	Area (sq in.)	Corrected free length, L (in.)	L/r
Series "B" tubes						
"B"-1	SS-1	8.05	171.7	0.481	11.82	14.95
"B"-2	SS-2	8.11	169.1	.470	11.88	15.00
"B"-1	ES-1	11.38	238.9	.474	15.23	19.25
"B"-2	ES-2	11.39	238.6	.473	15.24	19.25
"B"-1	S-1	17.48	368.7	.476	21.45	27.15
"B"-2	S-2	17.49	366.6	.474	21.46	27.15
"B"-1	M-1	26.00	551.8	.478	30.02	37.95
"B"-1	M-2	26.00	549.2	.476	30.02	37.95
"B"-2	I-1	32.34	677.3	.473	36.37	45.95
"B"-2	I-2	32.36	677.2	.473	36.39	45.95
"B"-2	I-3	32.36	676.2	.472	36.39	45.95
"B"-3	ML-1	36.35	771.4	.479	40.38	51.00
"B"-3	L-1	40.23	853.0	.479	44.26	56.00
"B"-3	L-2	40.23	850.2	.477	44.26	56.00
Series "D" tubes						
"D"-4	SS-1	17.31	346.2	0.452	21.25	21.23
"D"-1	S-1	38.88	780.0	.452	43.03	43.00
"D"-2	RM-1	67.00	1349.7	.455	71.09	71.02
"D"-4	MS-1	72.16	1446.0	.452	76.25	76.17
"D"-3	I-2	81.78	1635.2	.452	85.87	85.78
"D"-1	I-1	81.81	1641.0	.453	85.90	85.81
"D"-5	L-1	123.49	2545.0	.465	127.58	127.45

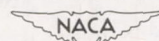


TABLE 3.- TEST RECORD OF SERIES "B" TUBES

[Dimensions: 2 by 2 by 0.062 in.]

Designation		Theoretical			Experimental		$P_{ult}/P_{cr}$
Tube	Column	Plate $\sigma_{cr}$	Column $\sigma_{cr}$	$P_{cr}$	$P_{ult}$	$\sigma_{ult}$	
"B"-1	SS-1	37,250	43,500	17,900	17,850	37,150	0.997
"B"-2	SS-2	37,250	43,500	17,500	17,700	37,650	1.010
"B"-1	ES-1	37,250	42,700	17,630	17,900	37,800	1.015
"B"-2	ES-2	37,250	42,700	17,600	17,400	36,800	.988
"B"-1	S-1	37,250	40,900	17,720	17,750	37,270	1.001
"B"-2	S-2	37,250	40,900	17,630	17,450	36,810	.988
"B"-1	M-1	37,250	38,500	17,800	17,500	36,600	.983
"B"-1	M-2	37,250	38,500	17,720	17,250	36,200	.972
"B"-2	I-1	37,250	37,250	17,600	16,900	35,750	.960
"B"-2	I-2	37,250	37,250	17,600	17,400	36,800	.988
"B"-2	I-3	37,250	37,250	17,590	17,150	36,350	.975
"B"-3	ML-1	37,250	36,500	17,470	17,150	35,800	.980
"B"-3	L-1	37,250	33,600	16,100	15,400	32,200	.959
"B"-3	L-2	37,250	33,600	16,030	15,400	32,350	.963



TABLE 4.- TEST RECORD OF SERIES "D" TUBES

[Dimensions:  $2\frac{1}{2}$  by  $2\frac{1}{2}$  by 0.047 in.]

Designation		Theoretical			Experimental			Ratio of experimental to theoretical values	
Tube	Column	Plate $\sigma_{cr}$	Column $\sigma_{cr}$	$P_{cr}$	$P_{ult}$	$\sigma_{ult}$	$\bar{\sigma}_{cr}$ (a)	$P_{ult}/P_{cr}$	Plate $\bar{\sigma}_{cr}/\sigma_{cr}$
"D"-4	SS-1	14,325	42,000	6470	9670	21,390	14,290	1.491	0.997
"D"-1	S-1	14,325	37,650	6470	9200	20,350	14,200	1.420	.991
"D"-2	RM-1	14,325	20,700	6520	6800	14,920	13,850	1.042	.967
"D"-4	MS-1	14,325	18,000	6470	6525	14,420	14,260	1.007	.995
"D"-3	I-2	14,325	14,325	6480	6230	13,790	-----	.963	-----
"D"-1	<sup>b</sup> I-1	14,325	14,325	6500	6050	13,330	-----	.930	-----
"D"-5	L-1	14,325	6,500	3020	2900	6,240	-----	.960	-----

<sup>a</sup>Experimental plate  $\sigma_{cr}$  as determined by NACA top-of-knee method.<sup>b</sup>Two tests on same column.

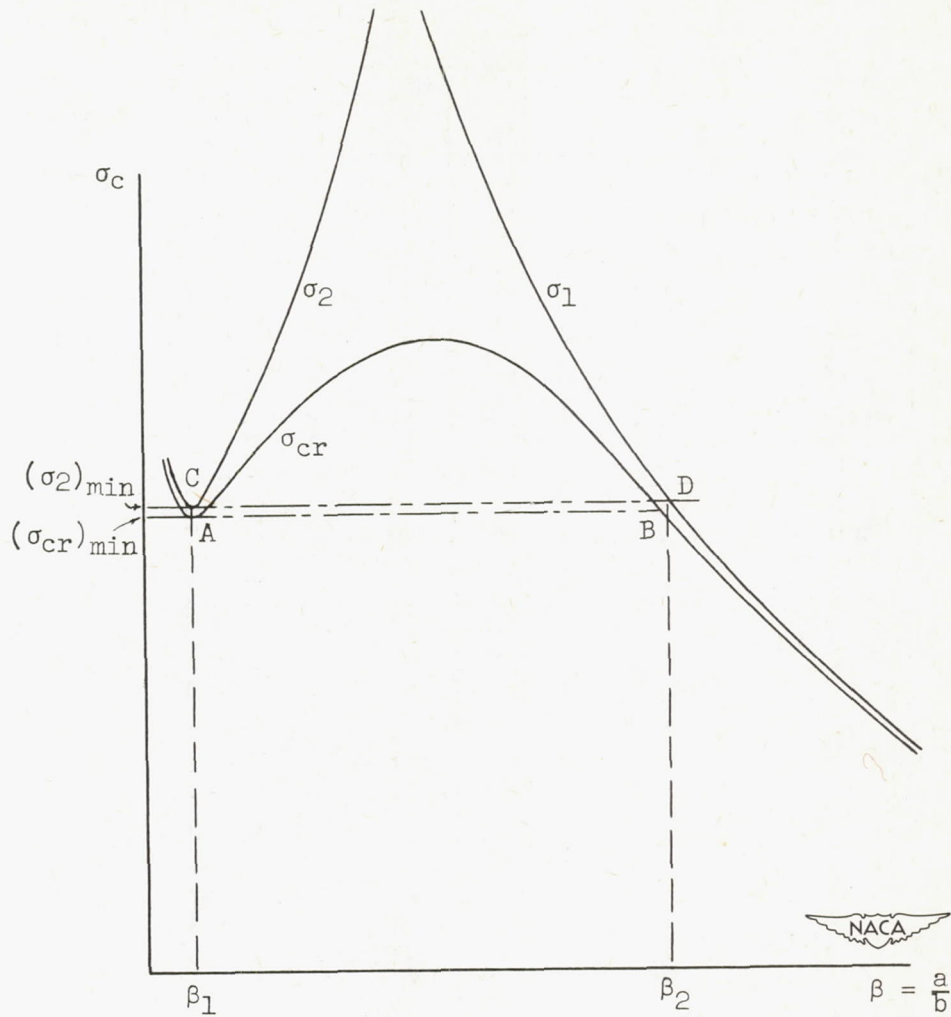
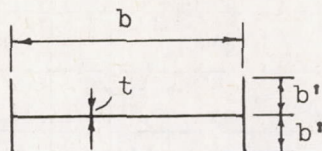
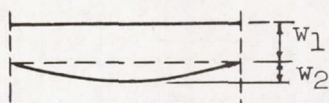


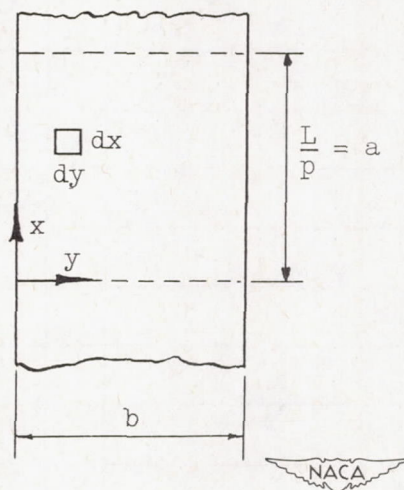
Figure 1.- Diagram of buckling stresses plotted against ratio of half wave length to web width  $\beta = a/b$ .



(a) Cross-sectional sketch of column.



(b) Cross-sectional sketch of web showing interaction of column and plate buckling.



(c) Sketch of column showing axis notation.

Figure 2.- I-section column showing various notations.

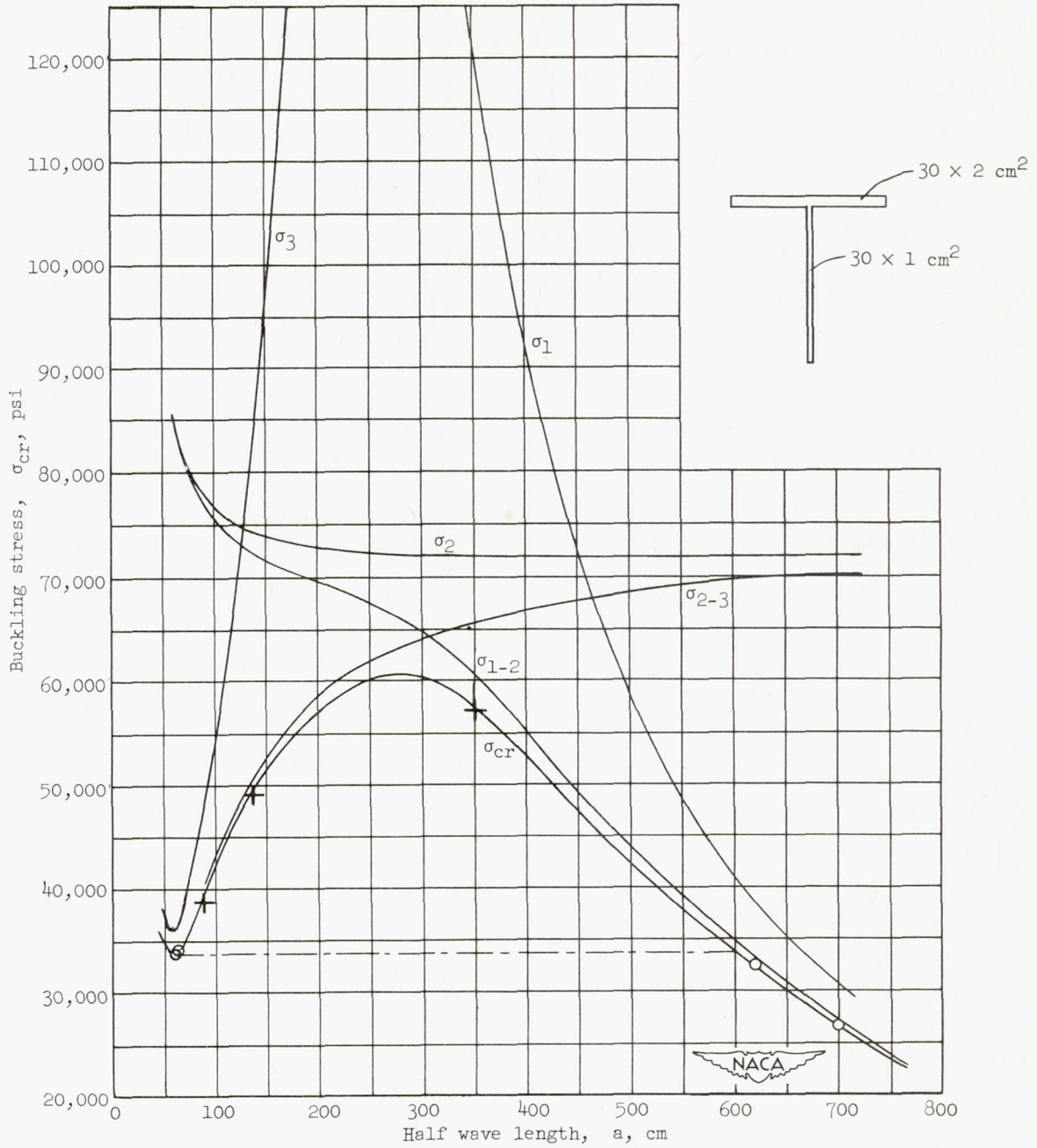
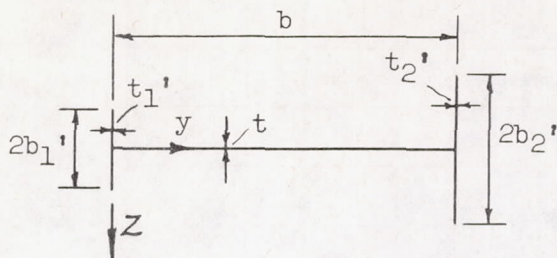
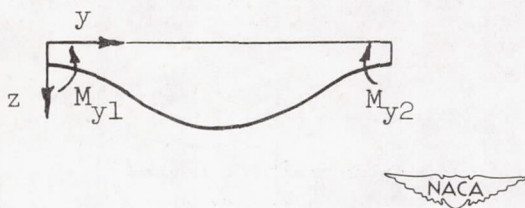


Figure 3.- Calculated buckling stresses of T-section of figure 16 for several half wave lengths  $a$ .



(a) Cross-sectional sketch of column.



(b) Cross-sectional sketch of web showing instability.

Figure 4.- Asymmetric column supported at both unloaded edges by flanges of different width and thickness.

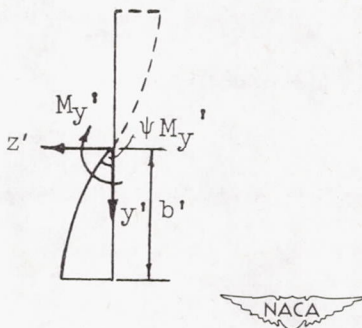


Figure 5.- Sketch of lower half of flange.

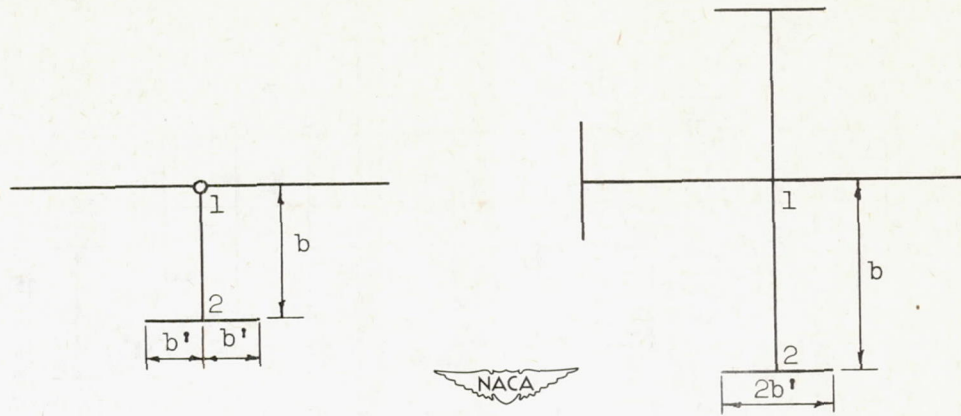
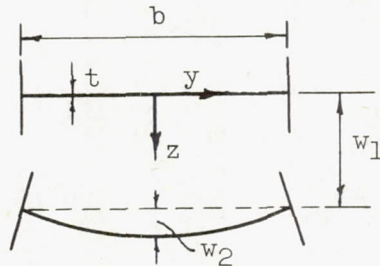
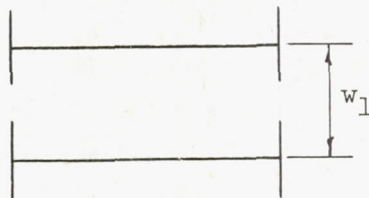


Figure 6.- Sketch of T-stiffener and column made of T-sections.



(a) Sketch of column showing various notation.



(b) Buckling as column without distortion of cross section.



(c) Buckling as plate with distortion of cross section.

Figure 7.- Sketch of I-section with narrow and thin flanges.

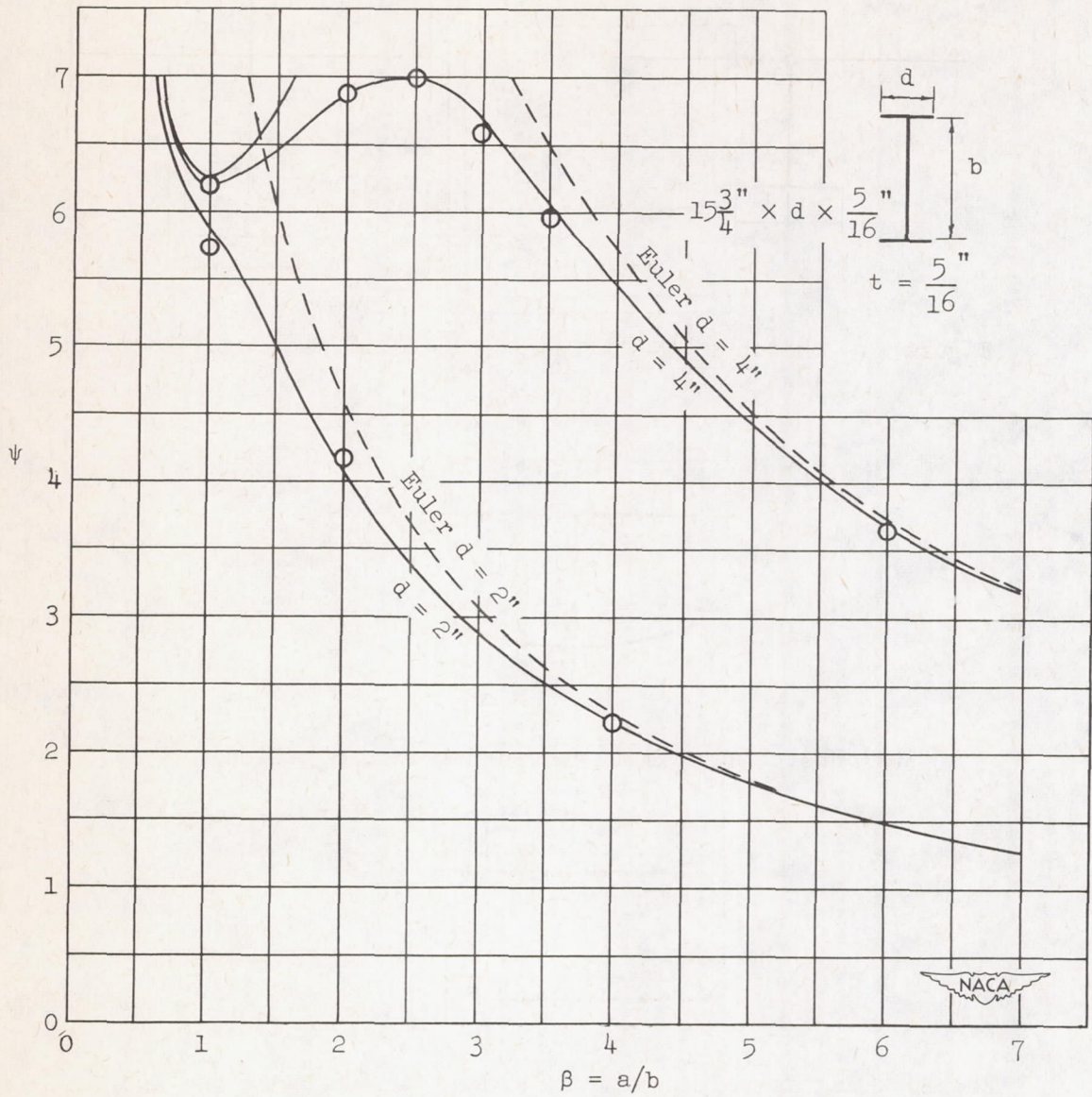


Figure 8.- Curves of  $\psi$  against  $\beta$  in elastic range for I-section columns with flanges of 4- and 2-inch width.

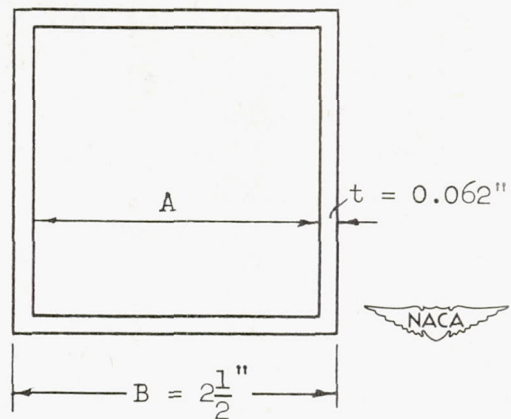


Figure 9.- Diagram of square tube or box section.

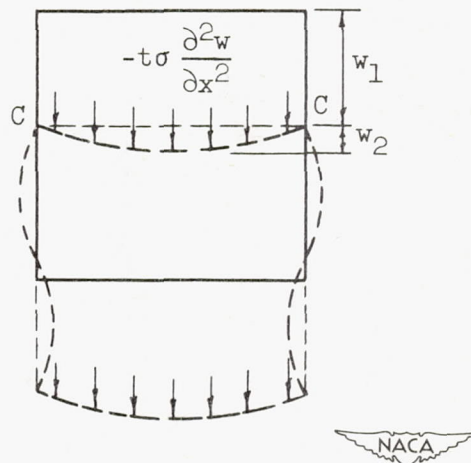


Figure 10.- Deflective forces  $-t\sigma \frac{\partial^2 w}{\partial x^2}$  caused by deflection  $w_1$  of box section.

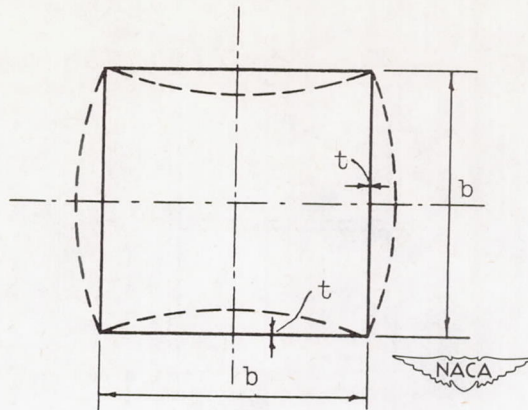


Figure 11.- Square tube with plates buckling symmetrically with respect to vertical and horizontal axes.

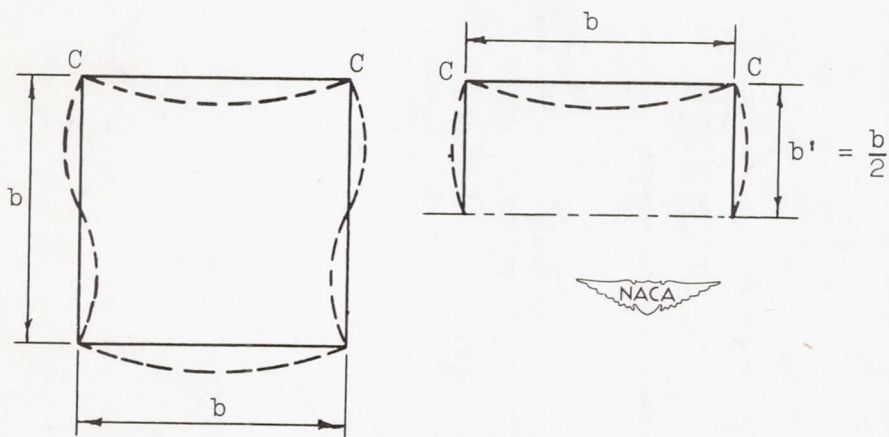


Figure 12.- Square tube showing alternate mode of web buckling.

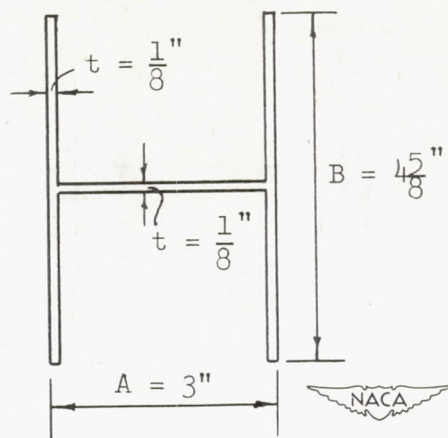


Figure 13.- H-section where width of flanges is such that they are rotationally restrained from buckling by web.

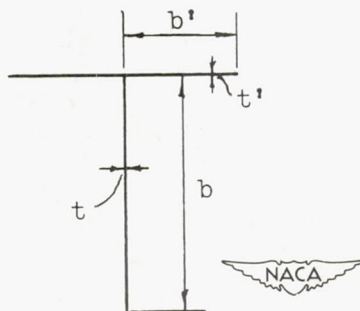


Figure 14.- Sketch of T-section showing notations.

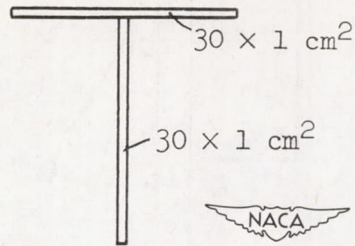


Figure 15.- T-section with small rotational restraint of web.

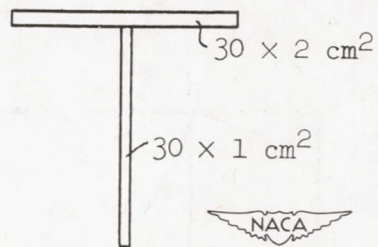


Figure 16.- T-section where flange has relatively large torsional rigidity and is much more stable than the web, so that web is substantially rotationally restrained.

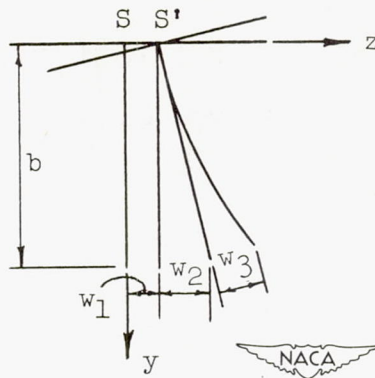


Figure 17.- Deflection of cross section in figure 16 consisting of translation  $w_1$ , rotation with respect to shear center  $S$ , and plate buckling of web with maximum deflection  $w_3$ .

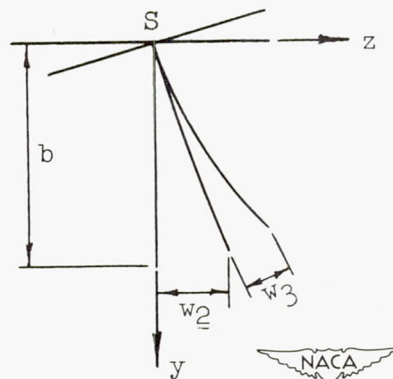


Figure 18.- Deflections of case (2) ( $w_2$ ) and case (3) ( $w_3$ ).

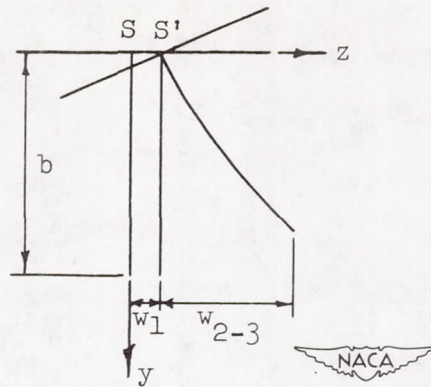


Figure 19.- Deflections of case (1) and of combined case (2-3).

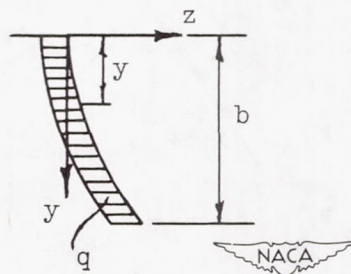


Figure 20.- Distortion of cantilever beam under uniform load  $q$ .

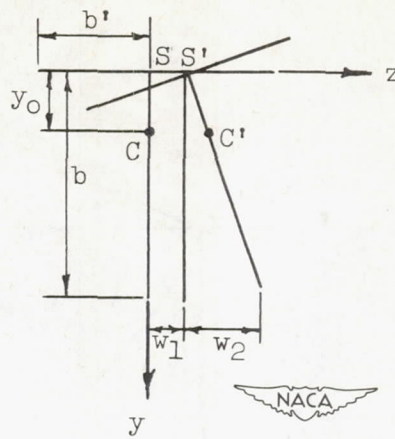


Figure 21.- Flexural and torsional buckling of T-section showing displacement  $CC'$  of center of gravity  $C$ .

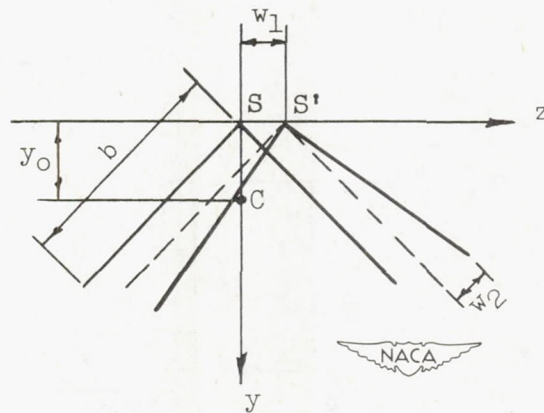


Figure 22.- Flexural and torsional buckling of angle section.

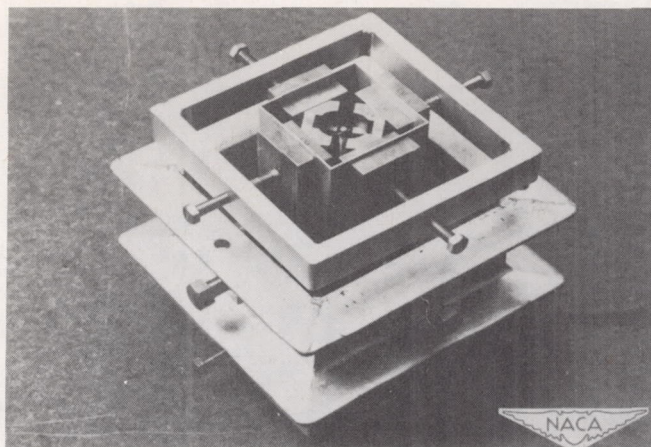


Figure 23.- Stress-strain test blocking assembly.

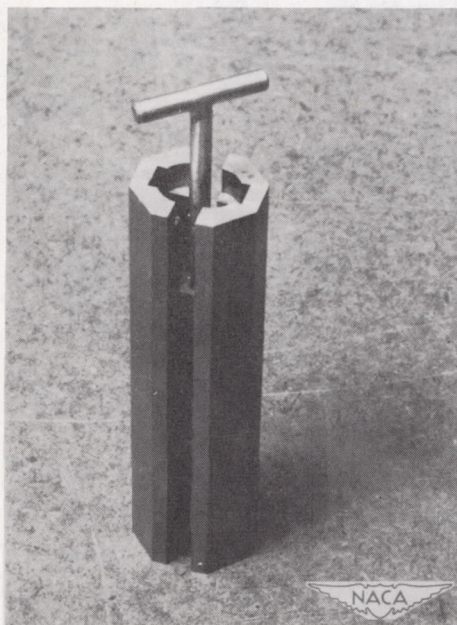


Figure 24.- Internal expander for tube specimens, assembled.

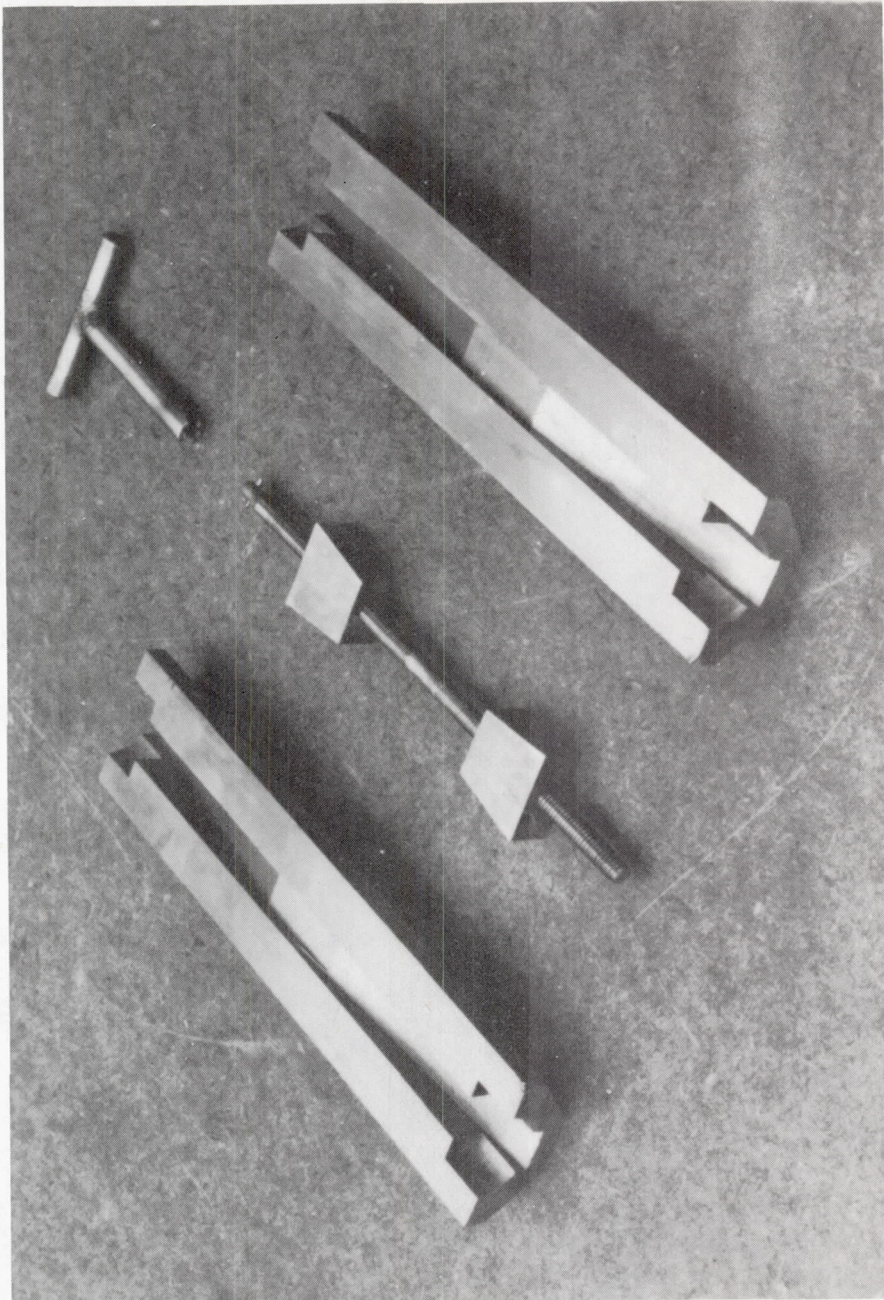


Figure 25.- Internal expander showing individual parts.

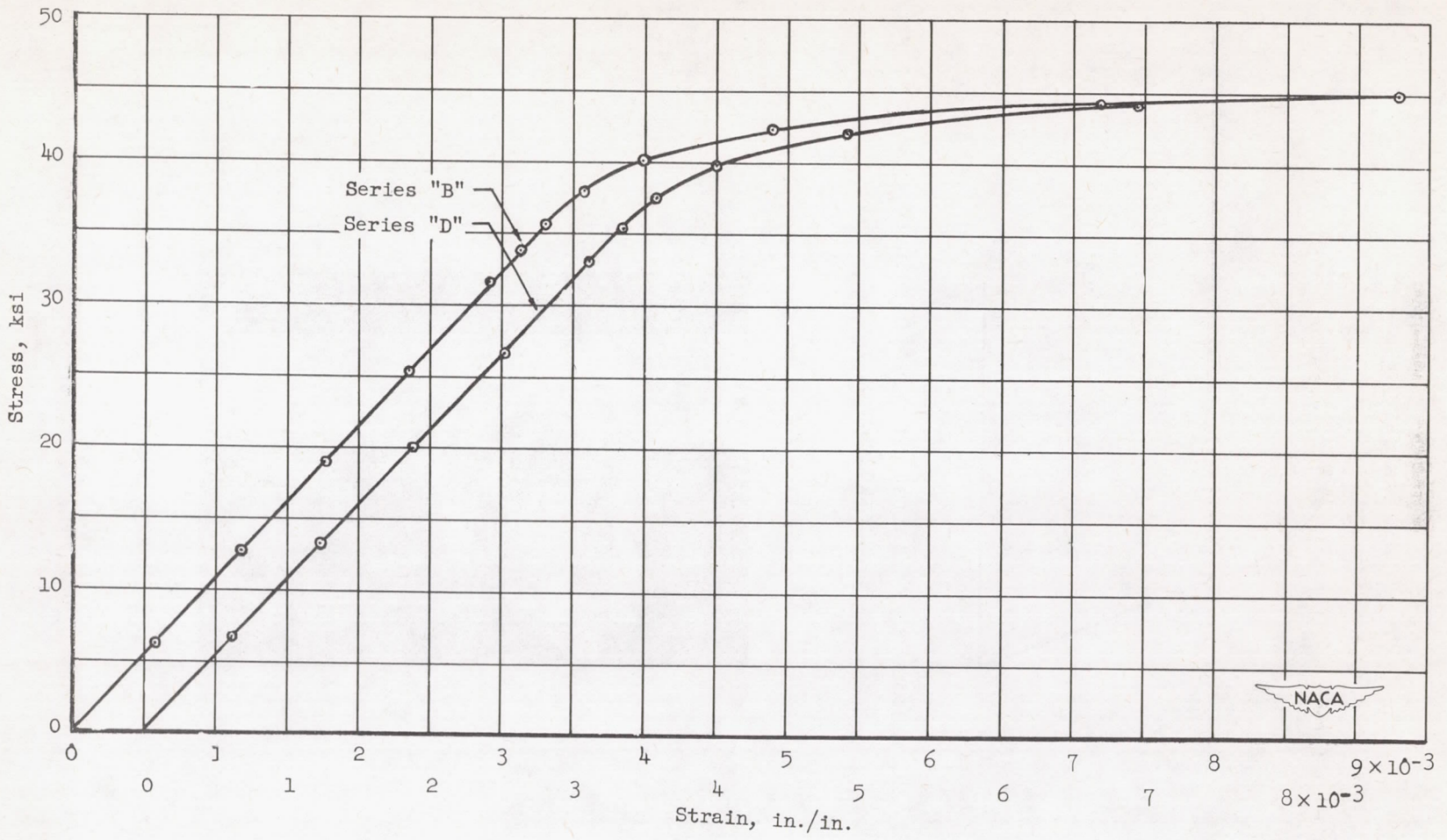


Figure 26.- Typical stress-strain curves for square-tube specimens.

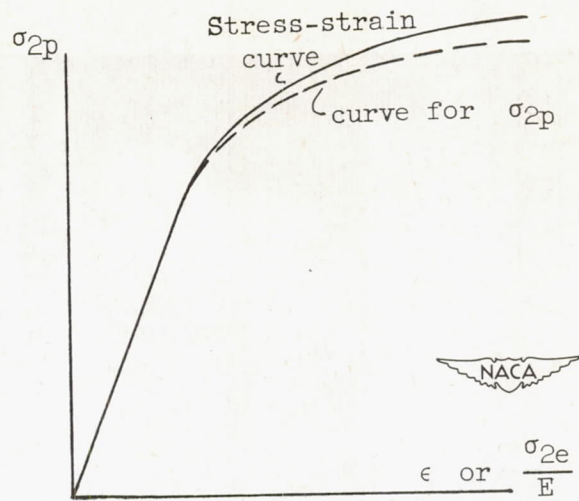


Figure 27.- Curve for  $\sigma_{2p}$  plotted on same coordinate system as stress-strain curve.

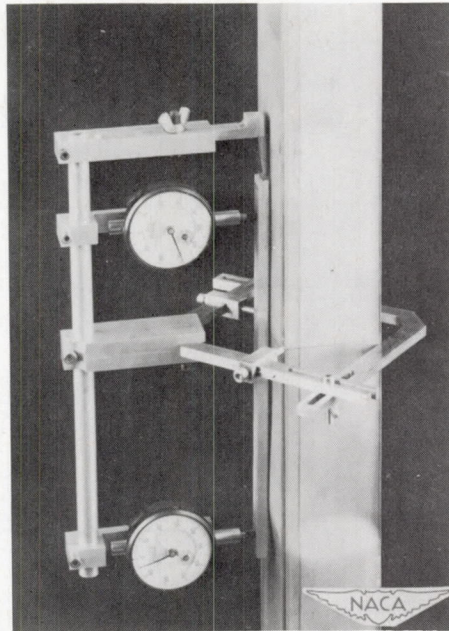


Figure 28.- Local buckling gage and supporting collar.

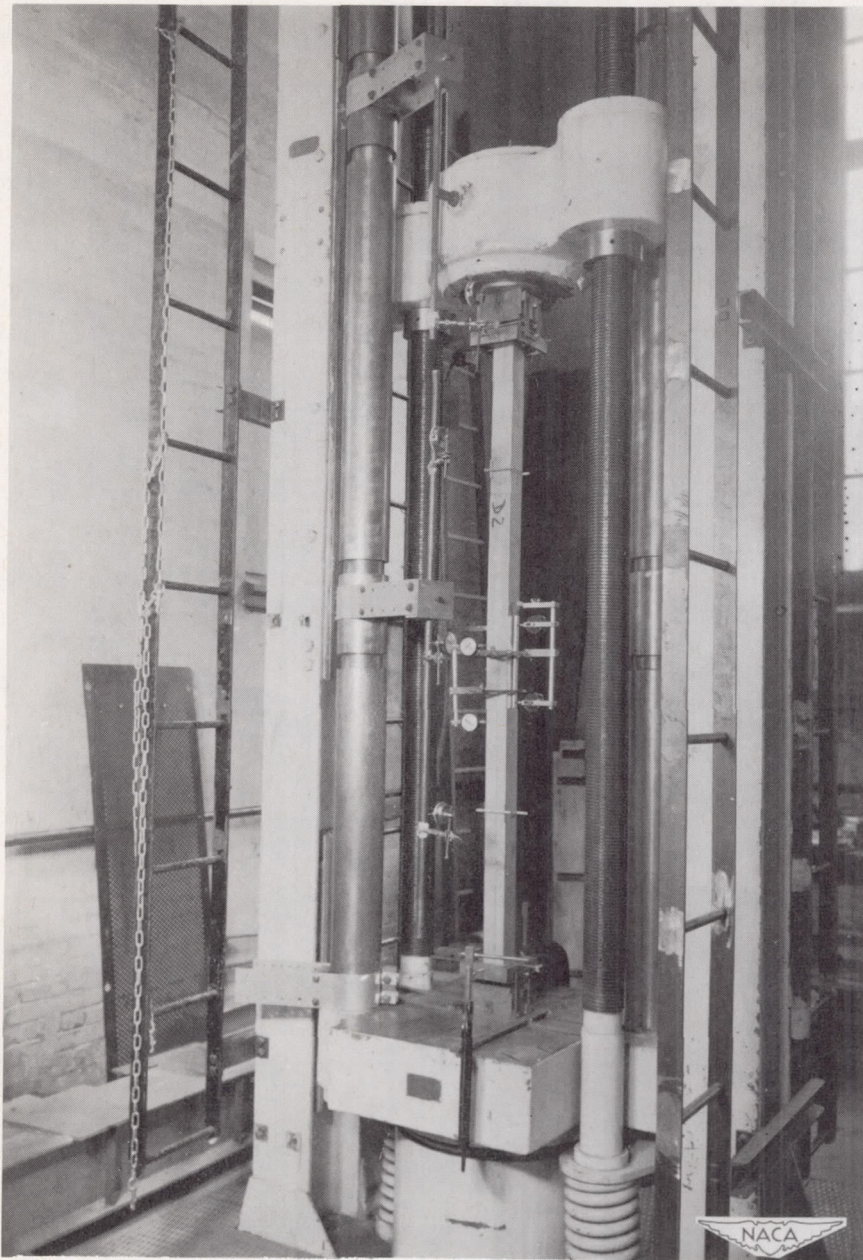


Figure 29.- General view of test arrangement.

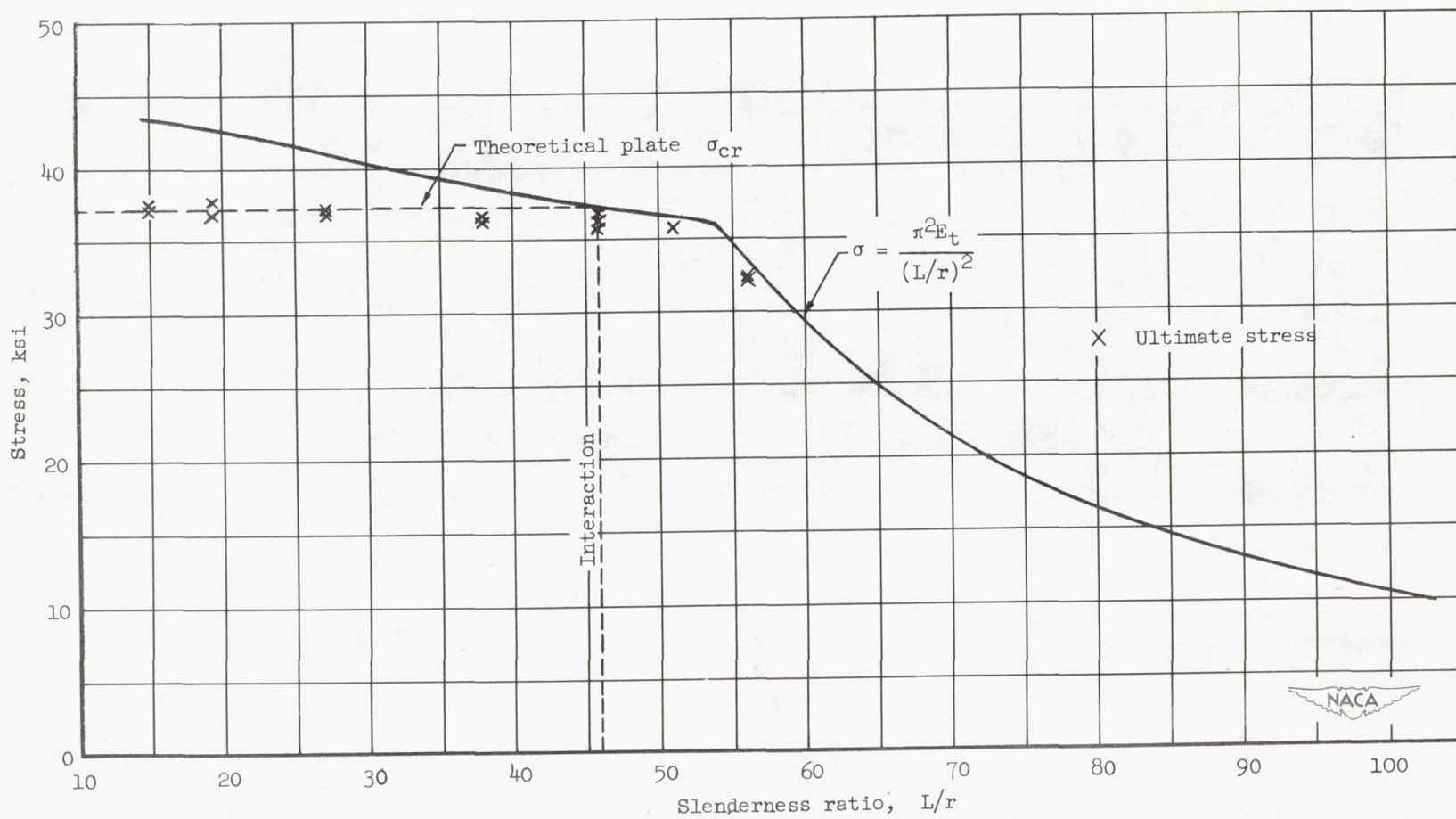


Figure 30.- Test results for series "B" specimens.

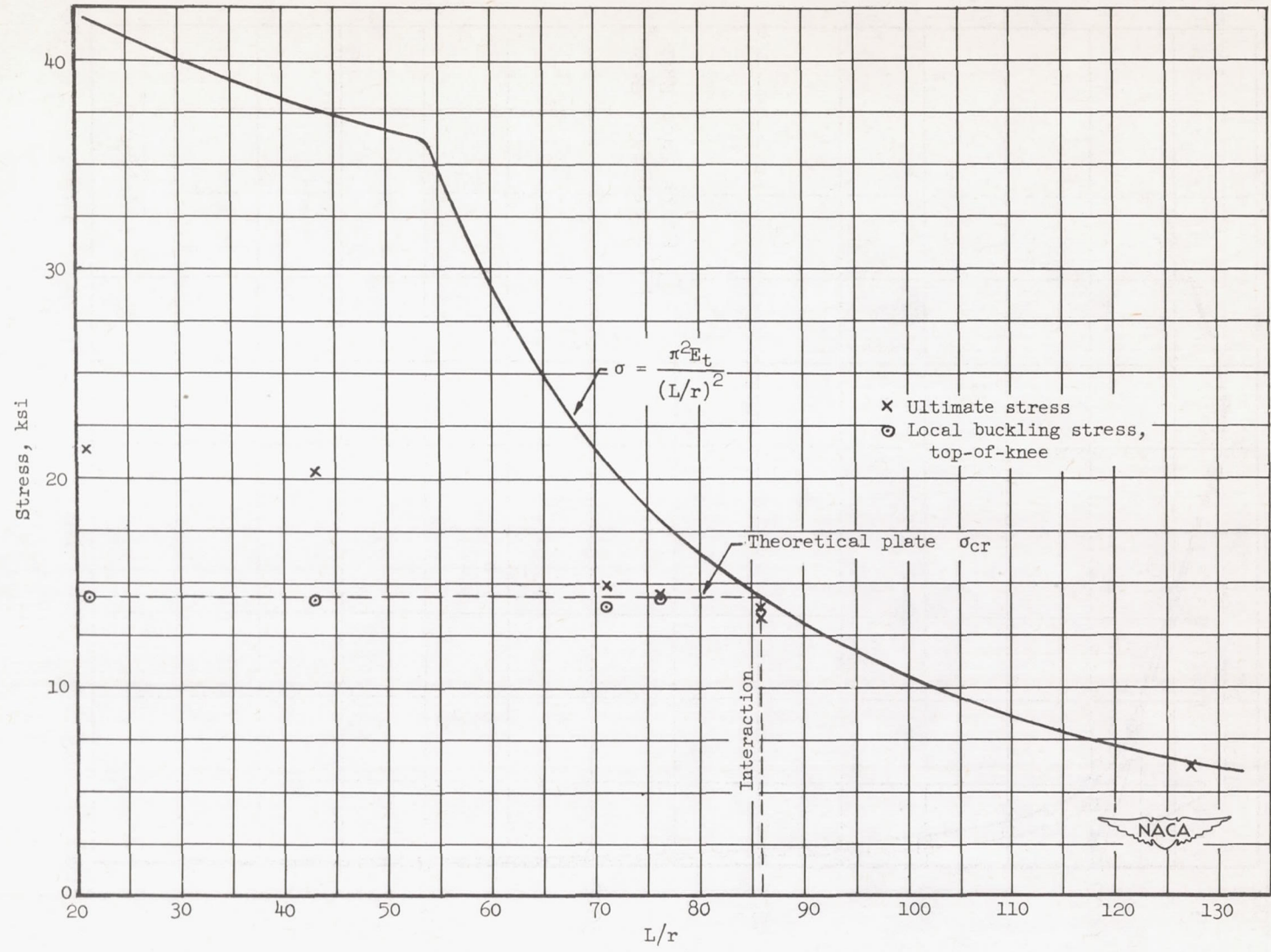


Figure 31.- Test results for series "D" specimens.

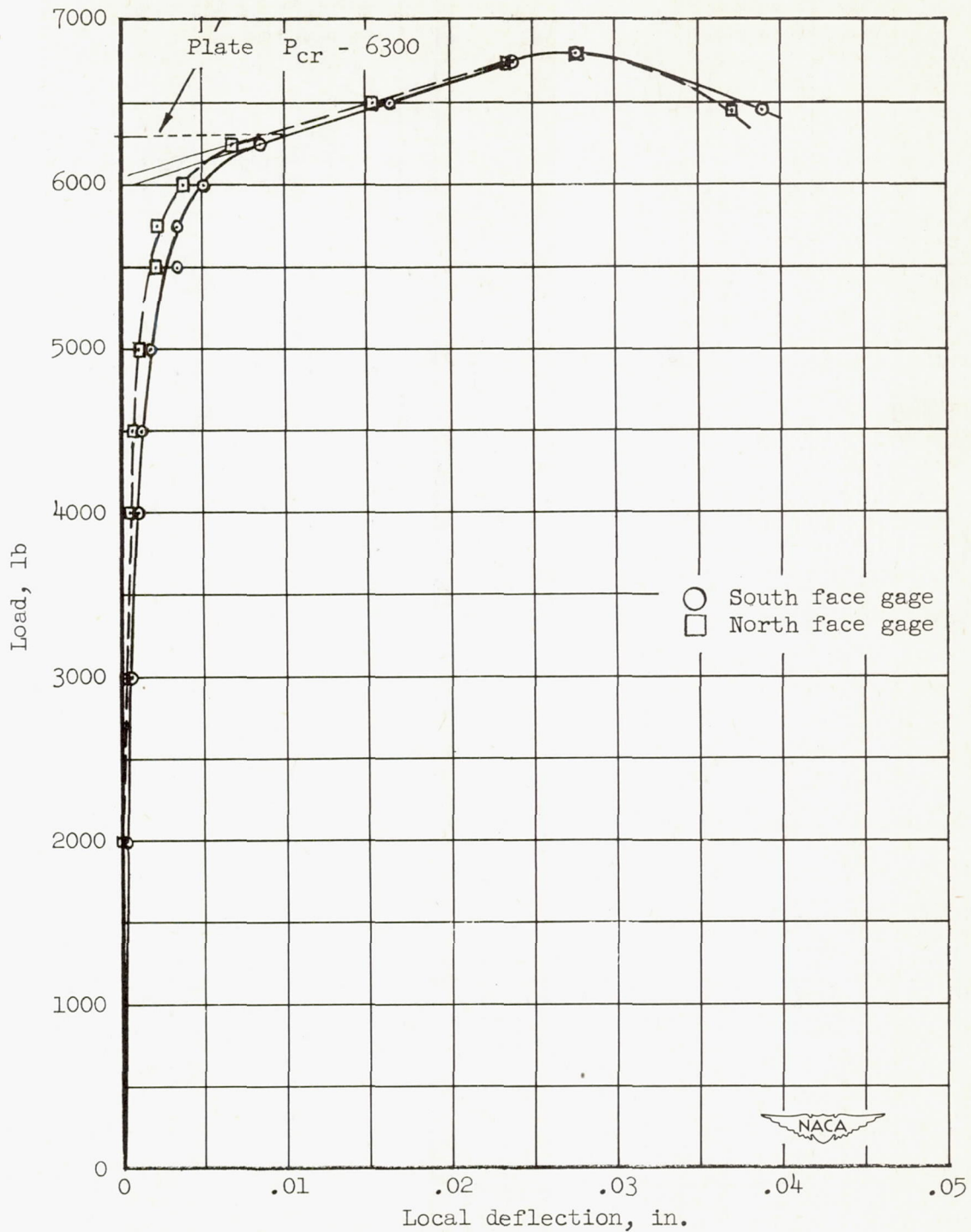


Figure 32.- Local buckling curves for square tube specimen "D"-2-RM1.